

AMERICAN UNIVERSITY OF BEIRUT

EFFECT OF HYPERGLYCEMIA ON EPIGENETICS OF
TARGET GENES IN VASCULAR CELLS

by
MOHAMAD MUSBAH RYAD ALMEDAWAR

A thesis
submitted in partial fulfillment of the requirements
for the degree of Master of Science
to the Department of Biochemistry and Molecular Genetics
of the Faculty of Medicine
at the American University of Beirut

Beirut, Lebanon
September 2014

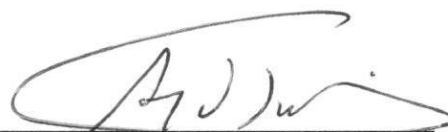
AMERICAN UNIVERSITY OF BEIRUT

EFFECT OF HYPERGLYCEMIA ON EPIGENETICS OF
TARGET GENES IN VASCULAR CELLS

by
MOHAMAD MUSBAH RYAD ALMEDAWAR

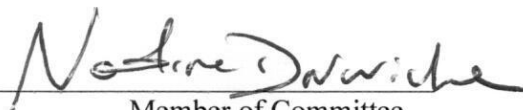
Approved by:

Dr. Ayad Jaffa, Professor and Chair
Biochemistry and Molecular Genetics



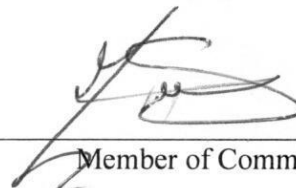
Advisor

Dr. Nadine Darwiche, Professor
Biochemistry and Molecular Genetics



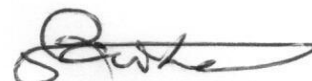
Member of Committee

Dr. Soha Yazbek, Assistant Professor
Medical Laboratory Sciences Program (MLS)



Member of Committee

Dr. Firas Kobeissy, Assistant Professor
Biochemistry and Molecular Genetics



Member of Committee

Dr. Fuad Ziyadh, Professor
Biochemistry and Molecular Genetics



Member of Committee

Date of thesis defense: September 9, 2014

ACKNOWLEDGMENTS

First and Foremost, I would like to thank my thesis advisor Dr. Ayad Jaffa, Chair and Professor of the Biochemistry and Molecular Genetics Department at AUB, for allowing me to join the cardiovascular and renal research laboratory to conduct the experiments needed to complete the requirements for a Masters of Science in Biochemistry. Dr. Jaffa supported my research in every aspect and encouraged me to become an independent scientist, to look for the answers, and to troubleshoot failures. I would like to thank the committee members, Dr. Ayad Jaffa, Dr. Firas Kobeissy, Dr. Nadine Darwiche and Dr. Soha Yazbeck, for reviewing my thesis and their technical and educational support in my master's study.

My recognition and gratitude are addressed to the 2-12 laboratory members Moustafa, Lamis, Joe, Oula, Nahed, Rana, Ruwaida, and Maya, for teaching me all that I need to know and more about laboratory techniques, and more importantly, for being my family outside home and tolerating my occasional insanity. Moustafa, I cannot thank you enough, you've really went out of your way to help me all along.

I would like to thank my mentor and lifelong friend Dr. Hussain Isma'eel for giving me an opportunity that very few people offered, an opportunity that got me to where I am today, and for guiding me throughout the past 2 and a half years in research, work ethics, and life. I would also like to thank Dr. Mohamad Samir Arnaout who also believed in my abilities and entrusted me with huge responsibilities.

Special thanks to Dr. Nathalie Khoueiry-Zgheib who provided us with priceless tips, ideas, and even materials to proceed with our experiments and was very supportive and open for consultation and advisory. My recognition and gratitude are addressed to Dr. Soha Yazbeck who also provided essential consultation and advisory for the project.

Special thanks to Dr. Firas Kobbaisy for throwing every possible opportunity my way, for helping our lab establish a collaboration with Dr. Yehia Mechref at the Department of Chemistry and Biochemistry, Texas Tech University, which greatly enriched my thesis data and helped validate our research.

My appreciation and gratitude to Dr. Ayad Jaffa, Dr. Rihab Nasr, Dr. Julnar Ousta, Dr. George Nembr and Dr. Marwan Sabban for encouraging critical thinking, looking for evidence as opposed to taking things as they are, and pragmatism in research, through their teaching methods. It was a true honor to sit in your classes.

None of this, of course, would have been possible if it was not for my parents, Riyadh and Bassima, and my siblings, Rima, Siba, and Majed to whom I dedicate this work. The sacrifice my parents go through every day, and the unconditional love, trust, and support have inspired me to do my best and give unconditionally as well. My inspiration also comes from my sister, Dr. Siba, whose footsteps I follow in science and life, and to Dr. Rami Diab who's been the perfect best friend in every sense of the term.

AN ABSTRACT OF THE THESIS OF

Mohamad Musbah Ryad Almedawar for Master of Science
Major: Biochemistry

Title: Effect of Hyperglycemia on Epigenetics of Target Genes in Vascular Cells

Background: Epigenetic alterations in vascular cells have been found to be implicated in microvascular and macrovascular complications in Diabetes Mellitus (DM). Metabolic memory is the phenomenon in which diabetic individuals who are chronically exposed to high blood glucose, exhibit diabetic complications even after achieving normoglycemia. This memory results partially from mitotically heritable changes in DNA methylation patterns on key genes involved in pathways that affect vascular remodeling.

Aims: To assess epigenetic control of expression of key genes involved in diabetic vascular complications through performing quantitative DNA methylation profiling in 5' promoter regions. To simulate the metabolic memory phenomenon by comparing DNA methylation signatures between control, diabetic, and insulin-treated diabetic rats.

Methods: Type-1 Diabetes Mellitus (T1DM) was induced by streptozotocin injection in Male Sprague Dawley rats. After 6 weeks, the aortas of T1DM rats, control rats and insulin-treated rats were harvested for isolation of genomic DNA (gDNA), mRNA, and proteins from smooth muscle cells. High glucose-treated and high mannitol-treated rat aortic smooth muscle cells for 4 weeks and their controls were also collected for isolation of gDNA and mRNA. Real-time qPCR (RTqPCR) followed by High-Resolution Melt PCR and global proteomics analysis were done to assess gene expression, differential DNA methylation profiles, and protein synthesis and activity, respectively. Genes of interest included *Bradykinin Receptor B1 (BDKRB1)*, *B2 (BDKRB2)*, *Connective Tissue Growth Factor (CTGF)*, *Fibronectin1 (FN1)*, *C-Reactive Protein (CRP)*, *Interleukin 1 β (IL1 β)*, *Interleukin 6 (IL6)*, *Interleukin 10 (IL10)*, *Transforming Growth Factor beta 1 (TGF- β 1)*, *Transforming growth factor beta 2 (TGF- β 2)*, *Tumor Necrosis Factor alpha (TNF α)*, *NADPH oxidase 1 (Nox1)*, and *NADPH oxidase 4 (Nox4)*.

Results: RTqPCR on cDNA from *in vitro* and *in vivo* samples showed that high glucose treatment induces expression of all studied genes. However, fold change was higher for *in vitro* gene expression in comparison to *in vivo*. Analysis of CpG

methylation in promoter regions of *BDKRB1*, *BDKRB2*, *TGF- β 2*, and *TNF α* revealed that *BDKRB1* and *BDKRB2* were hypomethylated *in vivo* but remained unchanged *in vitro*, whereas *TGF- β 2*, and *TNF α* were hypomethylated *in vitro* but remained unchanged *in vivo*. Proteomics analysis revealed that proteins extracted from diabetic rat aortas clustered away from control and insulin-treated rat aortas, which were also clearly resolved. Proteomics and systems biology analysis revealed that pathways downstream of the kinin receptors have also been found to be up-regulated in the aorta and persist as such even after lowering blood glucose with intensive insulin treatment.

Conclusions: DNA methylation controls expression of BK receptor genes in addition to pro-inflammatory and fibrotic genes in T1DM in aortic vascular smooth muscle cells. The phenomenon of metabolic memory was evident through proteomics and systems biology analysis.

Keywords: Type-1 Diabetes, Vascular Complications, Metabolic Memory, Epigenetics, DNA Methylation

CONTENTS

ACKNOWLEDGMENTS	V
ABSTRACT.....	VI
LIST OF ILLUSTRATIONS	XI
LIST OF TABLES.....	XIII
LIST OF ABBREVIATIONS.....	XIV

Chapter

I.INTRODUCTION	1
A. Clinical Studies	2
B. Definitions of metabolic memory	3
C. Epigenetic mechanisms.....	4
D. Vascular complications in Diabetes.....	5
1. Molecular pathways of vascular complications.....	5
2. Downstream pathway of the kinin receptors in diabetes	8
3. Epigenetic regulation of gene expression in Diabetes Mellitus.....	11
a. Histone tail modifications in hyperglycemia.....	11
b. MicroRNAs in hyperglycemia.....	14
c. DNA methylation in hyperglycemia.....	14
II.RATIONAL AND AIMS	17
III.MATERIALS AND METHODS	19
A. Materials	19
B. Methods	20
1. In vitro Studies: Effect of high glucose on VSMC.....	20
a. <i>In vitro</i> Sample Preparation and Treatment (Cell Culture)	20
b. RNA Isolation.....	21
c. DNA Isolation	21
2. In vivo Studies: Effect of hyperglycemia on VSMCs	22
a. <i>In vivo</i> Laboratory Animal Handling and Treatment	22
b. Collection of rat aorta tissues	23

c. Immunohistochemistry	23
d. RNA and DNA Isolation	23
e. Extraction and tryptic digestion of proteins	24
3. Reverse Transcriptase Conversion of mRNA to cDNA	25
4. RTqPCR Primer Design	25
5. Gene Expression Quantitation by RTqPCR	27
6. DNA Methylation Studies	27
a. Bisulfite Conversion	27
b. Bisulfite Specific Primer Design	29
c. Preparation of Methylation Standards	30
d. Methylation Sensitive-High Resolution Melting (MS- HRM) PCR	30
7. Global Proteomics analysis.....	31
a. Liquid Chromatography-Tandem mass spectrometry (LC- MS/MS) assay	31
b. LC-MS/MS data analysis	32
c. Systems Biology Assessment	33
8. Statistical Analysis.....	34

IV.RESULTS –EPIGENETIC REGULATION OF GENE EXPRESSION

A. <i>In vitro</i> studies: Effect of high glucose on VSMCs	35
1. RT-qPCR	35
2. Melting Curve analysis of DNA methylation	36
B. <i>In vivo</i> studies: Effect of hyperglycemia on VSMCs	36
1. Characteristics of animal models.....	36
2. RT-qPCR	37
C. Melting Curve Analysis of DNA Methylation	39
D. Immunohistochemical staining	39
Bisulfite Conversion Efficiency	42

V.RESULTS – PROTEOMICS.....

A. Protein Extraction Efficiency.....	43
B. Spectral Count Quantification	43
C. Protein level variation (Shotgun Proteomics).....	44

D. Systems Biology Assessment	53
1. IPA analysis of dysregulated protein levels in the aorta.....	53
2. IPA analysis of dysregulated protein levels in the renal cortex.....	57
3. GO analysis.....	62
VI.DISCUSSION	68
VII.CONCLUSIONS	74
A. Main findings of the study	74
B. Limitations of the study	74
C. Future prospects	75
BIBLIOGRAPHY	76

ILLUSTRATIONS

Figure	Page
1: Cross - talk between BK B2 Receptor (B2R) and Sphingosine 1 Phosphate Receptor (S1PR)	10
2: Mechanisms of histone tail modifications observed in diabetes <i>via</i> posttranslational modifications on the N-terminal histone tails. Chromatin modifiers include Histone lysine methyltransferases (HMTs) and lysine demethylases (KDMs) which regulate histone lysine methyltransferases (HMTs) and lysine demethylases (KDMs) which regulate histone lysine methylation (Kme), while histone acetyltransferases (HATs) and histone deacetylases (HDACs) control histone acetylation (Ac) [85].	12
3: Activated epigenetic mechanisms by hyperglycemia and persistence of vascular complications [85].	13
4: Hyperglycemia activates several pathways leading to diabetic complications, these pathways include PKC, MAPKs, ROS, and AGE formation. These pathways lead to histone tail modifications and altered DNA methylation in downstream genes [85].	16
5 - in vivo and in vitro methods scheme on endothelium-denuded aorta and VSMC...	20
6 - Changes in body weight of rats during 6 weeks of exposure (n=3)	37
7 - Changes in non-fasting blood glucose levels of rats during 6 weeks of exposure (n=3)	37
8 - Endothelium-denuded rat aorta rings were stained with (A) Anti- α -SMA-Alexa Fluor (Red) (B) Anti-PECAM-1 (CD31)-Texas Red (Green), which showed presence of VSMC and absence of VEC. Regular rat aortic smooth muscle cells were stained with (C) Fluoro-Gel II with Dapi (blue) (D) Anti-PECAM-1-Texas Red (Green) (E) Anti- α -SMA-Alexa Fluor (Red), (F) Superimposed images (C to E), which showed presence of VSMC and VEC.....	41
9: PCA scoring plots of aorta proteome for controls, diabetic, and insulin-treated rats using Scaffold Q+ software	44
10: IPA map of diabetic rat aorta in comparison to control rat aorta on cellular processes and diseases that lead to atherosclerosis (n=3).....	55
11: IPA map of insulin-treated rats aorta in comparison to diabetic rat aorta on cellular processes and diseases that lead to atherosclerosis (n=3).....	56
12: IPA map of insulin-treated rat aorta in comparison to diabetic rat aorta on cellular processes and diseases that lead to atherosclerosis (n=3).....	57

13: IPA map of diabetic rat renal cortex in comparison to control rat renal cortex on cellular processes and diseases that lead to diabetic nephropathy (n=3).....	59
14: IPA map of insulin-treated rats renal cortex in comparison to diabetic rat renal cortex on cellular processes and diseases that lead to diabetic nephropathy (n=3).	61
15: IPA map of insulin-treated rats renal cortex in comparison to control rat renal cortex on cellular processes and diseases that lead to diabetic nephropathy (n=3).	62
16: GO analysis illustrating down-regulated pathways and cellular processes in the aorta due to untreated hyperglycemia in comparison to controls	64
17: GO analysis illustrating up-regulated pathways and cellular processes in the aorta due to untreated hyperglycemia in comparison to controls	64
18: GO analysis illustrating down-regulated pathways and cellular processes in the aorta due to Insulin-treated hyperglycemia in comparison to untreated hyperglycemia	65
19: GO analysis illustrating up-regulated pathways and cellular processes in the aorta due to Insulin-treated hyperglycemia in comparison to untreated hyperglycemia	65
20: GO analysis illustrating down-regulated pathways and cellular processes in the renal cortex due to untreated hyperglycemia in comparison to controls	66
21: GO analysis illustrating up-regulated pathways and cellular processes in the renal cortex due to untreated hyperglycemia in comparison to controls	66
22: GO analysis illustrating down-regulated pathways and cellular processes in the renal cortex due to Insulin-treated hyperglycemia in comparison to untreated hyperglycemia	67
23: GO analysis illustrating up-regulated pathways and cellular processes in the renal cortex due to Insulin-treated hyperglycemia in comparison to untreated hyperglycemia	67

TABLES

Table	Page
1 - List of primers and their properties for target genes used for RTqPCR gene expression quantification	26
2 - List of primers and their properties for target genes used for MS-HRM PCR.....	29
3 - Fold change in gene expression by high glucose in vitro (n=3).....	35
4 - Effect of high glucose on DNA Methylation in VSMC (n=3), (p<0.05)	36
5 - Fold change in gene expression by hyperglycemia in vivo (n=3).....	38
6 - Effect of T1DM on DNA Methylation in VSMC (n=3), (p<0.05).....	39
7 - Protein Extraction Efficiency (n=3)	43
8 - Regulation of protein levels in aorta of T1DM rats in comparison to control rats (n=3)	45
9 - Regulation of protein levels in aorta of insulin-treated rats in comparison to T1DM rats (n=3).....	47
10 - Regulation of protein levels in aorta of insulin-treated rats in comparison to control rats (n=3).....	48
11 Regulation of protein levels in renal cortex of T1DM rats in comparison to controls (n=3)	49
12 - Regulation of protein levels in renal cortex of insulin-treated rats in comparison to T1DM rats (n=3).....	51
13 - Regulation of protein levels in renal cortex of insulin-treated rats in comparison to control rats (n=3)	52

ABBREVIATIONS

α -SM.....	Alpha Smooth Muscle
ACE.....	Angiotensin I converting enzyme
AGEs.....	Advanced glycation end products
AIFM1.....	Mitochondrial apoptosis-inducing factor
ANOVA.....	Analysis of Variance
ANXA1.....	Annexin A1
BK.....	Bradykinin
B1R.....	Bradykinin Receptor type 1
B2R.....	Bradykinin Receptor type 2
BDKRB1.....	gene for B1R
BDKRB2.....	gene for B2R
BSP.....	Bisulfite sequencing PCR
CKD.....	Chronic kidney disease
CTGF.....	Connective Tissue Growth Factor
CRP.....	C-Reactive Protein
CVD.....	Cardiovascular disease
DAG.....	Diacylglycerol
DM	Diabetes Mellitus
DMEM.....	Dulbecco's Modified Eagle Medium
DNMT.....	DNA methyltransferase
DTT.....	Dithiothreitol
ECM.....	Extracellular matrix
eNOS.....	Endothelial nitric oxide synthase

FBS..... Fetal Bovine Serum

FFPE..... Formalin fixed paraffin-embedded

FN1..... Fibronectin1

GDM..... Gestational diabetes mellitus

gDNA..... Genomic DNA

GNAI2..... Guanine nucleotide binding protein

GO..... Gene Ontology

H3K4me2..... Di-methylation of the lysine 4 residue on histone 3

Hmgb1..... High mobility group box 1

HMOX1..... Heme oxygenase 1

HMT..... Histone-lysine N-methyltransferase

IAA..... Iodoacetamide

IDF..... International Diabetes Federation

IL..... Interleukin

IPA..... Ingenuity Pathway Analysis

KKS..... Kinin-Kallikrein system

LC-MS/MS..... Liquid Chromatography-Tandem mass spectrometry

LRP2..... Low density lipoprotein receptor-related protein 2

MENA..... Middle East and North Africa

MCP1..... Monocyte chemoattractant protein-1

MI..... Myocardial infarction

MRM..... Multiple reaction monitoring

MS-HRM..... Methylation Sensitive-High Resolution Melting

NAC..... N-acetylcysteine

NFκB..... Nuclear factor κB

NO..... Nitric Oxide

Nox1..... NADPH Oxidase 1

Nox4..... NADPH Oxidase 4

PBS..... Phosphate buffer Solution

PCA..... Principal component analysis

PKC..... Protein Kinase C

PLC..... Phospholipase C

PTM..... Posttranscriptional modifications

PRDX..... Peroxiredoxin

Rac1..... Ras-related C3 botulinum toxin substrate 1

ROS..... Reactive oxygen species

RTqPCR..... Real-Time quantitative Polymerase Chain Reaction

SD..... Standard deviation

SE..... Standard error

S1PR..... Sphingosine-1 Phosphate Receptor

SphK1..... Sphingosine Kinase 1

STZ..... Streptozotocin

STRING..... Search Tool for the Retrieval of Interacting Genes/Proteins

Suv39h1..... Suppressor of variegation 3-9 homolog 1

T1DM Type-1 Diabetes Mellitus

T2DM Type-2 Diabetes Mellitus

TGF-β..... Transforming growth factor beta

Tm..... Melting temperature

TNF α Tumor Necrosis Factor alpha

VEC..... Vascular endothelial cells

VSMC..... Vascular smooth muscle cells

CHAPTER I

INTRODUCTION

Diabetes is a set of metabolic diseases that are characterized by chronic hyperglycemia. Several types exist including Type-1 Diabetes Mellitus (T1DM), Type-2 Diabetes Mellitus (T2DM), Gestational Diabetes Mellitus (GDM), and other subtypes. The International Diabetes Federation (IDF) estimates that Diabetes Mellitus (DM) currently affects 382 million people worldwide, projected to increase by 55% (592 million) in 2035. In the Middle East and North Africa (MENA) region, IDF estimates 34.6 million to have DM, with 67.9 million cases projected by 2035 [1].

T1DM, also termed insulin dependent diabetes mellitus, results from the impairment of the pancreatic beta cells that produce insulin by autoantibodies. Hence, a loss of insulin production leads to hyperglycemia and causes irreversible damage to blood vessels and highly vascularized organs. In the MENA region, 64 thousand children, up to 14 years of age, are affected, with 10,700 newly diagnosed cases per year. In terms of mortality, 367,700 total annual deaths in the MENA region are attributed to T1DM [1]. Furthermore, in the last two decades, an annual increase in the incidence of T1DM in children of around 3% has been reported worldwide [2], the highest rates of which are reported among children younger than 5 years of age [3]. Recent data indicate that among children diagnosed with T1DM at 10 years of age, the number of life-years lost is 18.7 for boys and 19.0 for girls [4], thus underscoring the burden of this disease. The causes of T1DM are diverse, but mainly include genetic predisposition and environmental stimuli that trigger autoimmunity. Other minor causes include ingestion of toxins or pharmacological agents that destroy the beta cells.

A. Clinical Studies

Observations from large-scale prospective clinical trials on diabetes have concluded that poor control of hyperglycemia at the early stages of diabetes would accelerate the incidence and progression of vascular complications, regardless of glycaemia control at later stages. These trials stress on the long-term benefit from early and tight glycemic control in the prevention from macrovascular and microvascular diabetic complication. In 1993, outcomes from The Diabetes Control and Complications Trial (DCCT) [5] and the Epidemiology of Diabetes Intervention and Complications (EDIC) [6] have proven that the primary modifiable risk factor of the long-term vascular complications of T1DM is hyperglycemia. Moreover, the development and progression of diabetic retinopathy, nephropathy, and neuropathy can be halted with intensive blood glucose lowering therapy, in addition to reducing the risk of cardiovascular disease in T1DM. More importantly, the phenomenon of metabolic memory was observed and defined as the benefits of early, intensive therapy versus conventional therapy in delaying the onset of vascular complications of T1DM [7].

The United Kingdom Prospective Diabetes Study (UKPDS) [8] had a unique feature which most other trials did not offer which was the recruitment of early onset newly diagnosed T2DM patients, which gave it the opportunity to verify the observation that early intensive treatment would prevent long-term vascular complications [9]. Indeed, in 1998, results showed that early intensive glucose control with metformin significantly reduced diabetes-related mortality and myocardial infarction (MI) compared with conventional treatment. Whereas early intensive treatment with sulfonylurea or insulin reduced any diabetes related end point by 12%, microvascular end points by 25%, retinopathy by 21%, albuminuria by 33%, and MI by 16% [10]. Similarly, results from the Steno Diabetes Study [11] showed that risk of cardiovascular

disease (CVD), nephropathy, and autonomic neuropathy were significantly lower by 53%, 58% and 63%, respectively, upon administering a target-driven, long-term, intensified treatment [12]. Outcomes from the Steno-2 Study, also on T2DM patients, noted a lower risk of CVD events and mortality, in addition to lower End Stage Renal Disease after implementing intensive multifactorial therapy [13].

In the last decade, numerous trials for assessment of efficacy of pharmacological agents in improving cardiovascular outcomes and control of hyperglycemia. These included the PROspective pioglitAzone Clinical Trial In macroVascular Events (PROACTIVE) in 2005 [14], the Action in Diabetes and Vascular disease: PreterAx and DiamicroN MR Controlled Evaluation (ADVANCE) in 2008 [15], the Action to Control CardiOvascular Risk in Diabetes (ACCORD) in 2008 [16], the Veterans Affairs Diabetes Trial (VADT) in 2008 [17], and the Rosiglitazone Evaluated for Cardiac Outcomes and Regulation of glycemia in Diabetes (RECORD) trial reported in 2009 [18]. Interesting outcomes from these trials suggested that aggressive treatment to patients with established vascular complications is counterproductive, as opposed to progressive incremental treatment to reduce hyperglycemia which, in turn, reduced the long-term complications [16].

B. Definitions of metabolic memory

There are several terms and definitions of metabolic memory that essentially mean the same thing, but give different perspectives on how to tackle the mechanisms of this phenomenon. It has been also called hyperglycemic memory, glycemic memory, legacy effect, metabolic imprint, and latent hyperglycemic damage [19]. It can be described as the progression of multiple organ vascular complications in diabetic patients after a period of exposure to metabolic derangement, including hyperglycemia.

According to the phenomenon, previous chronic exposure to hyperglycemia leads to delayed onset of long-term complications. It occurs as a result of poor control of hyperglycemia at the early stages of diabetes which would accelerate the incidence and progression of vascular complications, regardless of glycaemia control at later stages [20]. In other words, early intensive treatment would reduce the incidence and progression of vascular complications. Hence, early glycaemic intervention would have the greatest impact on halting the rate of progression of these diabetic complications [21]. On the molecular level, it can be explained as the persistence of the chronic inflammation and oxidative stress observed in vascular complications even after establishing tight glycaemic control [22]. This persistence in expression has been attributed to epigenetic mechanisms.

C. Epigenetic mechanisms

Epigenetics refers to changes that alter gene expression independent of changes in the sequence of DNA [23]. These changes persist following their induction and are maintained following cell division and are thus mitotically and/or meiotically heritable [24]. Several types of epigenetic regulation processes exist and can be categorized based on relative stability. For example, X chromosome inactivation is more stable than the dynamic acetylation of histone proteins. Epigenetic memory is a term that describes a sustained and transmissible change in gene expression or function that is induced by a previous environmental or developmental stimulus. Epigenetic mechanisms include genomic DNA methylation of CpG dinucleotides at the promoter region of genes, histone protein modifications, and variation in complexes responsible for chromatin remodeling, all of which fall under chromatin-based changes [25]. Other mechanisms include the dysregulation of short non-coding RNAs such as miRNAs that suppress

expression [23]. Propagation of DNA methylation marks mitotically and meiotically has been documented to occur through methylation of hemimethylated sites following DNA replication by maintenance DNA methyltransferase (DNMT) 1, whereas most histone tail modifications are not heritable the mechanism behind heritability of few of them is much less understood than DNA methylation [26].

D. Vascular complications in Diabetes

Chronic hyperglycemia is an independent risk factor for vascular complications [27] and T1DM is associated with long-term vascular complications [21]. It results in microvascular complications such as retinopathy, nephropathy, and neuropathy. It also results in macrovascular complications such as atherosclerosis, stroke, coronary heart disease, and peripheral vessel disease. Atherosclerosis is the primary complication leading to impaired life expectancy. It is an inflammatory disease that progressively damages and clots medium and large size vessels throughout the body.

1. Molecular pathways of vascular complications

Several clinical parameters and morbidities are taken into consideration when assessing the risk of atherosclerosis including the onset of diabetes and hypertension, and having elevated levels of oxidized low density lipoprotein (LDL), reactive oxygen species (ROS), and homocysteine, in addition to genetic factors [28]. The vascular tone is dictated by several factors including the vascular endothelial cells (VEC), which form the innermost layer of cells in the blood vessels. Under physiological conditions, VEC maintain the homeostasis of the vascular smooth muscle cells (VSMCs) to favor a vasoprotective state, primarily through the release of Nitric Oxide (NO), a potent endogenous vasodilator [29]. However, dysfunction of these cells due to pathological

states such as diabetes may cause injury to this layer and allow cells and vasoactive peptides in the blood to come in contact with VSMCs, often leading to vascular constriction, inflammation, migration and proliferation; the hallmarks of atherosclerosis [28; 30]. It is worth to note that NO also acts as a protective factor from these events. However, its production is impaired in diabetic conditions, thus allowing and exacerbating these complications [29; 31]. Moreover, experiments on rabbits showed that when exposed to hyperglycemia, the aorta no longer exhibits endothelium-dependent relaxation when treated with endothelium-derived vasoactive peptides such as acetylcholine or bradykinin (BK) [32]. In fact, BK has been shown to cause synthesis and release of NO from VEC, leading to vasodilation [33; 34]. However, BK causes vascular constriction and increased mitogenesis through increased intracellular calcium influx when it directly interacts with VSMC upon endothelial injury [35; 36]. BK is a 9-amino acid peptide that results from proteolytic cleavage of its kininogen precursor, high-molecular-weight kininogen (HMWK or HK), by the enzyme kallikrein. BK acts on its receptors BK B2 Receptor (B2R) and BK B1 Receptor (B1R) with less affinity, in an autocrine or paracrine fashion [37] to mediate numerous functions including regulation of local blood flow, stimulation of cell proliferation, and inflammatory responses [38].

Certain cell types do not exhibit a rapid decline in glucose transport rate during hyperglycemia compared to others. These cells are involved in vascular complications due to hyperglycemia [39; 40]. As a result, high glucose inside these cells activates numerous alternative intracellular pathways, four of which have been tightly associated with vascular complications. These include the polyol pathway whereby the aldose reductase enzyme reduces glucose to sorbitol, consuming all available NADPH. This in

turn increases the susceptibility of the cell to oxidative stress [41]. The second pathway involves the production of advanced glycation end products (AGEs) that modify the structure and function of receptors and mitochondrial proteins [42; 43] leading to increased oxidative stress and production of pro-inflammatory and sclerotic cytokines and growth factors [44], in addition to reduced mitochondrial function. AGEs also modify extracellular matrix molecules by cross-linking collagen and causing vascular stiffness [45], in addition to modifying circulating proteins [44]. Combined, these modifications lead to changes in transcription and cellular dysfunction [46]. In the third pathway, termed the hexosamine pathway, the glutamine:fructose-6 phosphate amidotransferase (GFAT) enzyme converts the glycolysis intermediate fructose-6 phosphate into Uridine diphosphate (UDP) N-acetyl glucosamine, which pathologically modifies gene transcription when it is added to the serine and threonine residues of transcription factors, contributing to cellular dysfunction [47]. Finally, the Protein Kinase C (PKC) pathway is activated through the increased synthesis of diacylglycerol (DAG) [48]. This leads to the activation of a variety of signals that contribute to oxidative stress, chronic inflammation, and vascular complications. In one signaling route, the increase in Transforming Growth Factor- β 1 (TGF- β 1) and Fibronectin 1 (FN1) contributes to capillary occlusion, a major event in microvascular complications. PKC isoforms also activate the transcription factor nuclear factor κ B (NF κ B), leading to overexpression of pro-inflammatory genes [49]. They also contribute to overexpression of *NAD(P)H oxidase* isoforms (*Nox*), that produce ROS [50], which have deleterious effects in vascular complications [51]. Although low levels of ROS are a vital part of the cell's defense mechanisms against foreign invaders, the excess production of ROS exceeds the capacity of cellular antioxidants defense [52] and activates pro-inflammatory molecules such as NF κ B in VSMCs [5355]. ROS has also been shown to

cause uncoupling of the endothelial nitric oxide synthase (eNOS) thus leading to a diminished NO production [56]. ROS can be induced by cytokines and growth factors such as Tumor Necrosis Factor alpha (TNF α) [57], the expression of which has been documented to be increased in diabetes [54; 58]. TNF α has also been found to increase expression of interleukin-1 β (IL-1 β), IL-6, MCSF, and MCP-1 in VSMC from T2DM mice [59].

2. Downstream pathway of the kinin receptors in diabetes

Another downstream effect of PKC activation is the increased expression of the B2R [60]. In fact, studies have shown that the binding of BK to B2R leads to G α_q -dependent activation of PKC leading to increased proliferation and migration of VSMC [36]. This occurs through activation of Phospholipase C (PLC) that leads to formation of DAG, which in turn activates PKC and the intracellular calcium influx [35; 61]. The kinin receptors are 7 transmembrane G-protein-coupled receptors (GPCRs) expressed on the cell surface [62; 63]. Their expression has been documented on VEC and VSMC of the aorta [64; 65] and studies have shown that they regulate the vascular tone, hypertension, and atherogenesis [66; 67]. While B2R is expressed constitutively on the cell surface, B1R expression is increased under pathological conditions [38]. It is believed that induction of B1R follows the inflammatory response by B2R and remains chronically active throughout the inflammatory phase [68; 69]. Knockout of *BK B2 Receptor gene (BDKRB2)* in mice has been shown to exacerbate hypertension [70], in addition to a marked increase in genes that contribute to end-stage renal disease, meaning that *BDKRB2* plays a protective role [71]. However, in diabetic nephropathy, diabetic B2R^{-/-} null mice are at less risk of developing proteinuria as they display reduced albumin excretion rate, and reduced glomerular and tubular injury compared to

diabetic B2R^{+/+} mice [72]. As for *BK B1 Receptor (BDKRB1)*, its deletion was found to ameliorate renal fibrosis, which could mean a role for it in mediating fibrosis [73]. In T1DM, the expression of *BDKRB1* and *BDKRB2* on the surface of retinal cells were found to be up-regulated in streptozotocin (STZ)-induced diabetic rats by 256% and 215% compared to controls, respectively [74]. In another study, exposure of mesenteric VEC to high glucose (25×10^{-3} mol/L) *in vitro* also showed a 450% increase in *BDKRB1* mRNA and protein expression levels [75]. Fibrosis in VSMCs has also been attributed to the binding of BK to its receptors, which was observed to lead to autocrine activation of TGF- β 1 [76]. In fact, studies have shown that in T1DM patients, increased synthesis and deposition of extracellular matrix (ECM) such as collagen I in plaque areas of the aorta was found to be induced by TGF- β [77]. This transformation leads to an impaired contractility of VSMC and a change into a synthetic proliferative state [78]. This process involves increased inflammation and is one of the very first events occurring in the pathophysiology of atherosclerosis [79]. Moreover, studies on patients with diabetic nephropathy showed increased expression of *Connective Tissue Growth Factor (CTGF)* as a result of demethylation of *CTGF* gene promoter region, allowing for increased transcription rate [80]. CTGF is a cysteine rich protein that enhances ECM production [81]. Studies have shown that TGF- β could induce the expression of *CTGF* in human aortic endothelial cells thus contributing to exacerbation of fibrosis in the hyperglycemic state [82].

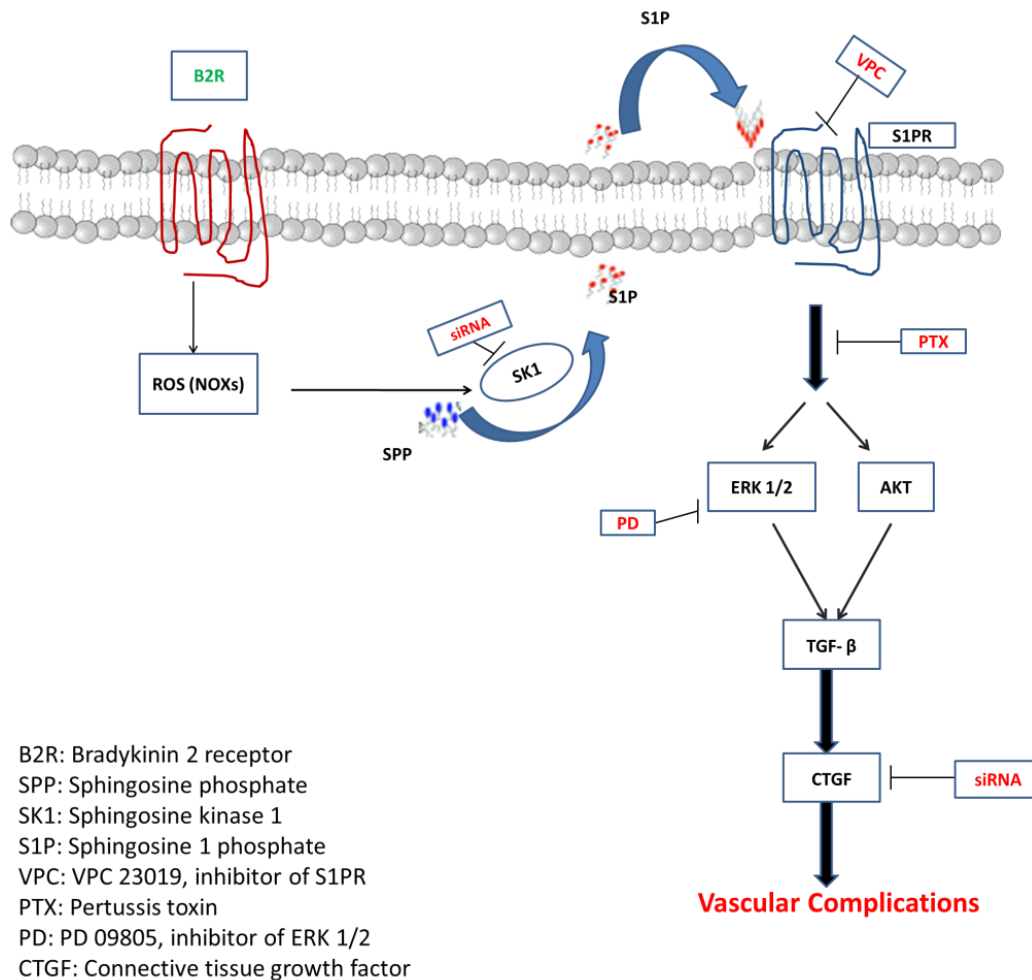


Figure 1: Cross - talk between BK B2 Receptor (B2R) and Sphingosine 1 Phosphate Receptor (S1PR)

Preliminary data from our laboratory have determined a definitive link between B2R activation and CTGF expression through crosstalk of B2R with Sphingosine-1 Phosphate Receptor (S1PR). The enzyme that links the two receptors is Sphingosine Kinase 1 (SphK1), and its inhibition using a scavenger of ROS called N-acetylcysteine (NAC) indicates that B2R activates this enzyme through generation of ROS. Moreover, our lab has established the link between B2R and ROS generation whereby treatment of rat podocytes with BK induced the expression of *Nox1* and *Nox4* (Unpublished data) (Figure 1).

3. Epigenetic regulation of gene expression in Diabetes Mellitus

Although numerous studies have linked genetic mutations and genetic factors to the pathophysiology behind diabetic complications, mounting evidence and reports suggest that environmental stimuli weigh in more than anticipated in determining the diabetic pathogenesis, and that the interplay between genetics and these stimuli produce the observed outcomes [83; 84]. Further evidence to this theory comes from research on aging whereby risk of developing T2DM increases with age due to the cumulative effect of genetic mutations, telomere shortening, and environmental stimuli. The platform on which both genetic and environmental stimuli exert their effects is the chromatin, where posttranscriptional modifications (PTMs) of histone tails and addition or removal of methyl groups from CpG sites occur. These modifications lead to changes in transcription rate of key genes involved in processes that lead to or prevent the complications [85].

Recent studies have demonstrated that several epigenetic mechanisms are involved in maintaining the phenomenon of metabolic memory by changing the expression level of key genes involved in vascular complications [23]. So far, research on epigenetic modifications in VEC and VSMC has been geared towards studying histone tail modifications and miRNAs.

a. Histone tail modifications in hyperglycemia

Increased expression of inflammatory genes such as interleukin 6 (IL-6) and monocyte chemoattractant protein-1 (MCP1) was noted in VSMC from T2DM mice and humans has been attributed to elevated di-methylation of the lysine 4 residue on histone 3 (H3K4me2), a histone activating mark [86] that renders DNA more accessible for transcription. Moreover, levels of a histone repressive mark, H3k9me3, were lower

in the promoters of these genes (Figure 2). The mechanism behind the decrease was attributed to lower protein levels of Suppressor of variegation 3-9 homolog 1 (Suv39h1), a histone-lysine N-methyltransferase (HMT) that methylates Lysine-9 of histone H3. The method by which these changes become heritable is that Suv39h1 has been found to interact with DNMT 1 and DNMT 3A disrupting their function, suggesting a possible variation in DNA methylation levels [87]. All these marks are correlated with a more open chromatin and higher transcriptional activity. The sustained decrease levels of H3K9me3 and Suv39h1 occupancy at the promoter region of these genes can also be induced by $TNF\alpha$ [59].

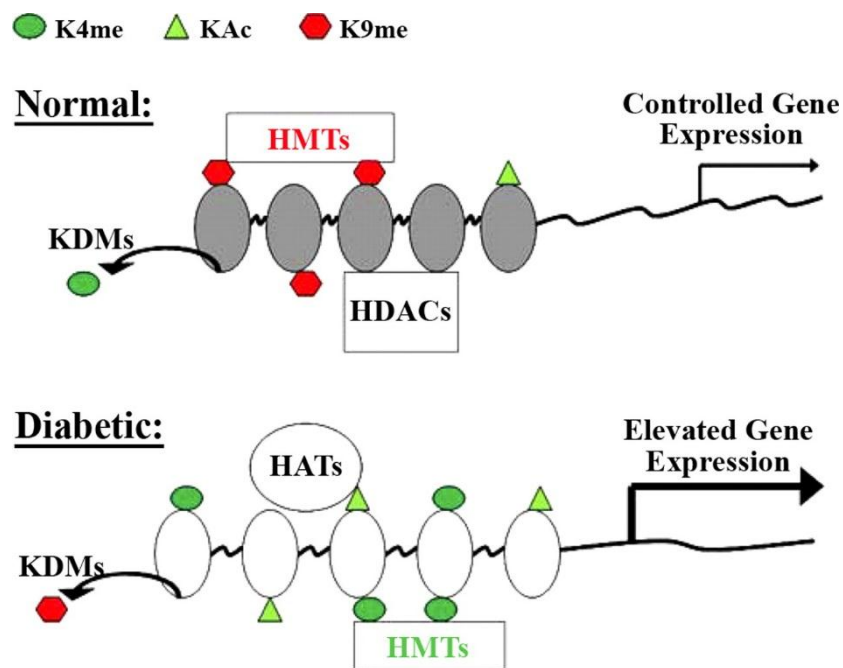


Figure 2: Mechanisms of histone tail modifications observed in diabetes *via* posttranslational modifications on the N-terminal histone tails. Chromatin modifiers include Histone lysine methyltransferases (HMTs) and lysine demethylases (KDMs) which regulate histone lysine methylation (Kme), while histone acetyltransferases (HATs) and histone deacetylases (HDACs) control histone acetylation (Ac) [85].

In human microvascular endothelial cells, H3K4m1 levels increased in the promoter region of NF- κ B-p65 gene leading to its increased expression and downstream

inflammatory process [88]. Similar studies on normal human VSMC that were transiently exposed to high glucose demonstrated similar histone modifications, proving yet again the persistence of the epigenetic dysregulation and further evidence in favor of metabolic memory [59]. The interesting finding from this study is that even short-term exposure to hyperglycemia causes persisting chromatin modifications, especially on promoter regions of inflammatory genes such as NF- κ B p65 subunit, MCP-1, and vascular cell adhesion molecule-1 (VCAM-1). A noteworthy report revealed that inhibiting ROS production such as mitochondrial superoxide production by overexpressing manganese superoxide dismutase would prevent these histone tail modifications [20].

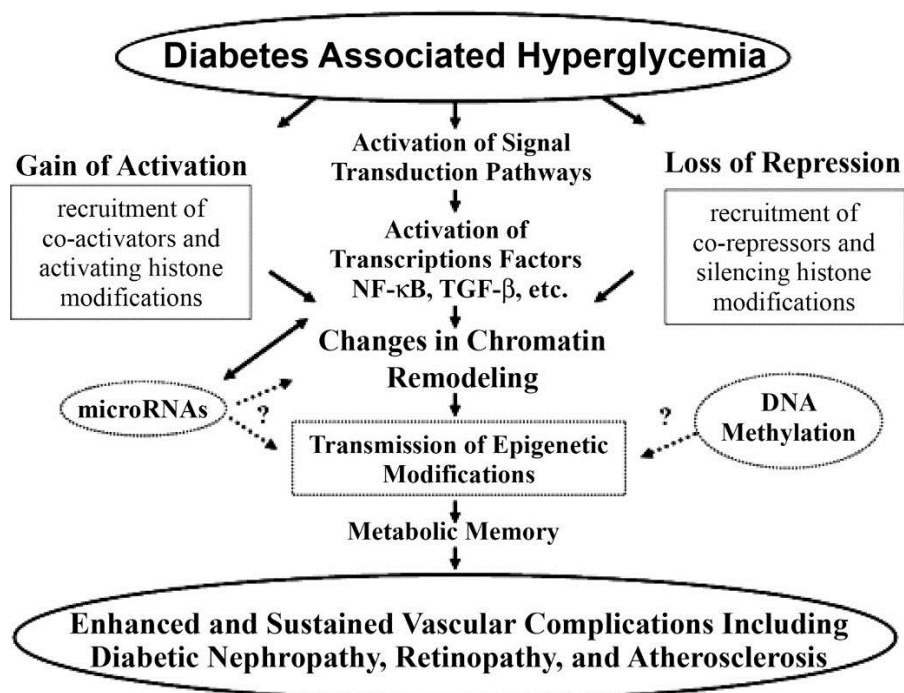


Figure 3: Activated epigenetic mechanisms by hyperglycemia and persistence of vascular complications [85].

b. MicroRNAs in hyperglycemia

MicroRNAs (miRNAs) are short (22 nucleotide long) noncoding RNA that are involved in the posttranscriptional regulation of gene expression. They down regulate gene expression through inhibiting translation of messenger RNA (mRNA) gene transcripts and promoting their degradation. They negatively regulate signaling molecules and transcription factors, in addition to targeting chromatin-modifying enzymes, resulting in epigenetic modifications.

Their role in diabetes has been recently documented. One study found that increased levels of microRNA-125b in VSMCs of T2DM Mice lead to increased inflammatory gene expression by a decrease in repressive histone H3 lysine-9 trimethylation (H3K9me3). The study concluded that this was achieved by targeting Suv39h1 [89]. Hyperglycemia also up regulates miR-377 and miR-29a that have been shown to induce FN1, and collagen IV production, respectively, leading to ECM deposition and fibrosis [90; 91]. Another study explored the role miR-200 family members in inhibiting a transcriptional repressor, Zeb1, thus allowing increased expression of inflammatory genes cyclooxygenase-2 and MCP-1 [92].

c. DNA methylation in hyperglycemia

The presence of methyl groups at promoter CpG islands leads to recruitment of proteins that inhibit transcription and hence gene repression. In cancer, there is strong evidence that suppression of tumor suppressor genes results from DNA hypermethylation and leads to cancer [93]. In diabetes, however, few studies have studied DNA methylation of key genes involved in diabetic complications. Rather, in developmental studies, a recent report suggested that insulin expression is controlled at the promoter region by DNA methylation whereby embryonic stem cells that do not

excrete insulin shown hypermethylation at the promoter. They only become insulin producing cells after these cells differentiate into pancreatic cells and are demethylated at the insulin promoter [94]. Another study focused on intrauterine growth retardation in rats and found that the transcription factor Pdx1, which regulates insulin gene expression and beta cell differentiation, is silenced by both histone tail modifications and DNA methylation [95].

In a recent study on epigenetic signatures of primary VEC exposed to hyperglycemia, a genome wide analysis was conducted to describe H3K9/K14 hyperacetylation and DNA methylation using Chromatin Immunoprecipitation and CpG methylation assays, respectively [96]. The study concluded that several genes linked to cardiovascular disease, endocrine regulation, and diabetes were up-regulated using gene ontology (GO) softwares such as Ingenuity pathway analysis and GO annotations. Of interest to the pathway discussed in our study, a gene set was identified that was associated with regulation of NF κ B, possibly leading to overexpression of pro-inflammatory genes [49]. Moreover, this study suggested that hyperglycemia causes both DNA hypomethylation and H3K9/K14 hyperacetylation, a gene-activating epigenetic mark, leading to increased expression of the associated set of genes which include heme oxygenase 1 (HMOX1), known for activating interleukin-10 (IL-10) and conferring anti-inflammatory activity. However, no studies have looked at the DNA methylation status of key genes in VSMC involved in vascular complications in T1DM. Interestingly, hyperglycemia also increased the expression of interleukin-8 (IL-8) and MCP-1, well-known pro-inflammatory mediators [96].

Moreover, the relationship between chronic kidney disease (CKD) and increased risk of CVD [97] involves excess homocysteine levels in CKD that lead to

inhibition of DNMTs, which in turn elicits global DNA hypomethylation and increased inflammation in VEC [98; 99]. In peripheral blood leukocytes, however, increased homocysteine levels in CKD lead to global DNA hypermethylation associated with inflammation and increased mortality [100]. Moreover, increased homocysteine levels in the blood are associated with inhibition of endothelial growth [101] and exacerbated atherogenesis [98; 102].

Overall, these studies prove that previous exposure to hyperglycemia activates epigenetic changes in key genes, causing long-lasting alterations in gene expression levels that lead to micro- and macrovascular complications (Figure 3). However, no studies have looked at the DNA methylation status of pro-inflammatory genes in VSMC involved in vascular complications in T1DM.

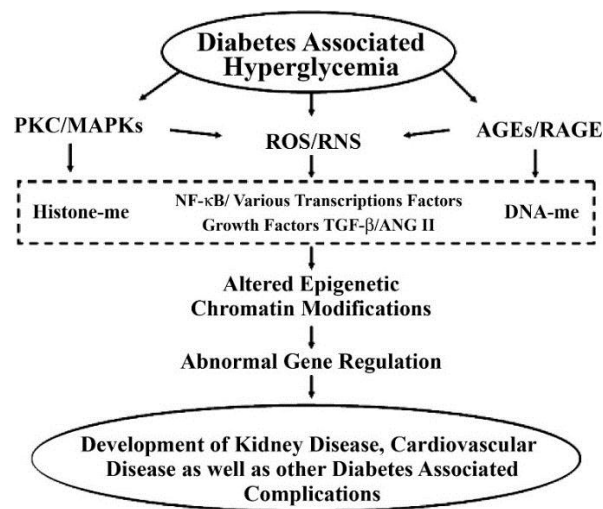


Figure 4: Hyperglycemia activates several pathways leading to diabetic complications, these pathways include PKC, MAPKs, ROS, and AGE formation. These pathways lead to histone tail modifications and altered DNA methylation in downstream genes [85].

CHAPTER II

RATIONAL AND AIMS

So far, research on epigenetic modifications in VSMCs have been limited to studying the mechanisms behind histone tail modifications and miRNAs. No studies, however, have looked at the DNA methylation status of key genes in VSMC involved in vascular complications in T1DM. Many examples exist regarding a coordinated effect between DNA methylation and histone tail modifications synergistically leading to overexpression of epigenetically regulated genes [103106], which warrants the quest towards studying DNA methylation profile of these genes. Accordingly, we aim to attribute the overexpression of target genes involved in oxidative stress, inflammation, fibrosis, and the kinin-kallikrein system, in part, to DNA hypomethylation of CpG islands in promoter regions of these genes in VSMC in T1DM. Genes of interest include *BDKRB1*, *BDKRB2*, *CTGF*, *FN1*, *C-reactive protein (CRP)*, *IL-1 β* , *IL-6*, *IL-10*, *TGF- β 1*, *TGF- β 2*, *TNF α* , *Nox1*, *Nox4*, and *SphK1*. This will be accomplished through examining the effects of hyperglycemia *in vivo* and high glucose *in vitro* on:

- 1- The mRNA expression level of the aforementioned genes in VSMC using Real-Time quantitative Polymerase Chain Reaction (RTqPCR).
- 2- The alteration of DNA methylation level in promoter regions Methylation Sensitive-High Resolution Melting (MS-HRM) PCR amplification of bisulfite converted DNA.
- 3- Assess the effect of metabolic memory on persistence of DNA methylation

Moreover, diabetic nephropathy has been correlated to increased risk of cardiovascular disease and atherosclerosis. Hence, studying molecular pathways dysregulated in both tissues is warranted. Accordingly, we also aim to:

- 4- Examine the effects of hyperglycemia *in vivo* and high glucose *in vitro* on the global protein expression level in aorta and kidney (renal cortex) tissue using Liquid Chromatography-Tandem Mass Spectrometry (LC-MS/MS) to complement the results of epigenetic and gene expression studies on the aorta and find common pathways dysregulated in both tissues.

CHAPTER III

MATERIALS AND METHODS

A. Materials

Company	Item
Abbott Laboratories Ltd., Kent, UK	Forane (isoflurane)
Abcam Inc (Cambridge, MA, USA)	Anti-mouse conjugated to Alexa fluor
AMRESCO Inc. (Solon, OH, USA)	D-glucose, HEPES, and sodium chloride
Applied Biosystems, Inc. (Foster City, CA, USA)	MeltDoctor™ HRM Master Mix kit, The Cells-to-CpG™ Bisulfite Conversion Kit, Cells-to-CpG™ Bisulfite Conversion & Quantitation Control Kit, Methyl Primer Express® Software
BioRad (Hercules, CA, USA)	iQ™ SYBR® Green Supermix, iScript™ cDNA Synthesis, Multiplate Low-Profile 96-Well PCR Plates, iCycler iQ™ Real-Time PCR, CFX96 PCR, Tris
Corning	All Plasticware for Cell Culture
Electron Microscopy Sciences	Fluoro-Gel II with Dapi
Eli Lilly and company (Indianapolis, IN)	HUMULIN N
Fisher Scientific (London, UK)	Formaldehyde and ethylene diamine tetraacetate (EDTA)
J.T.Baker (Phillipsburg, NJ)	HPLC grade acetonitrile
Mallinckrodt Chemicals (Phillipsburg, NJ)	HPLC grade water
Molecular Probes	SYBR® Safe DNA gel stain
Promega (Madison, WI)	Trypsin gold, mass spectrometry grade
QIAGEN, Hilden, Germany	QIAamp DNA Mini Kit
Santa Cruz Biotechnology (CA, USA)	Rabbit Anti-PECAM-1 antibody
Sigma-Aldrich (St. Louis, MO, USA)	Mannitol, Collagenase A, Streptozotocin, Mouse Monoclonal Anti- α Smooth Muscle Actin antibody, Sodium citrate dehydrate, Phosphate buffer Solution (PBS) containing Ca^{2+}/Mg^{2+} , Pharmacologic agent (+/-) methamphetamine hydrochloride, dithiothreitol (DTT), iodoacetamide (IAA), ammonium bicarbonate and MS-grade formic acid, Heat-inactivated Fetal Bovine Serum (FBS), Dulbecco's Modified Eagle Medium (DMEM), penicillin, streptomycin, L-glutamine, and trypsin
Thermo Scientific (Rockford, IL).	Urea
TIB Molbiol (Berlin, Germany)	PCR primers
UniChem (Mumbai, India)	Chloroform and Isopropanol

B. Methods

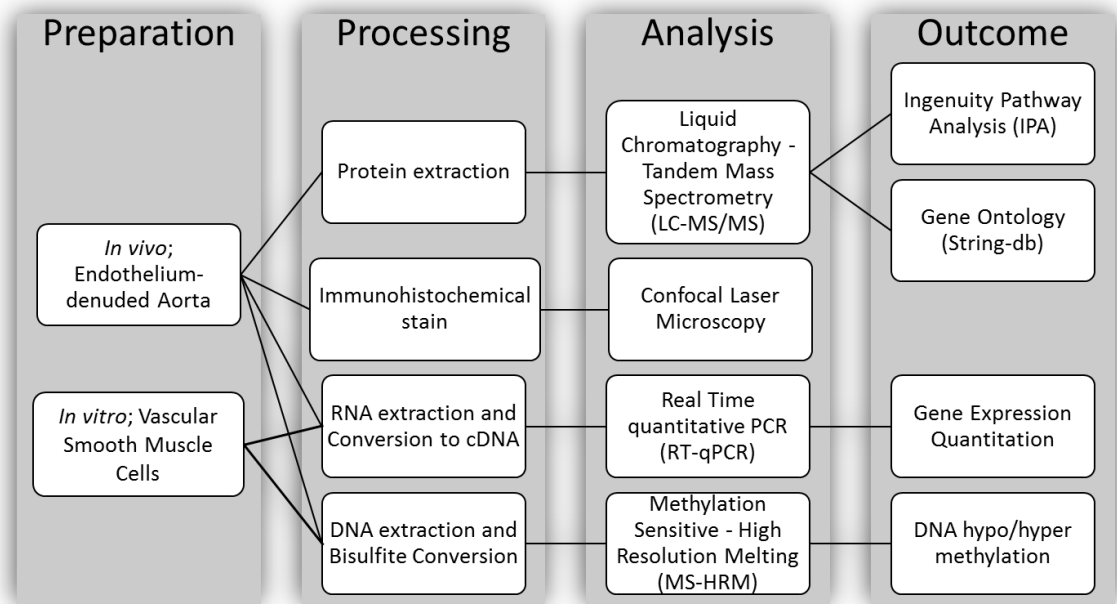


Figure 5 - *in vivo* and *in vitro* methods scheme on endothelium-denuded aorta and VSMC

1. *In vitro* Studies: Effect of high glucose on VSMC

a. *In vitro* Sample Preparation and Treatment (Cell Culture)

Primary rat VSMC were obtained from one healthy male Sprague-Dawley rat that was aged 60 days and weighed 150 g. Rat aorta tissue was acquired as explained but was directly processed by performing tissue explant. After dissection, the tissue was cleared from blood with PBS containing $\text{Ca}^{2+}/\text{Mg}^{2+}$ and cut longitudinally and incubated in 3-5ml collagenase A solution (dilution 1:20) for 1h, 37°C in a shaking water-bath followed by removal of the adventitia and endothelium with bent-head forceps. The aorta was grinded into fine pieces using forceps and transferred into T75-flasks with DMEM media containing 1 g/L glucose, 10% FBS, 1% penicillin, 1% streptomycin, 20 mM HEPES (pH 7) and 1% L-glutamine. The flasks were placed at 37°C and 5% CO₂ incubator for 10-7 days to allow adherence and growth of cells. Cells were used at passage 4 where they were transferred into T75-flasks with starvation DMEM media

containing 1 g/L glucose, 0% FBS, 1% penicillin, 1% streptomycin, 20 mM HEPES (pH 7) and 1% L-glutamine for 24 hours. This was followed by transfer into four 6-well plates with 2 ml treatment DMEM media per well containing 1 g/L glucose, 0.5% FBS, 1% penicillin, 1% streptomycin, 20 mM HEPES (pH 7) and 1% L-glutamine. Each plate had 2 wells treated with 25 mM D-glucose and 2 other wells with 25 mM mannitol as osmotic control, and 2 control wells left untreated. At day 1, the cells were treated and placed at 37°C and 5% CO₂ incubator for 7 days. At day 8, media was aspirated with Pasteur pipettes connected to vacuum suction pump. Then 2 ml of warm (37°C) treatment DMEM media cells was added per well followed by glucose and mannitol treatment. This was repeated for day 15 and day 22. At day 28, cells were removed from culture plates for DNA and RNA isolation.

b. RNA Isolation

RNA was isolated from VSMCs using GenElute kit as per the manufacturer's protocol. Briefly, 250 µl of cell lysis solution containing β-mercapto-ethanol was added to cells, followed by Cell scraping and transfer into 1.5 ml tubes. Using designated buffers and enzymes the solution is filtered in columns and washed. Then RNA was eluted with 50 µl Elution buffer and stored at - 80°C.

c. DNA Isolation

DNA was isolated from VMSCc using QIAamp DNA Mini Kit as per the manufacturer's protocol. Briefly, 200 µl PBS with Ca²⁺ and Mg²⁺ was added to cells, followed by Cell scraping and transfer into 1.5 ml tubes. Using designated buffers and

enzymes the cells are lysed and the solution is filtered in columns and washed. Then DNA was eluted with 50 µl Elution buffer and stored at - 80°C.

2. In vivo Studies: Effect of hyperglycemia on VSMCs

a. In vivo Laboratory Animal Handling and Treatment

All animal experiments were approved by and conducted in accordance with the guidelines of the Animal Care Facility and Institutional Animal Care and Use Committee (IACUC) at the American University of Beirut by trained and certified personnel. Rats were kept under standard condition throughout the study period, which included constant access to water and standard rat chow, at ambient room temperature, under a cycle of 12 hours light-12 hours dark. A T1DM model was induced with a non-specific cytotoxic pharmacologic agent STZ in 10 male Sprague-Dawley rats over a period of 6 weeks. STZ destroys the insulin-producing β -cells of the pancreas, thus simulating insulin dependent diabetes [107]. All experiments were performed using 15 male Sprague-Dawley rats that were aged 60 days and weighed between 250 and 275 g at day 0. STZ was dissolved in Citrate buffer (vehicle). After brief anesthesia with Forane (isoflurane), 10 rats were intravenously injected through the tail-vein with 65 mg STZ per kg of body weight once on day 0, while 5 control rats received physiological Citrate buffer injections through the tail-vein as well. 2 weeks post-intravenous injection, 5 out of the 10 T1DM rats received subcutaneous insulin (HUMULIN N) injections twice daily (total 6 Units) for 4 weeks while the other 5 T1DM rats and 5 controls received subcutaneous saline (vehicle) injections. Accordingly, rats were divided into controls, diabetic, diabetic under insulin treatment starting at day 14. The weight and blood glucose of each rat was measured weekly, except for insulin-treated rats who blood glucose was measured daily.

b. Collection of rat aorta tissues

After 6 weeks, all rats were euthanized by carbon dioxide (CO₂) followed by cervical dislocation. Rat aorta tissue was acquired using a published method [108]. Briefly, a midline incision and opening of the peritoneum was followed by displacement of intestines to expose the posterior abdominal wall. The aorta was cut from the level of the left renal artery to its bifurcation at the aortic arch. Aorta samples were placed under a biosafety cabinet in Phosphate buffer Solution (PBS) containing Ca²⁺/Mg² to be cleaned from blood and endothelium-denuded with bent-head forceps. This was followed by further washing with PBS, snap-freeze in liquid nitrogen, and storage at -80 °C for further processing.

c. Immunohistochemistry

To confirm that the origin of the extracted DNA, RNA, and proteins is from VSMC only, the formalin fixed paraffin-embedded (FFPE) endothelium-denuded aorta tissues of the control and T1DM rats and were stained with specific anti-rat antibodies. anti-PECAM-1 antibody was used as negative control antibodies to confirm that visualized cells were not VEC whereas anti- α Smooth Muscle Actin (α -SMA) antibody was used as a positive control antibody to confirm that visualized cells are VSMCs. The tissue section was mounted with Fluoro-Gel II with Dapi to stain nucleic acids blue.

d. RNA and DNA Isolation

Frozen rat aorta tissues were homogenized by grinding with mortar and pestle immersed in liquid nitrogen and transferred to 2 ml microcentrifuge tubes containing 1 ml RiboZol RNA Extraction reagent. Phase separation by centrifugation at 12000 g for

15 min at 4°C resulted in a top colorless layer containing pure RNA. This layer was transferred into a new 1.5 ml microcentrifuge tube to perform RNA precipitation with isopropanol. This was followed by washing with 75% ethanol, air drying, and reconstituting with 30 µl deionized water. The middle white layer that remained in the RiboZol/chloroform solution contains DNA. This was transferred into a new 1.5 ml microcentrifuge tube to perform DNA precipitation with ethanol/phenol mixture. This was followed by washing with Sodium Citrate/10% ethanol solution and 75% ethanol solution, air drying, and reconstituting with 100 µl deionized water. RNA and DNA samples were stored at - 80°C until further processing.

e. Extraction and tryptic digestion of proteins

Frozen rat aorta tissues that were sent to Dr. Yahia Mechref's Laboratory in Texas Tech University USA were processed as follows:

“Tissues were homogenized using VWR® Disposable Pellet Mixers (VWR International, Radnor, PA) in 500-µL extraction buffer (5M urea, 40mM Tris, 0.2%w/v CHAPS). Next, the samples were sonicated for 1 hour at 4°C prior to centrifugation for 45 min at 14,800 rpm with the centrifuge held at 4°C. The supernatant was then collected in separate containers. The buffer of the extracted protein was exchanged into 50 mM ammonium bicarbonate using 5kDa MWCO spin concentrators (Agilent Technologies, Santa Clara, CA). This buffer is needed for efficient tryptic digestion.

A 10-µg aliquot of each sample, determined by BCA protein assay (Thermo Scientific/Pierce, Rockford, IL), was diluted to 20-µL by 50 mM ammonium bicarbonate. Thermal denaturation was performed at 65°C for 10 min. A 0.75-µL aliquot of 200 mM DTT was added to reduce the sample at 60°C for 45 min. A 3-µL aliquot of 200 mM IAA was added to alkylate the sample at 37.5°C for 45 min in the

dark. Excess IAA was consumed by the addition of another 0.75- μ L aliquot of 200 mM DTT and incubation at 37.5 $^{\circ}$ C for 30 min. The tryptic digestion was performed at 37.5 $^{\circ}$ C for 18 hours followed by microwave digestion at 45 $^{\circ}$ C and 50W for 30 min. A 0.5- μ L aliquot of neat formic acid was added to quench the digestion. Finally, a 3- μ L aliquot of 5 ng/ μ L reduced and permethylated dextran was added to each sample as internal standard to offset any potential injection variance.”

3. Reverse Transcriptase Conversion of mRNA to cDNA

iScript™ cDNA Synthesis kit was used to convert isolated mRNA to cDNA to be followed by RTqPCR. The procedure was done according to the manufacturer’s protocol. Briefly, 1 μ g of total mRNA was mixed with 5X RT buffer, deionized water, mRNA, and iScript reverse transcriptase and run on iCycler iQ™ Real-Time PCR Detection System according to the following program:

Temperature	Time
25 $^{\circ}$ C	5 minutes
45 $^{\circ}$ C	30 minutes
85 $^{\circ}$ C	5 minutes
4 $^{\circ}$ C	Hold

4. RTqPCR Primer Design

The primers were designed using the Primer Blast tool in the NCBI database. Table 1 contains a list of primers used for the amplification of coding region of target genes.

Table 1 - List of primers and their properties for target genes used for RTqPCR gene expression quantification

Gene	Accession Number		Sequence (5'→3')	Primer Length	Tm	Product length
<i>BDKRB1</i>	NM_030851.1	F	5'-GCGACGGCAA GCCCAAGCTA-3'	20	60.0	147
		R	5'-TGCCAAGCCTC GTGGGGGAA-3'	20	60.4	
<i>BDKRB2</i>	NM_173100.1	F	5'-GCTTGGCGTGCT GTCGGGAT-3'	20	60.0	130
		R	5'-TCGGAAGCGCTTG CCCACAA-3'	20	59.6	
<i>CTGF</i>	NM_022266.2	F	5'-CCCCCGCCAACCG CAAGATT-3'	20	60.0	135
		R	5'-CGGCCCATCCAG GCAAGTG-3'	20	60.0	
<i>FNI</i>	NM_019143.2	F	5'-CCACAGCCATTCC TGCGCCA -3'	20	60.0	114
		R	5'-TCACCCGCACTCG GTAGCCA-3'	20	59.9	
<i>Nox1</i>	NM_053683.1	F	5'-ATAGCTACTGCCCA CCCCAAGT-3'	22	63.2	97
		R	5'-TTGAGTACCGC CGACAGCA-3'	19	61.6	
<i>Nox4</i>	NM_053524.1	F	5'-GAACCTCAACTG CAGCCTGATC -3'	22	61.5	111
		R	5'-CTTTTGTCCAACA ATCTTCTTGTTCTC-3'	27	59.6	
<i>IL-6</i>	NM_012589.2	F	5'-CACTTCACAAGTCG GAGGCT-3'	20	60.0	114
		R	5'-TCTGACAGTGCAT CATCGCT-3'	20	59.5	
<i>TNF α</i>	NM_012675.3	F	5'-ACCTTATCTACTCC CAGTTTCT-3'	22	57.4	108
		R	5'-GGCTGACTTTCT CCTGGTATG-3'	21	58.1	
<i>IL-1β</i>	NM_031512.2	F	5'TCCTCTGTGACTC GTGGGAT -3'	20	60.0	109
		R	5'-TCAGACAGCAC GAGGCATTT-3'	20	60.0	
<i>CRP</i>	NM_017096.3	F	5'-GGCTTTGACGCG AATCAGTC -3'	20	59.9	134
		R	5'-GCCCCGCCAGTTC AAAACATT -3'	20	60.0	
<i>IL10</i>	NM_012854.2	F	5'-CCTCTGGATACAG CTGCGAC-3'	20	60.3	122
		R	5'-TCATGGCCTTGTAGA CACCTT-3'	21	59.0	
<i>TGF-β1</i>	NM_021578.2	F	5'-CTGAACCAAGGAG ACGGAATAC -3'	22	58.5	106
		R	5'-GTTTGGGACTGATCC CATTGA -3'	21	57.9	

TGF-β2	NM_031131.1	F	5'-CCATACAGTCCCA GGTGCTC-3'	20	59.8	150
		R	5'-GCAAGCGAAAGAC CCTGAAC-3'	20	59.8	
SphK1	NM_133386.3	F	5'- AGCATATGGACCTC GACTGC -3'	20	59.6	85
		R	5'- AACACTCCCCTCTG GTT CCT-3'	20	60.1	
GAPDH	NM_017008.3	F	5'-GGGGCTCTCTGCTC CTCCCTG-3'	21	60.0	107
		R	5'-CGGCCAAATCCGTT CACACCG-3'	21	59.0	

F: Forward primer; R: Reverse primer; Tm: Melting Temperature.

5. Gene Expression Quantitation by RTqPCR

iQ™ SYBR® Green Supermix was used to amplify and quantitate the expression of target genes according to the manufacturer's protocol. Briefly, iQ SYBRGreen supermix, deionized water, Forward and Reverse primers (10 μ M), and cDNA samples were added to each well in 96-well plates and were run on iCycler iQ™ Real-Time PCR Detection System according to the following program:

Temperature		Time
95°C		5 minutes
40 cycles	95°C	9 seconds
	57-63°C (depending on primer melt temperature)	12 seconds
	72°C	9 seconds
4°C		Hold

6. DNA Methylation Studies

a. Bisulfite Conversion

The Cells-to-CpG™ Bisulfite Conversion Kit was used to perform direct and fast conversion of unmethylated cytosines to uracil in isolated genomic DNA (gDNA) and prepared methylated standards according to the manufacturer's protocol. The Cells-to-CpG™ Bisulfite Conversion & Quantitation Control Kit was used simultaneously

with the conversion kit for quality control and quantitation purposes. Briefly, 45 µl of denaturation reagent was added to both rat gDNA and the Control Unconverted gDNA and incubated at 50°C for 10 minutes. Then, 100 µl freshly prepared conversion reagent was added to the mixture and tubes were run in iCycler PCR according to the following program:

Temperature	Time
65°C	30 minutes
95°C	1.5 minutes
65°C	30 minutes
95°C	1.5 minutes
65°C	30 minutes
4°C	Hold up to 4 hours

After conversion, the DNA was desalted, desulfonated, and washed to remove salts and sulfonic groups from the DNA samples. Then 40 µl elution buffer was passed through column to retrieve the purified DNA.

Bisulfite conversion was followed by an assessment of the yield and quality of the bisulfite-converted DNA using the Cells-to-CpG™ Bisulfite Conversion and Quantitation Control Kit according to the manufacturer's protocol. Briefly, real-time qPCR was performed on selected samples and controls from the kit to determine the amount of unconverted gDNA using 20x Non-Conversion Control Primer Mix, and the amount of converted human gDNA using 20x Conversion Control Primer Mix. Using the Ct values resulting from real-time qPCR, the efficiency of bisulfite conversion was determined using the following formula:

$$\text{Conversion efficiency} = \left(\frac{2^{(-\Delta C_T + 1)}}{2^{(-\Delta C_T + 1)} + 1} \right) \times 100 \quad \text{Equation 1}$$

b. Bisulfite Specific Primer Design

The Methprimer online software [109] and Methyl Primer Express® Software were used to design and verify methylation primers for bisulfite sequencing PCR (BSP) based on a specific set of criteria that take into account changes in DNA due to bisulfite treatment. Other criteria taken into account include specificity, binding stability, self-annealing, self-end annealing, pair complementarity, melting temperature (T_m) difference between left and right primers, and maximal allowable length of a mononucleotide repeat in primer sequence. The softwares also have a CpG island prediction feature based on the GC content and the observed/expected (obs/exp) CpG dinucleotide ratio of the promoter sequence [109]. Criteria for a CpG island include a 200 Bp DNA stretch, that has a GC content >50% and an obs/exp ratio >0.6 [110].

Table 2 - List of primers and their properties for target genes used for MS-HRM PCR

Gene	Accession Number		Sequence (5'→3')	Primer Length	T _m	Product length
<i>BDKRB1</i>	NM_030851.1	F	5'- TGTTTTTTTTGA GTTAGGTTTAGG -3'	25	55	194
		R	5'- CAACCAAAAATCC ATCAATATAAAC -3'	25	54	
<i>BDKRB2</i>	NM_173100.1	F	5'- TGGGAGAGTTTG GTTTTTAAAGTTA-3'	25	66	201
		R	5'-ATCTTCACACTT TCCAAAACCTCC-3'	25	68	
<i>TNF α</i>	NM_012675.3	F	5'- TGTGAGATGTG TTGTAATTAAGA -3'	25	56	152
		R	5'- AATAAACTCAACC CTAAAATTCAC -3'	25	56	
<i>TGF-β2</i>	NM_031131.1	F	5'- TTGGAGGTTGGTT TTTTTTGTAG -3'	23	60	296
		R	5'- ACTAAACCCTACC TTCCACAC -3'	21	55	

c. Preparation of Methylation Standards

Methylated and unmethylated DNA standards were prepared from control rat genomic DNA that was amplified by qPCR using iQ™ SYBR® Green Supermix. This was followed by DNA Gel purification and extraction using GenElute™ Gel Extraction Kit. Finally, 2 µl from purified DNA was completely methylated using CpG Methyltransferase (M.SssI) kit.

d. Methylation Sensitive-High Resolution Melting (MS-HRM) PCR

HRM methylation studies were performed using MeltDoctor™ HRM Master Mix kit according to the manufacturer's protocol to determine the percentage of methylated DNA in unknown samples in comparison to the prepared standards. Briefly, real-time PCR was performed in a total reaction mixture of 20 µl containing 10 µl of MeltDoctor HRM Master Mix from, 1.2 µl of each primer (0.3 µM), approximately 1 ng/µl of genomic DNA and sterile deionized water on CFX96 PCR according to the following program:

Temperature		Time
95°C		10 minutes
40 cycles	95°C	15 seconds
	60-66°C (depending on primer melt temperature)	1 minute
Melt Curve/ dissociation	95°C (Denature)	15 seconds
	60°C (Anneal)	1 minute
	95°C (High Resolution Melting)	9 seconds
	60°C (Anneal)	15 seconds
4°C (Hold)		10 minutes

Genomic DNA of positive controls (standards) and Non-Template Control (NTC) samples without DNA were included in each PCR run. Different ratios of 100% methylated and 0% methylated DNA of equal concentration were mixed to obtain a

standard curve from which the % methylation of unknown samples can be calculated. The ratios used were 100%, 25%, 10%, 5%, 1%, and 0% as the expected variability was hypomethylation. Following real-time PCR, a Melt Curve program in the same real-time PCR machine immediately started amplicon dissociation. In this process, the PCR amplicons were allowed to denature and re-anneal before the high resolution melting recording changes in fluorescence with changes in temperature (-dRFU)/dT as a function of increasing temperature. The high resolution melting curve profile was then analyzed using Bio-Rad precision Melt Analysis software with fluorescence normalization by selecting the linear region before and after the melting transition. T_m was inferred from the normalized data as the temperature at 50% fluorescence. Differences in methylation levels were distinguished by plotting the fluorescence difference between normalized melting curves. All samples and standards were examined in triplicates to obtain the standard deviation (SD) for the T_m .

7. Global Proteomics analysis

a. Liquid Chromatography-Tandem mass spectrometry (LC-MS/MS) assay

Extracted protein samples by Dr. Yahia Mechref's Laboratory in Texas Tech University USA were processed by LC-MS/MS for global proteomics study as follows:

“LC-MS/MS was acquired using Dionex 3000 Ultimate nano-LC system (Dionex, Sunnyvale, CA) interfaced to LTQ Orbitrap Velos and TSQ Vantage mass spectrometers (Thermo Scientific, San Jose, CA) equipped with nano-ESI source. The separation was attained using Acclaim PepMap RSLC columns (75 μm I.D. x 15 cm, 2 μm particle sizes, 100 \AA pore sizes) (Dionex, Sunnyvale, CA) with a flow rate of 350 nL/min. The column compartment was maintained at 29.5 $^\circ\text{C}$. The LC elution gradient of solvent B used in both LC-MS/MS analysis was: 5% over 10 min, 5%-20%

over 55 min, 20-30% over 25 min, 30-50% over 20 min, 50%-80% over 1 min, 80% over 4 min, 80%-5% over 1 min and 5% over 4 min. Solvent B consisted of 100% ACN with 0.1% formic acid while solvent A composed of 2% ACN with 0.1% formic acid. The LTQ Orbitrap Velos mass spectrometer was operated in positive mode with the ESI voltage set to 1500V. Data dependent acquisition mode was employed to achieve two scan events. The first scan event was a full MS scan of 380-2000 m/z at a mass resolution of 15,000. The second scan event was CID MS/MS of parent ions selected from the first scan event with an isolation width of 3.0 m/z , at a normalized collision energy (CE) of 35%, and an activation Q value of 0.250. The CID MS/MS scans were performed on the 30 most intense ions observed in the MS scan event. The dynamic exclusion was set to have repeat count of 2, repeat duration of 30s, exclusion list size 200 and exclusion duration of 90s.

The TSQ Vantage mass spectrometer was operated in positive mode with an ESI voltage of 1800V. Data independent acquisition mode was used for a multiple reaction monitoring (MRM) experiment. Predefined precursor and transition ions were monitored to select specifically targeted peptides corresponding to each candidate protein with 10.0 sec chromatogram filter peak width. The MRM experiments were performed at a cycle time of 2.000 sec and a Q1 peak width of 0.70 min for 400-1500 m/z mass range. The normalized collision energy value was 30% with a collision gas pressure of 1.5 mTorr in Q2.”

b. LC-MS/MS data analysis

The data resulting from LC-MS/MS processing of samples by Dr. Yahia Mechref’s Laboratory in Texas Tech University USA were analyzed as follows:

“Liquid chromatography-electrospray ionization-tandem mass spectrometry (LC-ESI-MS/MS) data was used to generate mascot generic format file (*.mgf) by Proteome Discover version 1.2 software (Thermo Scientific, San Jose, CA) then searched using SwissProt database (Rattus) in MASCOT version 2.4 (Matrix Science Inc., Boston, MA). Iodoacetamide modification of cysteine was set as a fixed modification, while oxidation of methionine was set as a variable modification. An m/z tolerance of 5 ppm was set for the identification of peptides with maximum 2 missed cleavages. Also, tandem MS ion tolerance was set within 0.8 Da with label-free quantification. Scaffold Q+ (Proteome Software, Portland, OR) was employed for spectral counts quantitation. Proteins shown significant difference ($p < 0.05$, unpaired student t-test) in spectral counts quantitation results were confirmed by MRM LC-MS/MS experiment. Each sample was injected three times to make a technical triplicate of MRM experiment. The most intense 1 or 2 peptides corresponding to each candidate protein were selected as target peptides. The three transitions of each target peptide were suggested by Pinpoint (Thermo Scientific, San Jose, CA). The MRM experiment results were investigated using Pinpoint. Peak area of each target peptide was normalized by the peak area of the glycan with 4 glucose units ($m/z = 896.507$). The normalized intensity of target peptides corresponding to each candidate protein were summed up to represent the abundance of the certain protein. A t-test ($\alpha = 0.05$) was performed to evaluate the statistical significance.

c. Systems Biology Assessment

Ingenuity Pathway Analysis software (Ingenuity® Systems) was employed to examine functional correlations within the different treatment groups. Data sets containing protein identifiers (Uniprot-KB) and corresponding expression values were

uploaded into the application. Each protein identifier was mapped to its corresponding protein object in the Ingenuity Pathways Knowledge Base. All mapped proteins were differentially expressed with $p < 0.01$ and overlaid onto global molecular networks developed from information contained in the knowledge base. Networks were then algorithmically generated based on their connectivity. Networks were “named” on the most prevalent functional group(s) present.

GO analysis is commonly used for functional studies of large-scale genomic or transcriptomic data [111]. KEGG pathway database [112] contains information on how molecules or genes are networked. The Search Tool for the Retrieval of Interacting Genes/Proteins (STRING-db) [113] is a database that integrates known and predicted protein associations from various sources, such as BioGRID [114], BIND [115], DIP [116], MINT [117], and gene co-expression data aimed at systematically extracting biological meaning from large gene or protein lists. In this study, STRING-database was used to identify the over-represented biological processes and significant pathways, and to generate the KEGG pathways of the different groups.

8. Statistical Analysis

Results of RTqPCR and MS-HRM were expressed as mean \pm Standard Error (SE) of at least three independent experiments. SigmaStat Version 3.1 and Microsoft Office Excel 2010 were used to calculate the mean, SE, and significant difference between the sample values compared to the controls using the Paired t-test. Statistical significance of differences between compared samples was claimed when the P-value was less than 0.05.

CHAPTER IV

RESULTS –EPIGENETIC REGULATION OF GENE EXPRESSION

A. *In vitro* studies: Effect of high glucose on VSMCs

1. RT-qPCR

Table 3 summarizes the Results of *in vitro* gene expression profiling that showed fold change differences due to high glucose treatment of VSMCs for 4 weeks compared to controls. High glucose induced gene expression of all studied genes from high glucose treatment. However, only *BDKRB1*, *BDKRB2*, *CTGF*, *Nox4*, *TNF α* , *IL-10*, and *TGF- β 2* showed statistical significance in difference.

Table 3 - Fold change in gene expression by high glucose *in vitro* as assessed by RT-qPCR (n=3)

Gene	Fold change relative to control VSMCs (\pm SE)	
	Glucose-treated VSMCs	Mannitol-treated VSMCs
<i>BDKRB1</i>	24.8 \pm 9.9 *	2.1 \pm 1.5 [#]
<i>BDKRB2</i>	9.1 \pm 3.1 *	1.5 \pm 0.5 [#]
<i>Nox1</i>	5.0 \pm 3.0	1.1 \pm 0.3
<i>Nox4</i>	0.4 \pm 0.2 *	1.0 \pm 0.1 [#]
<i>TNFα</i>	4.2 \pm 0.9 *	1.5 \pm 0.9 [#]
<i>IL-1β</i>	2.0 \pm 1.0	0.7 \pm 0.3
<i>IL-6</i>	2.9 \pm 1.3	1.9 \pm 1.0
<i>IL-10</i>	9.7 \pm 4.0 *	7.8 \pm 2.4
<i>CRP</i>	5.2 \pm 3.2	3.2 \pm 2.2
<i>SphK1</i>	1.1 \pm 0.1	0.4 \pm 0.2
<i>CTGF</i>	2.7 \pm 0.7 *	1.2 \pm 0.2
<i>FN1</i>	1.3 \pm 0.3	0.9 \pm 0.1
<i>TGF-β1</i>	1.1 \pm 0.1	1.0 \pm 0.1
<i>TGF-β2</i>	4.0 \pm 0.55 *	0.7 \pm 0.2

Significant change relative to control * p<0.05, **p<0.01,
Significant change relative to high glucose # p<0.05, ##p<0.01

2. Melting Curve analysis of DNA methylation

In vitro results of MS-HRM methylation studies have shown 1.75 fold decrease in methylation of TNF α promoter region compared to the control, while TGF β 2 demonstrated 1.45 fold decrease (Table 4).

Table 4 - Effect of high glucose on DNA Methylation in VSMC as assessed by MS-HRM (n=3), (p<0.05)

Gene	Methylation status	Fold Change in hypomethylation compared to	
		Control	Mannitol-treated
TNF α	Hypomethylated	1.75	-----
TGF- β 2	Hypomethylated	1.45	-----

B. *In vivo* studies: Effect of hyperglycemia on VSMCs

1. Characteristics of animal models

Figure 6 illustrates the change in body weight of controls, diabetic, and insulin-treated rats during the 6 weeks experiment. T1DM rats demonstrated a loss of weight after the third week of T1DM in comparison to control and insulin-treated rats which demonstrated an almost linear increase in body weight.

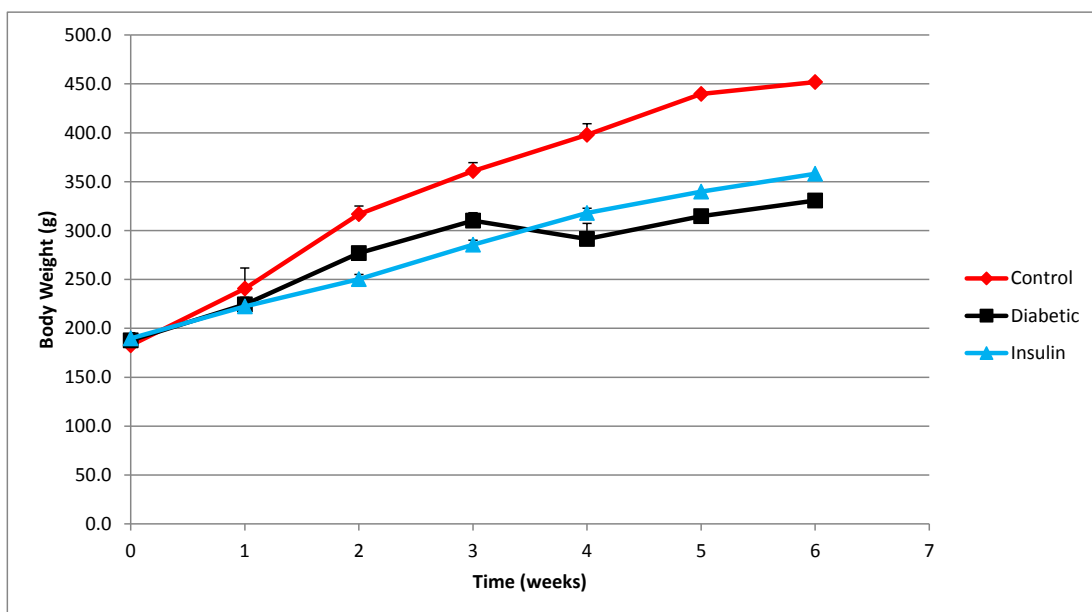


Figure 6 - Changes in body weight of rats during 6 weeks of exposure (n=3)

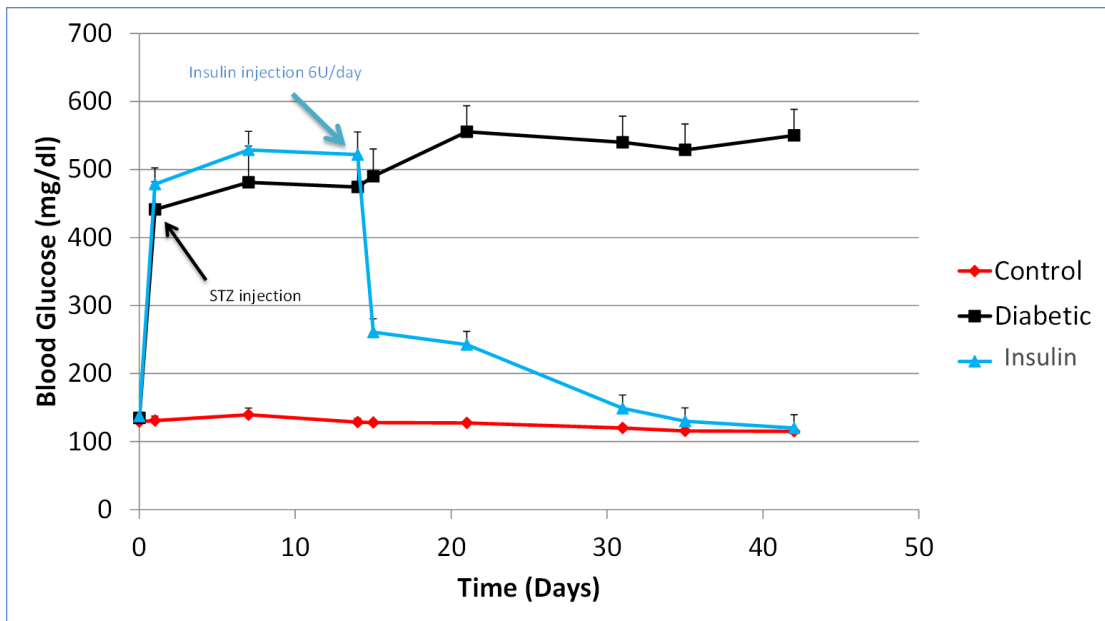


Figure 7 - Changes in non-fasting blood glucose levels of rats during 6 weeks of exposure (n=3)

Figure 7 illustrates the change in non-fasting blood glucose of controls, diabetic, and insulin-treated rats during the 6 weeks experiment. Controls, however, maintained a low level (<300 mg/dl) throughout the 6 weeks as expected. Diabetic and insulin-treated rats demonstrated the highest blood glucose level (>300 mg/dl) at day 1 after the STZ injection. While T1DM rats maintained this level until the end of the experiment, insulin-treated rats demonstrated a sharp decline at day 14 upon commencing daily injections of 5 insulin units to reach control group level by the end of the 6 weeks.

2. RT-qPCR

Results from *in vivo* studies on aortic smooth muscle cells from T1DM rats were similar but less pronounced than those of *in vitro* studies where we also noted

overexpression of all studied genes from hyperglycemia, with statistical significance noted for *BDKRB1*, *CTGF*, *FNI*, *Nox1*, *TNF α* , *IL-10*, *CRP*, *SphK1*, *TGF- β 1*, and *TGF- β 2* (Table 5).

Table 5 - Fold change in gene expression by hyperglycemia *in vivo* as assessed by RT-qPCR (n=3)

Gene	Fold change relative to control rats (\pm SE)	
	Diabetic rats	Insulin-treated rats
<i>BDKRB1</i>	5.6 \pm 1.6 *	16.2 \pm 5.5 *. [#]
<i>BDKRB2</i>	1.9 \pm 1.0	1.8 \pm 0.7
<i>Nox1</i>	1.3 \pm 0.1 *	4.3 \pm 1.2 *. [#]
<i>Nox4</i>	1.8 \pm 0.4	6.1 \pm 0.7 *. [#]
<i>TNFα</i>	1.3 \pm 0.1 *	1.9 \pm 0.5 *. [#]
<i>IL-1β</i>	1.3 \pm 0.3	1.9 \pm 0.2
<i>IL-6</i>	1.1 \pm 0.3	0.7 \pm 0.2
<i>IL-10</i>	3.0 \pm 0.7 *	0.3 \pm 0.1 *
<i>CRP</i>	3.5 \pm 0.3 *	1.5 \pm 0.3 *
<i>SphK1</i>	5.2 \pm 0.8 *	20.5 \pm 5.4, *
<i>CTGF</i>	2.3 \pm 1.5 **	0.6 \pm 0.1
<i>FNI</i>	3.2 \pm 0.7 *	13.9 \pm 5.3 *. [#]
<i>TGF-β1</i>	1.4 \pm 0.1 *	1.3 \pm 0.3
<i>TGF-β2</i>	1.3 \pm 0.1 *	0.8 \pm 0.2 *

Significant change relative to control * p<0.05, **p<0.01,
Significant change relative to diabetic # p<0.05, ##p<0.01

Moreover, to eliminate the osmotic pressure effect induced by glucose on VSMCs in culture, each sample had an osmotic control achieved by adding mannitol in concentration equivalent to that of high glucose added to samples. Mannitol does not bind or directly induce signaling pathways in VSMCs. It only simulates the high osmotic pressure environment. To test the metabolic memory phenomenon in these genes, five rats were treated with insulin for 4 weeks, 2 weeks after inducing T1DM with STZ.

C. Melting Curve Analysis of DNA Methylation

Table 6 demonstrates results of *in vivo* melt curve analysis of DNA methylation levels. *BDKRB1* and *BDKRB2* promoter regions demonstrated 8.91 and 4.75 fold decrease in DNA methylation level, respectively.

Table 6 - Effect of T1DM on DNA Methylation in VSMC as assessed by MS-HRM (n=3), (p<0.05)

Gene	Methylation status	Fold Change in hypomethylation compared to	
		control	Insulin-treated
<i>BDKRB1</i>	Hypomethylated	8.91	-----
<i>BDKRB2</i>	Hypomethylated	4.75	0.95

D. Immunohistochemical staining

To confirm that DNA, RNA, and proteins extracted from the aorta are from VSMC only, the FFPE endothelium-denuded aortas that were extracted from control and T1DM rats were stained with specific anti-rat antibodies and visualized under confocal laser microscopy to check for presence or absence of specific markers for VEC and VSMC.

Endothelium-denuded aorta rings were stained with anti- α -SMA (primary antibody) and Anti-mouse conjugated to Alexa Fluor fluorophore (secondary antibody). The tissue section was mounted with Fluoro-Gel II with Dapi to stain nucleic acids. Upon visualization at 40X magnification with oil immersion, well resolved red stains were present, verifying specificity of the primary antibody (Figure 8A).

To test the VEC-specific antibody, normal aortic rings not subjected to removal of endothelium were paraffin embedded and placed on rat aortic ring was stained with anti-PECAM-1 (CD31) (primary antibody) and anti-rabbit conjugated to Texas Red fluorophore (secondary antibody). The tissue section was mounted with Fluoro-Gel II

with Dapi to stain nucleic acids blue. Upon visualization at 40X magnification with oil immersion, tissue showed both green and red stain indicating presence of VEC and α -SMA (Figures C to F). Faint nonspecific green stain seems to be spread throughout the tissue and on what seems to be elastin fibers. However, specific, bright green staining on the right of the image is visible and corresponds to VEC. After testing the antibody on a positive control tissue sample, it was then used to test for the presence of endothelial cells in our test tissue samples. Accordingly, endothelium-denuded rat aortic ring was stained with anti-PECAM-1 (primary antibody) and anti-rabbit conjugated to Texas Red fluorophore (secondary antibody). The tissue section was mounted with Fluoro-Gel II with Dapi to stain nucleic acids blue. Upon visualization at 40X magnification with oil immersion, no trace of green stain was visualized. Hence, the tissue was successfully endothelium-denuded as no green stain appears.

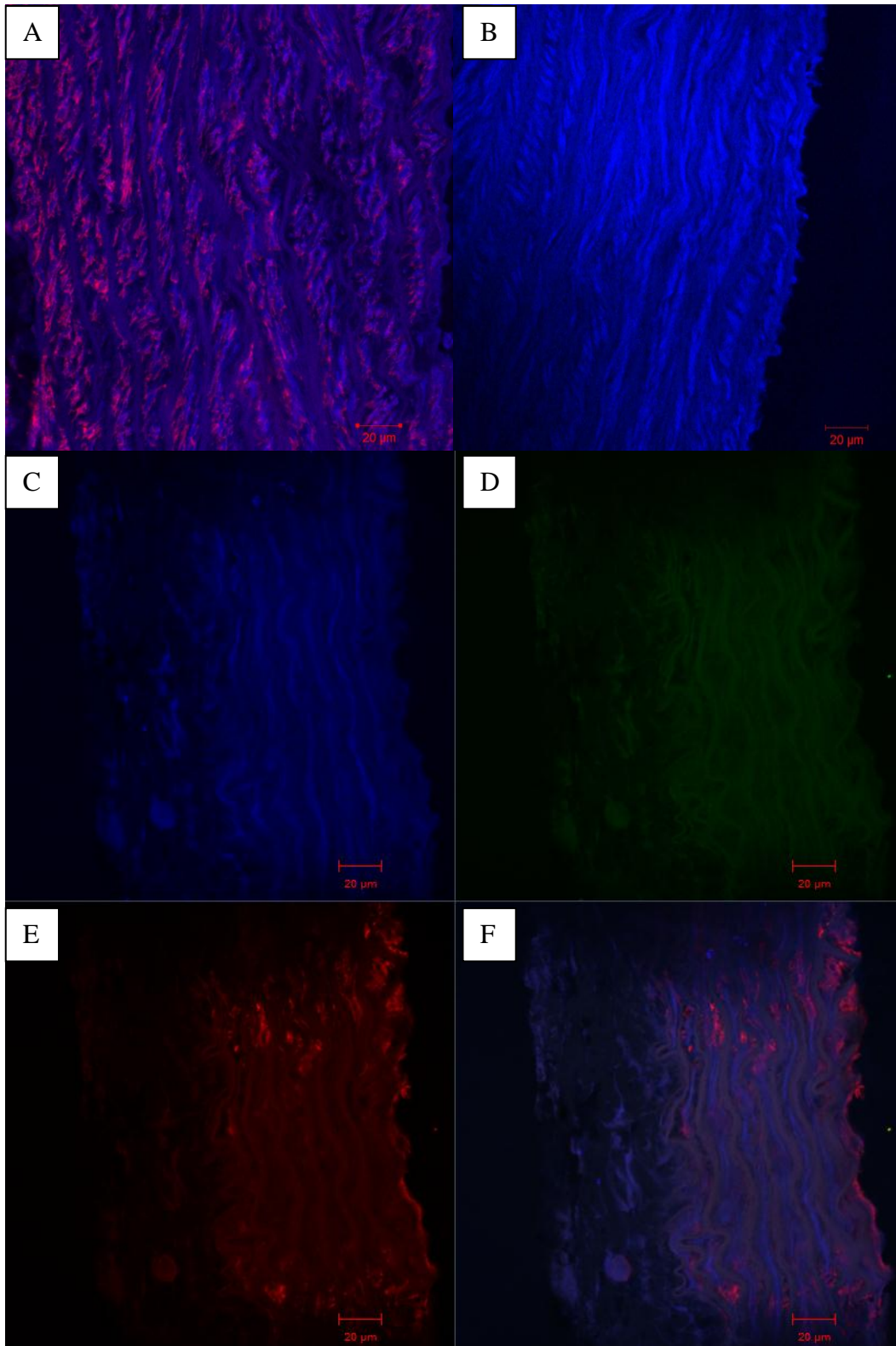


Figure 8 - Endothelium-denuded rat aorta rings were stained with **(A)** Anti- α -SMA-Alexa Fluor (Red) **(B)** Anti-PECAM-1 (CD31)-Texas Red (Green), which showed presence of VSMC and absence of VEC. Regular rat aortic smooth muscle cells were stained with **(C)** Fluoro-Gel II with Dapi (blue) **(D)** Anti-PECAM-1- Texas Red (Green) **(E)** Anti- α -SMA-Alexa Fluor (Red), **(F)** Superimposed images (C to E), which showed presence of VSMC and VEC.

Bisulfite Conversion Efficiency

Based on equation 1, the calculated bisulfite conversion efficiency for the unconverted control sample was 99.99%, while that of the selected samples converted ranged from 99.65 to 99.90. As for the standards, the conversion efficiency ranged from 99.78 to 99.99%. Samples that had efficiency lower than 99.5 were excluded from DNA methylation studies.

CHAPTER V

RESULTS – PROTEOMICS

A. Protein Extraction Efficiency

Table 7 shows the extraction efficiency of rat brain tissues. In general, the average protein extraction efficiencies were highest for control rats (n=3), and lowest for insulin-treated rats (n=3).

Table 7 - Protein Extraction Efficiency (n=3)

Sample	Weight(mg)	Extracted Proteins (ug)	Extraction Efficiency	Average efficiency \pm SD
Control	49.3	603.67	1.22%	1.28% \pm 0.005
	34.97	269.25	0.77%	
	24.5	451.32	1.84%	
Diabetic	24.59	246.05	1.00%	1.06% \pm 0.005
	27.49	173.12	0.63%	
	37.45	578.13	1.54%	
Insulin-treated	40.83	123.05	0.30%	0.29% \pm 0.002
	26.95	26.84	0.10%	
	28.94	133.25	0.46%	

B. Spectral Count Quantification

A principal component analysis (PCA) plot was performed on the spectral count data to investigate internal variation between controls, diabetic, and insulin-treated. A PCA plot transforms a set of observations of possibly correlated variables into a set of values of linearly uncorrelated variables called principal components [118]. It is a 3 dimensional graph. Each dimension is a factor or component, whereas the blue, yellow, and green points are data points. For each treatment, we get different data points that give a score based on protein characteristics. This score defines the location of the coordinates of the plane seen here. Figure 9 depicts the PCA scoring plots of aorta

proteome. According to PCA, principal components from controls, diabetic, and insulin-treated were clustered with components of their respective groups but clearly resolved from principal components in other groups. Although the components of insulin-treated rats could be clustered together in the PCA plot away from diabetic components, they were grouped away from control rats components. This fact might suggest that insulin treatment might reduce hyperglycemia and change the protein expression of diabetics but it will not return it to normal levels, emphasizing the concept of metabolic memory.

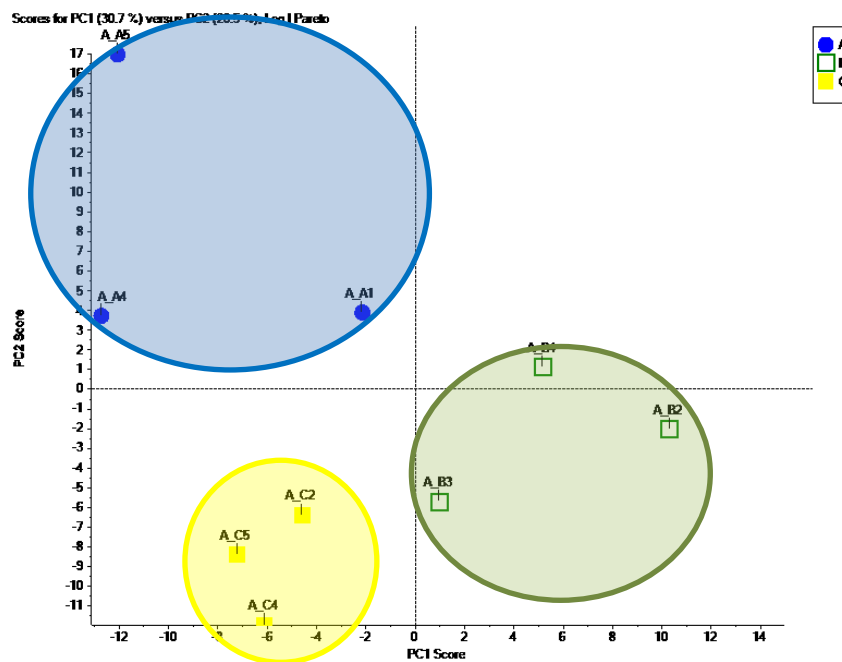


Figure 9: PCA scoring plots of aorta proteome for controls, diabetic, and insulin-treated rats using Scaffold Q+ software

C. Protein level variation (Shotgun Proteomics)

LC-MS/MS analyses of aorta tissue extracted from rats permitted the total identification of 101 unique proteins. For T1DM rats (n=3), 71 proteins had altered expression level in comparison to controls. For insulin-treated rats (n=3), 53 proteins had altered

expression level in comparison to diabetic rats. There are 48 proteins unique to T1DM rats while there are 30 proteins unique to the insulin-treated rats. Table 8 lists all modified aortic proteins levels in T1DM rats in comparison to control rats while table 9 lists all modified aortic proteins levels in insulin-treated rats in comparison to diabetic rats.

Table 8 - Regulation of protein levels in aorta of T1DM rats in comparison to control rats (n=3)

Accession Number	Protein Name	Fold Change	p-value	Regulation
B0BNE5	S-formylglutathione hydrolase	3.93	0.0195	up
D3Z8L7	Ras-related protein R-Ras	1.84	0.0199	up
P04692	Tropomyosin alpha-1 chain	2.65	0.0366	up
P04797	Glyceraldehyde-3-phosphate dehydrogenase	1.65	0.0253	up
P04937	Fibronectin	2.78	0.0484	up
P05197	Elongation factor 2	3.41	0.0170	up
P08009	Glutathione S-transferase Yb-3	4.33	0.0072	up
P20070	NADH-cytochrome b5 reductase 3	ND in Control	0.0448	up
P23764	Glutathione peroxidase 3	ND in Control	0.0150	up
P25113	Phosphoglycerate mutase 1	1.53	0.0439	up
P29457	Serpin H1	11.53	0.0027	up
P35565	Calnexin	2.45	0.0017	up
P36201	Cysteine-rich protein 2	ND in Control	0.0492	up
P48679	Prelamin-A/C	2.56	0.0456	up
P49134	Integrin beta-1	2.33	0.0309	up
P50399	Rab GDP dissociation inhibitor beta	3.46	0.0021	up
P52296	Importin subunit beta-1	11.27	0.0008	up
P53534	Glycogen phosphorylase, brain form (Fragment)	4.36	0.0251	up
P58775	Tropomyosin beta chain	2.01	0.0309	up
P61589	Transforming protein RhoA	1.82	0.0154	up
P62142	Serine/threonine-protein phosphatase PP1-beta catalytic subunit	8.83	0.0072	up
P69897	Tubulin beta-5 chain	2.02	0.0035	up
P85515	Alpha-centractin	5.06	0.0345	up
P85973	Purine nucleoside phosphorylase	2.99	0.0232	up
Q00438	Polypyrimidine tract-binding protein 1	7.20	0.0106	up
Q00657	Chondroitin sulfate proteoglycan 4	5.05	0.0427	up
Q08163	Adenylyl cyclase-associated protein 1	4.52	0.0330	up
Q5XI07	Lipoma-preferred partner homolog	5.62	0.0132	up
Q62636	Ras-related protein Rap-1b	4.65	0.0295	up
Q62812	Myosin-9	3.86	0.0082	up
Q62952	Dihydropyrimidinase-related protein 3	11.57	0.0051	up

Q63598	Plastin-3	3.15	0.0482	up
Q63862	Myosin-11 (Fragments)	4.13	0.0391	up
Q6P742	Proteolipid protein 2	ND in Control	0.0492	up
Q7M0E3	Dextrin	1.81	0.0252	up
Q8CFN2	Cell division control protein 42 homolog	4.41	0.0246	up
Q99PD6	Transforming growth factor beta-1- induced transcript 1 protein	7.08	0.0292	up
Q9EQT5	Tubulointerstitial nephritis antigen-like	13.68	0.0411	up
Q9ESN0	Protein Niban	9.40	0.0083	up
Q9HB97	Alpha-parvin	5.05	0.0387	up
Q9QXQ0	Alpha-actinin-4	3.15	0.0368	up
Q9WUH4	Four and a half LIM domains protein 1	7.37	0.0200	up
Q9Z0W7	Chloride intracellular channel protein 4	7.65	0.0143	up
Q9Z1B2	Glutathione S-transferase Mu 5	19.99	0.0014	up
Q9Z1P2	Alpha-actinin-1	3.73	0.0478	up
Q9Z1Z9	PDZ and LIM domain protein 7	5.69	0.0496	up
O35796	Complement component 1 Q subcomponent-binding protein, mitochondrial	0.23	0.0228	down
P13803	Electron transfer flavoprotein subunit alpha, mitochondrial	0.17	0.0305	down
P14046	Alpha-1-inhibitor 3	0.20	0.0060	down
P14604	Enoyl-CoA hydratase, mitochondrial	0.16	0.0023	down
P17764	Acetyl-CoA acetyltransferase, mitochondrial	0.38	0.0092	down
P18163	Long-chain-fatty-acid--CoA ligase 1	0.10	0.0302	down
P19944	60S acidic ribosomal protein P1	0.55	0.0078	down
P20788	Cytochrome b-c1 complex subunit Rieske, mitochondrial	0.20	0.0173	down
P32551	Cytochrome b-c1 complex subunit 2, mitochondrial	0.22	0.0236	down
P49432	Pyruvate dehydrogenase E1 component subunit beta, mitochon.	0.24	0.0157	down
P61983	14-3-3 protein gamma	0.57	0.0341	down
P62898	Cytochrome c, somatic	0.20	0.0332	down
P67779	Prohibitin	0.51	0.0028	down
Q00715	Histone H2B type 1	0.15	0.0083	down
Q03626	Murinoglobulin-1	0.47	0.0104	down
Q3KR86	Mitochondrial inner membrane protein (Fragment)	0.06	0.0158	down
Q5M9I5	Cytochrome b-c1 complex subunit 6, mitochondrial	0.00	0.0017	down
Q5SGE0	Leucine-rich PPR motif-containing protein, mitochondrial	0.00	0.0001	down
Q60587	Trifunctional enzyme subunit beta, mitochondrial	0.08	0.0007	down
Q64591	2,4-dienoyl-CoA reductase, mitochondrial	0.07	0.0075	down
Q66HF1	NADH-ubiquinone oxidoreductase 75 kDa subunit, mitochondrial	0.10	0.0001	down
Q68FU3	Electron transfer flavoprotein subunit beta	0.27	0.0108	down
Q6P6R2	Dihydrolipoyl dehydrogenase, mitochondrial	0.23	0.0176	down

Q99NA5	Isocitrate dehydrogenase [NAD] subunit alpha, mitochondrial	0.20	0.0379	down
Q9ER34	Aconitate hydratase, mitochondrial	0.22	0.0188	down

ND: not detected

Table 9 - Regulation of protein levels in aorta of insulin-treated rats in comparison to T1DM rats (n=3)

Accession Number	Protein Name	p-value	Fold Change	Regulation
B0BNN3	Carbonic anhydrase 1	0.0052	1.81	up
O35077	Glycerol-3-phosphate dehydrogenase [NAD(+)], cytoplasmic	0.0143	5.54	up
P02767	Transthyretin	0.0447	2.29	up
P06399	Fibrinogen alpha chain	0.0425	2.88	up
P08289	Alkaline phosphatase, tissue-nonspecific isozyme	0.0191	4.20	up
P11240	Cytochrome c oxidase subunit 5A, mitochondrial	0.0001	ND in B	up
P14046	Alpha-1-inhibitor 3	0.0483	4.05	up
P14562	Lysosome-associated membrane glycoprotein 1	0.0280	ND in B	up
P14841	Cystatin-C	0.0446	3.09	up
P31232	Transgelin	0.0294	2.04	up
P47820	Angiotensin-converting enzyme	0.0081	ND in B	up
P48500	Triosephosphate isomerase	0.0172	1.38	up
P62775	Myotrophin	0.0036	7.68	up
Q9QZQ5	Protein NOV homolog	0.0314	2.55	up
P02651	Apolipoprotein A-IV	0.0492	0.00	down
P04639	Apolipoprotein A-I	0.0450	0.36	down
P04692	Tropomyosin alpha-1 chain	0.0060	0.63	down
P05197	Elongation factor 2	0.0185	0.41	down
P11884	Aldehyde dehydrogenase, mitochondrial	0.0126	0.58	down
P15865	Histone H1.4	0.0008	0.00	down
P20070	NADH-cytochrome b5 reductase 3	0.0448	0.00	down
P25235	Dolichyl-diphosphooligosaccharide--protein glycosyltransferase subunit 2	0.0329	0.08	down
P36201	Cysteine-rich protein 2	0.0243	0.11	down
P46462	Transitional endoplasmic reticulum ATPase	0.0104	0.08	down
P48679	Prelamin-A/C	0.0427	0.30	down
P50398	Rab GDP dissociation inhibitor alpha	0.0192	0.25	down
P50399	Rab GDP dissociation inhibitor beta	0.0242	0.34	down
P52296	Importin subunit beta-1	0.0019	0.00	down
P53534	Glycogen phosphorylase, brain form (Fragment)	0.0170	0.12	down
P61980	Heterogeneous nuclear ribonucleoprotein K	0.0168	0.20	down
P62142	Serine/threonine-protein phosphatase PP1-beta catalytic subunit	0.0110	0.18	down
P85125	Polymerase I and transcript release factor	0.0162	0.44	down
P85515	Alpha-centractin	0.0248	0.00	down
Q00438	Polypyrimidine tract-binding protein 1	0.0015	0.00	down

Q05962	ADP/ATP translocase 1	0.0072	0.08	down
Q08163	Adenylyl cyclase-associated protein 1	0.0079	0.00	down
Q09073	ADP/ATP translocase 2	0.0018	0.00	down
Q4V7C7	Actin-related protein 3	0.0188	0.14	down
Q5XI07	Lipoma-preferred partner homolog	0.0059	0.00	down
Q5XIF6	Tubulin alpha-4A chain	0.0012	0.00	down
Q5XIH7	Prohibitin-2	0.0480	0.20	down
Q5XIM9	T-complex protein 1 subunit beta	0.0047	0.23	down
Q62812	Myosin-9	0.0062	0.00	down
Q62952	Dihydropyrimidinase-related protein 3	0.0224	0.18	down
Q63081	Protein disulfide-isomerase A6	0.0335	0.29	down
Q8VHV7	Heterogeneous nuclear ribonucleoprotein H	0.0464	0.00	down
Q99PD6	Transforming growth factor beta-1-induced transcript 1 protein	0.0437	0.00	down
Q9ESN0	Protein Niban	0.0374	0.32	down
Q9HB97	Alpha-parvin	0.0218	0.23	down
Q9QXQ0	Alpha-actinin-4	0.0001	0.00	down
Q9WUH4	Four and a half LIM domains protein 1	0.0340	0.71	down
Q9Z1B2	Glutathione S-transferase Mu 5	0.0027	0.08	down
Q9Z1P2	Alpha-actinin-1	0.0428	0.23	down

ND: not detected

Table 10 - Regulation of protein levels in aorta of insulin-treated rats in comparison to control rats (n=3)

Accession Number	Protein Name	p-value	Fold Change	Regulation
B0BNN3	Carbonic anhydrase 1	0.0067	1.47	up
D3Z8L7	Ras-related protein R-Ras	0.0250	1.74	up
Q35796	Complement component 1 Q subcomponent-binding protein, mitochondrial	0.0079	0.06	down
P04797	Glyceraldehyde-3-phosphate dehydrogenase	0.0125	2.33	up
P04906	Glutathione S-transferase P	0.0008	7.96	up
P07150	Annexin A1	0.0314	1.62	up
P08649	Complement C4	0.0320	0.59	down
P13803	Electron transfer flavoprotein subunit alpha, mitochondrial	0.0447	0.26	down
P14562	Lysosome-associated membrane glycoprotein 1	0.0280	100.00	up
P14604	Enoyl-CoA hydratase, mitochondrial	0.0080	0.13	down
P15650	Long-chain specific acyl-CoA dehydrogenase, mitochondrial	0.0387	0.12	down
P17764	Acetyl-CoA acetyltransferase, mitochondrial	0.0056	0.37	down
P18163	Long-chain-fatty-acid--CoA ligase 1	0.0274	0.13	down
P20788	Cytochrome b-c1 complex subunit Rieske, mitochondrial	0.0129	0.21	down
P32551	Cytochrome b-c1 complex subunit 2, mitochondrial	0.0064	0.14	down
P47820	Angiotensin-converting enzyme	0.0081	100.00	up

P54311	Guanine nucleotide-binding protein G(I)/G(S)/G(T) subunit beta-1	0.0115	0.14	down
P55260	Annexin A4	0.0272	1.52	up
P61980	Heterogeneous nuclear ribonucleoprotein K	0.0386	0.16	down
P67779	Prohibitin	0.0315	0.34	down
P85108	Tubulin beta-2A chain	0.0000	0.00	down
P85125	Polymerase I and transcript release factor	0.0149	0.28	down
Q3KR86	Mitochondrial inner membrane protein (Fragment)	0.0483	0.00	down
Q4V8H8	EH domain-containing protein 2	0.0279	0.33	down
Q5M9I5	Cytochrome b-c1 complex subunit 6, mitochondrial	0.0150	0.16	down
Q5SGE0	Leucine-rich PPR motif-containing protein, mitochondrial	0.0001	0.00	down
Q60587	Trifunctional enzyme subunit beta, mitochondrial	0.0042	0.12	down
Q64591	2,4-dienoyl-CoA reductase, mitochondrial	0.0092	0.09	down
Q66HF1	NADH-ubiquinone oxidoreductase 75 kDa subunit, mitochondrial	0.0019	0.17	down
Q68FU3	Electron transfer flavoprotein subunit beta	0.0263	0.36	down
Q6MG61	Chloride intracellular channel protein 1	0.0324	3.58	up
Q6P6Q2	Keratin, type II cytoskeletal 5	0.0287	5.12	up
Q6P6R2	Dihydrolipoyl dehydrogenase, mitochondrial	0.0160	0.23	down
Q9EQT5	Tubulointerstitial nephritis antigen-like	0.0228	10.46	up
Q9ER34	Aconitate hydratase, mitochondrial	0.0433	0.34	down
Q9WUH4	Four and a half LIM domains protein 1	0.0228	5.26	up

LC-MS/MS analyses of kidney (renal cortex) tissue extracted from rats permitted the total identification of 86 unique proteins. For T1DM rats (n=3), 54 proteins had altered expression level in comparison to controls. For insulin-treated rats (n=3), 51 proteins had altered expression level in comparison to diabetic rats. There are 38 proteins unique to T1DM rats while there are 33 proteins unique to the insulin-treated rats. Table 11 lists all modified renal cortex proteins levels in T1DM rats in comparison to controls while table 12 lists all modified renal cortex proteins levels in insulin-treated rats in comparison to diabetic rats.

Table 11 Regulation of protein levels in renal cortex of T1DM rats in comparison to controls (n=3)

Accession Number	Protein Name	p-value	Fold Change	Regulation
A2VCW9	Alpha-aminoacidic semialdehyde synthase, mitochondrial	0.0223	2.08	up
A7VJC2	Heterogeneous nuclear ribonucleoproteins	0.0115	2.15	up

	A2/B1			
O88994	MOSC domain-containing protein 2, mitochondrial	0.0299	4.52	up
P01048	T-kininogen 1	0.0207	100.00	up
P04182	Ornithine aminotransferase, mitochondrial	0.0168	1.20	up
P07871	3-ketoacyl-CoA thiolase B, peroxisomal	0.0028	2.76	up
P15650	Long-chain specific acyl-CoA dehydrogenase, mitochondrial	0.0090	1.56	up
P27653	C-1-tetrahydrofolate synthase, cytoplasmic	0.0410	2.28	up
P36511	UDP-glucuronosyltransferase 2B15	0.0028	2.97	up
P49432	Pyruvate dehydrogenase E1 component subunit beta, mitochondrial	0.0447	1.54	up
P50137	Transketolase	0.0222	1.23	up
P50554	4-aminobutyrate aminotransferase, mitochondrial	0.0211	1.66	up
P51647	Retinal dehydrogenase 1	0.0119	1.90	up
P52873	Pyruvate carboxylase, mitochondrial	0.0243	1.50	up
P57113	Maleylacetoacetate isomerase	0.0000	100.00	up
Q0V GK3	Glycerate kinase	0.0183	8.79	up
Q4KLP0	Probable 2-oxoglutarate dehydrogenase E1 component DHKTD1, mitochondrial	0.0099	2.47	up
Q4KM73	UMP-CMP kinase	0.0127	2.17	up
Q561S0	NADH dehydrogenase [ubiquinone] 1 alpha subcomplex subunit 10, mitochondrial	0.0141	1.28	up
Q5I0D7	Xaa-Pro dipeptidase	0.0386	2.69	up
Q63965	Sideroflexin-1	0.0016	1.45	up
Q6JE36	Protein NDRG1	0.0102	3.93	up
Q7TP48	Adipocyte plasma membrane-associated protein	0.0412	1.57	up
Q8CHM7	2-hydroxyacyl-CoA lyase 1	0.0343	100.00	up
Q91ZW6	Trimethyllysine dioxygenase, mitochondrial	0.0001	2.19	up
Q9JM53	Apoptosis-inducing factor 1, mitochondrial	0.0052	1.33	up
Q9QYU4	Thiomorpholine-carboxylate dehydrogenase	0.0452	2.69	up
Q9R063	Peroxiredoxin-5, mitochondrial	0.0270	1.24	up
Q9Z0V6	Thioredoxin-dependent peroxide reductase, mitochondrial	0.0427	1.39	up
Q9Z0Z5	Solute carrier family 13 member 3	0.0242	100.00	up
Q9Z339	Glutathione S-transferase omega-1	0.0346	6.14	up
A9UMV8	Histone H2A.J	0.0195	0.69	down
O08651	D-3-phosphoglycerate dehydrogenase	0.0225	0.00	down
P01026	Complement C3	0.0180	0.12	down
P02761	Major urinary protein	0.0007	0.33	down
P02770	Serum albumin	0.0062	0.78	down
P11517	Hemoglobin subunit beta-2	0.0149	0.66	down
P14046	Hemoglobin subunit beta-2	0.0014	0.05	down
P21913	Succinate dehydrogenase [ubiquinone] iron-sulfur subunit, mitochondrial	0.0218	0.55	down
P24090	Alpha-2-HS-glycoprotein	0.0205	0.47	down
P35704	Peroxiredoxin-2	0.0442	0.66	down
P48679	Prelamin-A/C	0.0390	0.12	down
P50878	60S ribosomal protein L4	0.0002	0.00	down
P55260	Annexin A4	0.0002	0.74	down
P61983	14-3-3 protein gamma	0.0001	0.70	down

P62815	V-type proton ATPase subunit B, brain isoform	0.0014	0.74	down
P63245	Guanine nucleotide-binding protein subunit beta-2-like 1	0.0296	0.54	down
P84850	D-2-hydroxyglutarate dehydrogenase, mitochondrial	0.0198	0.28	down
P98158	Low-density lipoprotein receptor-related protein 2	0.0036	0.70	down
Q03626	Murinoglobulin-1	0.0104	0.00	down
Q07523	Hydroxyacid oxidase 2	0.0000	0.64	down
Q6AYZ1	Tubulin alpha-1C chain	0.0016	0.92	down
Q6RUV5	Ras-related C3 botulinum toxin substrate 1	0.0147	0.15	down
Q9WU82	Catenin beta-1	0.0386	0.17	down

ND: not detected

Table 12 - Regulation of protein levels in renal cortex of insulin-treated rats in comparison to T1DM rats (n=3)

Accession Number	Protein Name	p-value	Fold Change	Regulation
A9UMV8	Histone H2A.J	0.0145	1.49	up
O35763	Moesin	0.0206	1.27	up
P01026	Complement C3	0.0096	6.60	up
P02650	Apolipoprotein E	0.0066	100.00	up
P02761	Major urinary protein	0.0001	2.66	up
P02770	Serum albumin	0.0481	1.33	up
P04897	Guanine nucleotide-binding protein G(i) subunit alpha-2	0.0120	8.84	up
P07335	Creatine kinase B-type	0.0074	1.21	up
P11884	Aldehyde dehydrogenase, mitochondrial	0.0168	1.21	up
P14046	Alpha-1-inhibitor 3	0.0012	17.43	up
P29457	Serpin H1	0.0481	2.02	up
P31000	Vimentin	0.0171	1.98	up
P54313	Guanine nucleotide-binding protein G(I)/G(S)/G(T) subunit beta-2	0.0150	2.73	up
P62630	Elongation factor 1-alpha 1	0.0346	1.49	up
P63159	High mobility group protein B1	0.0350	5.96	up
P69897	Tubulin beta-5 chain	0.0352	1.17	up
P85968	6-phosphogluconate dehydrogenase, decarboxylating	0.0314	1.62	up
P98158	Low-density lipoprotein receptor-related protein 2	0.0445	1.31	up
Q00438	Polypyrimidine tract-binding protein 1	0.0159	4.25	up
Q63598	Plastin-3	0.0185	5.48	up
Q6RUV5	Ras-related C3 botulinum toxin substrate 1	0.0450	4.79	up
Q7TP52	Carboxymethylenebutenolidase homolog	0.0151	1.81	up
Q9Z2Q1	Protein transport protein Sec31A	0.0240	3.03	up
A2VCW9	Alpha-aminoacidic semialdehyde synthase, mitochondrial	0.0090	0.43	down
P01048	T-kininogen 1	0.0126	0.14	down
P07871	3-ketoacyl-CoA thiolase B, peroxisomal	0.0007	0.43	down

P11598	Protein disulfide-isomerase A3	0.0041	0.57	down
P20673	Argininosuccinate lyase	0.0392	0.27	down
P20788	Cytochrome b-c1 complex subunit Rieske, mitochondrial	0.0302	0.26	down
P23785	Granulins	0.0041	0.30	down
P32551	Cytochrome b-c1 complex subunit 2, mitochondrial	0.0448	0.71	down
P32755	4-hydroxyphenylpyruvate dioxygenase	0.0096	0.15	down
P43428	Glucose-6-phosphatase	0.0011	0.07	down
P50137	Transketolase	0.0346	0.86	down
P68035	Actin, alpha cardiac muscle 1	0.0467	0.84	down
P81155	Voltage-dependent anion-selective channel protein 2	0.0466	0.72	down
Q00715	Histone H2B type 1	0.0209	0.49	down
Q07523	Hydroxyacid oxidase 2	0.0012	0.82	down
Q3KR86	Mitochondrial inner membrane protein (Fragment)	0.0249	0.50	down
Q3MIF4	Xylulose kinase	0.0259	0.61	down
Q4G069	Regulator of microtubule dynamics protein 1	0.0000	0.00	down
Q4KLP0	Probable 2-oxoglutarate dehydrogenase E1 component DHKTD1, mitochondrial	0.0227	0.59	down
Q4KM73	UMP-CMP kinase	0.0055	0.36	down
Q63965	Sideroflexin-1	0.0023	0.69	down
Q64057	Alpha-aminoadipic semialdehyde dehydrogenase	0.0362	0.77	down
Q642A7	Protein FAM151A	0.0000	0.00	down
Q68G31	Phenazine biosynthesis-like domain-containing protein	0.0443	0.44	down
Q6AXR4	Beta-hexosaminidase subunit beta	0.0228	0.28	down
Q7TP48	Adipocyte plasma membrane-associated protein	0.0079	0.54	down
Q8CHM7	2-hydroxyacyl-CoA lyase 1	0.0343	0.00	down
Q9QYU4	Thiomorpholine-carboxylate dehydrogenase	0.0233	0.21	down
Q9R063	Peroxisome oxidoreductin-5, mitochondrial	0.0252	0.79	down
Q9Z339	Glutathione S-transferase omega-1	0.0415	0.18	down

ND: not detected

Table 13 - Regulation of protein levels in renal cortex of insulin-treated rats in comparison to control rats (n=3)

Accession Number	Protein Name	p-value	Fold Change	Regulation
Q07523	Guanine nucleotide-binding protein G(i) subunit alpha-2	0.0000	0.53	down
P62815	Gamma-glutamyltranspeptidase 1	0.0024	0.78	down
P23785	Protein disulfide-isomerase A3	0.0116	0.33	down
P38652	Aldehyde dehydrogenase, mitochondrial	0.0132	0.25	down
P11598	ATP synthase-coupling factor 6, mitochondrial	0.0158	0.58	down
P21913	Succinate dehydrogenase [ubiquinone] iron-	0.0211	0.55	down

	sulfur subunit, mitochondrial			
Q3KR86	Granulins	0.0250	0.60	down
P21571	C-1-tetrahydrofolate synthase, cytoplasmic	0.0355	0.68	down
P35171	Cytochrome c oxidase subunit 7A2, mitochondrial	0.0369	0.00	down
P35434	ATP synthase subunit delta, mitochondrial	0.0437	0.19	down
Q6IRK9	Calnexin	0.0007	1.28	up
P27653	Phosphoglucosyltransferase-1	0.0067	1.49	up
P11884	V-type proton ATPase subunit F	0.0099	1.27	up
P04897	Guanine nucleotide-binding protein G(I)/G(S)/G(T) subunit beta-2	0.0116	9.08	up
P54313	V-type proton ATPase subunit B, brain isoform	0.0132	2.08	up
P35565	Mitochondrial 2-oxoglutarate/malate carrier protein	0.0136	1.43	up
Q64550	Polypyrimidine tract-binding protein 1	0.0193	3.66	up
P50408	Hydroxyacid oxidase 2	0.0249	3.02	up
Q66HF1	Mitochondrial inner membrane protein (Fragment)	0.0304	1.15	up
P97700	ATPase family AAA domain-containing protein 3	0.0324	1.19	up
Q00438	UDP-glucuronosyltransferase 1-1	0.0428	1.82	up
P07314	NADH-ubiquinone oxidoreductase 75 kDa subunit, mitochondrial	0.0463	1.54	up
Q3KRE0	Carboxypeptidase Q	0.0489	100.00	up

D. Systems Biology Assessment

For a more comprehensive understanding of the classes of proteins and their functional relationship to cell processes and disease in the aorta and renal cortex, Ingenuity Pathway Analysis (IPA) was run on the proteins listed in tables 8-13 to generate figures 10-15 that illustrate the predicted pathways and regulatory activities of these proteins. Protein lists derived from analysis of aorta tissue were investigated for pathways and processes that lead to atherosclerosis, which include VSMC migration, proliferation, inflammation, oxidative stress, and fibrosis.

1. IPA analysis of dysregulated protein levels in the aorta

Aorta tissue from hyperglycemic rats revealed that FN1 protein level was increased and was predicted to contribute to several atherosclerosis-promoting

pathologies including infarction of blood vessels, diabetes, accumulation of ECM and fibrosis. It also activated cell movement directly and through formation of cellular protrusions, focal adhesions, actin stress fibers, and filopodia, in addition to promotion of cell spreading, attachment, and adhesion. Cell movement and formation of cellular protrusions were also promoted by the elevated ITGB1 and cdc42 while increased RHOA and DPYSL3 were predicted to inhibit it. RHOA was also involved in inhibiting Nf-kB complex and cell spreading of VSMC, while promoting chemotaxis and movement of white blood cells. GPX3 was highly up-regulated and was involved in catabolism of hydrogen peroxide, indicating a high demand by the cell for reduction of oxidative stress (Figure 10).

protein level was noted for angiotensin I converting enzyme (ACE), an endogenous metalloproteases, known for involvement in blood pressure regulation (Figure 11).

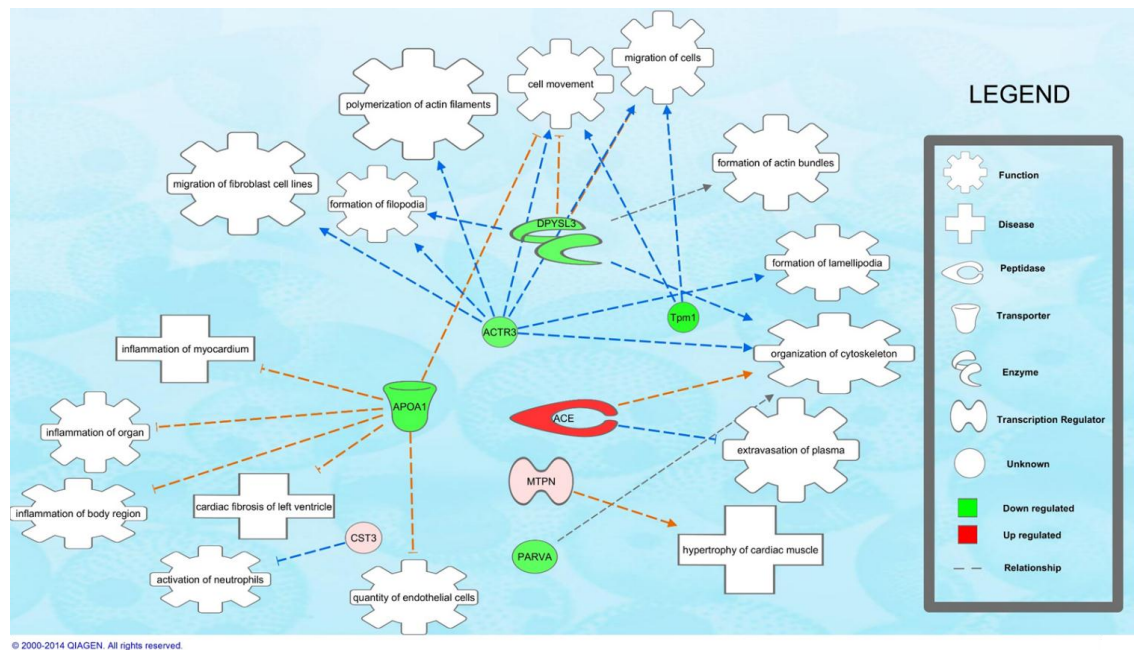


Figure 11: IPA map of insulin-treated rats aorta in comparison to diabetic rat aorta on cellular processes and diseases that lead to atherosclerosis (n=3).

ACE: angiotensin I converting enzyme; **ApoA1**: apolipoprotein A-I; **ACTR3**: ARP3 actin-related protein 3 homolog; **CST3**: Cystatin-3; **DPYSL3**: dihydropyrimidinase-like 3; **MTPN**: myotrophin; **PARVA**: parvin, alpha; **TPM1**: tropomyosin 1, alpha

To investigate whether insulin treatment permits the return of protein levels and activity to control level, figure 12 compares insulin-treated with control rats. It shows that ACE remained elevated and was predicted to promote apoptosis, kidney damage, and formation of neointima which is an early stage of atherosclerosis. GAPDH and Annexin A1 (ANXA1) were also elevated and promoted apoptosis. However, ANXA1 was also predicted to prevent heart injury, in addition to inhibition of neutrophil infiltration and nitric oxide release.

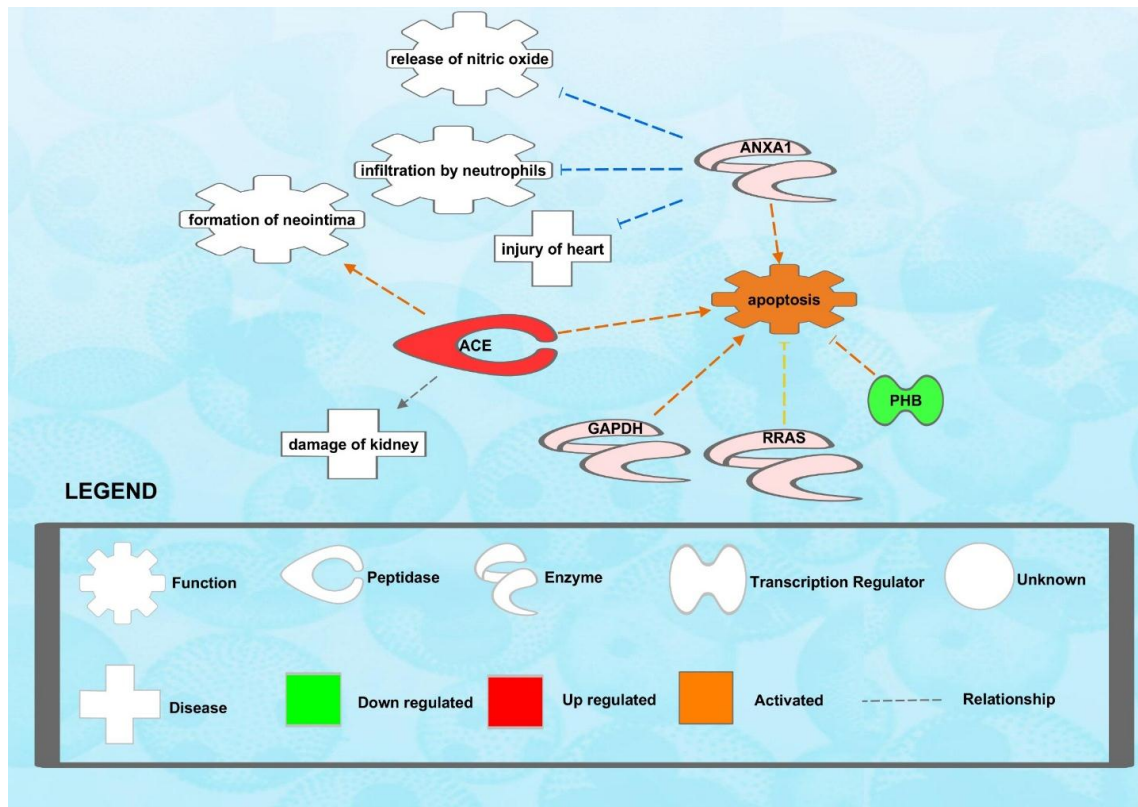


Figure 12: IPA map of insulin-treated rat aorta in comparison to diabetic rat aorta on cellular processes and diseases that lead to atherosclerosis (n=3).

ACE: angiotensin I converting enzyme; **ANXA1:** Annexin A1; **GAPDH:** Glyceraldehyde 3-Phosphate Dehydrogenase; **PHB:** Prohibitin; **RRAS:** Related Ras viral (r-ras) oncogene homolog

2. IPA analysis of dysregulated protein levels in the renal cortex

Protein lists derived from analysis of renal cortex tissue were investigated for pathways and processes that lead to diabetic nephropathy, which include nephrosis, nephritis, inflammation, oxidative stress, and fibrosis. Moreover, renal proteins that were predicted to influence cardiovascular pathways and diseases were also included to supplement earlier studies on effect of CKD on risk of CVD.

Peroxiredoxin 2 (PRDX2) is predicted to halt production of ROS and reduce its quantity, specifically that of hydrogen peroxide, in addition to inhibiting apoptosis and necrosis. In renal cortex tissue from hyperglycemic rats, however, its protein level is reduced, making the tissue more vulnerable to oxidative stress. Surprisingly, PRDX3 protein level was elevated, and it is also involved in reducing ROS quantity, specifically

that of lipid peroxide, which suggests a compensatory mechanism to withstand oxidative stress. Moreover, ras-related C3 botulinum toxin substrate 1 (Rac1) is predicted to increase production of ROS, but under hyperglycemia, its protein levels are lower than the control. Rac1 is also responsible for several disturbances in cell structure and mobility, in addition to causing cell necrosis, which is also aggravated by the elevated protein mitochondrial apoptosis-inducing factor (AIFM1) (Figure 13).

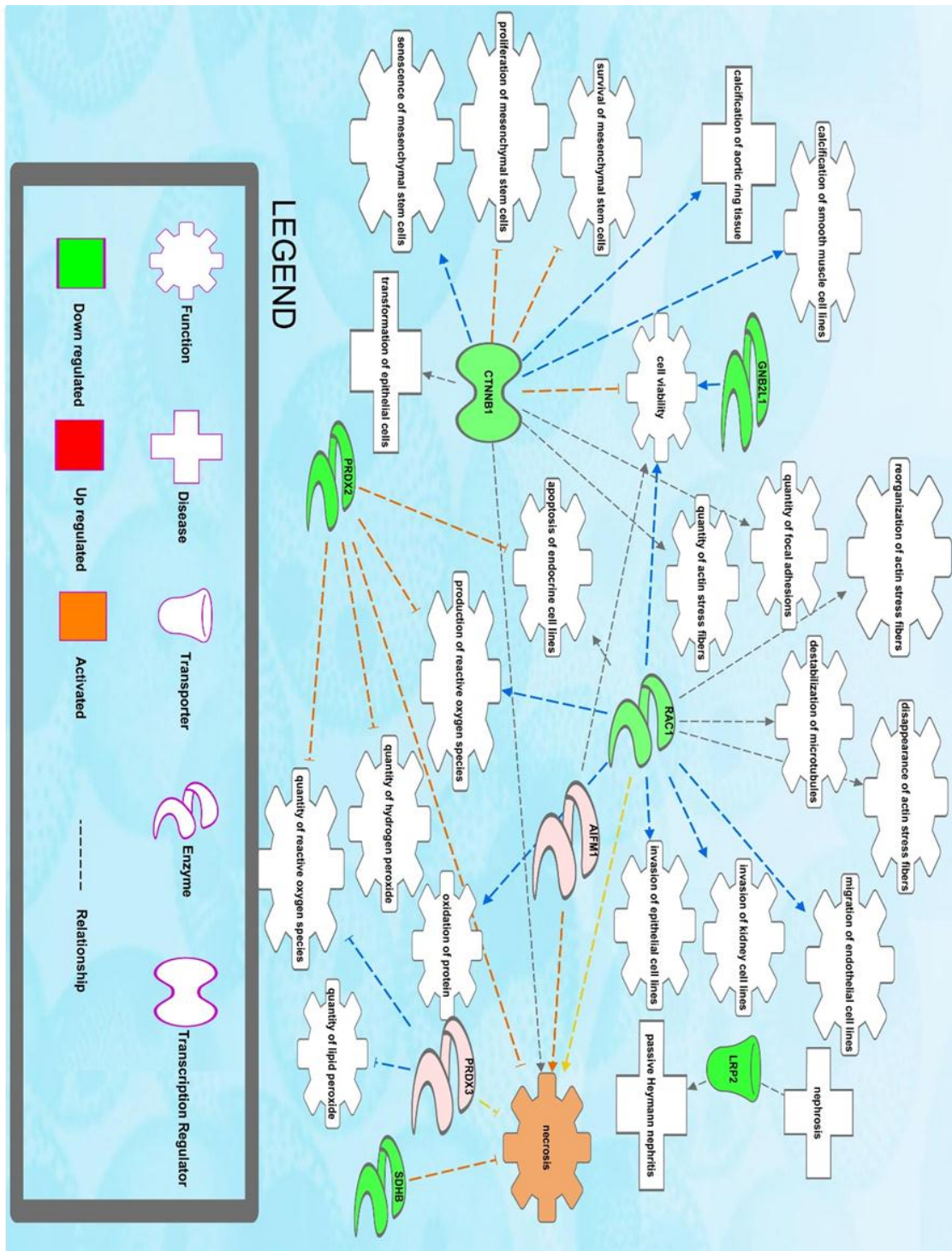


Figure 13: IPA map of diabetic rat renal cortex in comparison to control rat renal cortex on cellular processes and diseases that lead to diabetic nephropathy (n=3).

AIFM1: apoptosis-inducing factor, mitochondrion-associated 1; **CTNNB1**: catenin (cadherin associated protein), beta 1; **GNB2L1**: Guanine nucleotide binding protein (G-protein); **LRP2**: low density lipoprotein receptor-related protein 2; **PRDX2**: Peroxiredoxin 2; **PRDX3**: Peroxiredoxin 3; **RAC1**: ras-related C3 botulinum toxin substrate 1; **SDHB**: succinate dehydrogenase complex, subunit B

Upon insulin treatment, Rac1 protein level in the renal cortex was elevated in comparison to the hyperglycemic state. Besides causing structural and mobility disturbances in cooperation with elevated moesin protein (MSN), it was predicted to cause heart rate disturbances and promote migration and proliferation of VSMC. Other cardiovascular pathologies activated in these tissue include vessel infarction which is predicted to be caused by 2 elevated proteins, namely high mobility group box 1 (Hmgb1) and complement component 3 (C3). Low density lipoprotein receptor-related protein 2 (LRP2) was predicted to cause passive Heymann nephritis and nephrosis. In hyperglycemia, LRP2 levels were lower than controls. However, after insulin treatment, its levels exceeded that of the diabetic state. Moreover, Guanine nucleotide binding protein (GNAI2) was elevated and predicted to inhibit hypernatremia while promoting mitogen-activated protein kinase (MAPKKK) cascade and exocytosis of histamine from mast cells. Combined with the chemotaxis-inducing activity of RAC1 and Hmgb1, these factors suggest a pro-inflammatory function of those proteins. Even when compared to controls, GNAI2 levels remained elevated due to insulin treatment and was also predicted to inhibit hypernatremia while promoting natriuresis to reduce blood pressure (Figure 15).

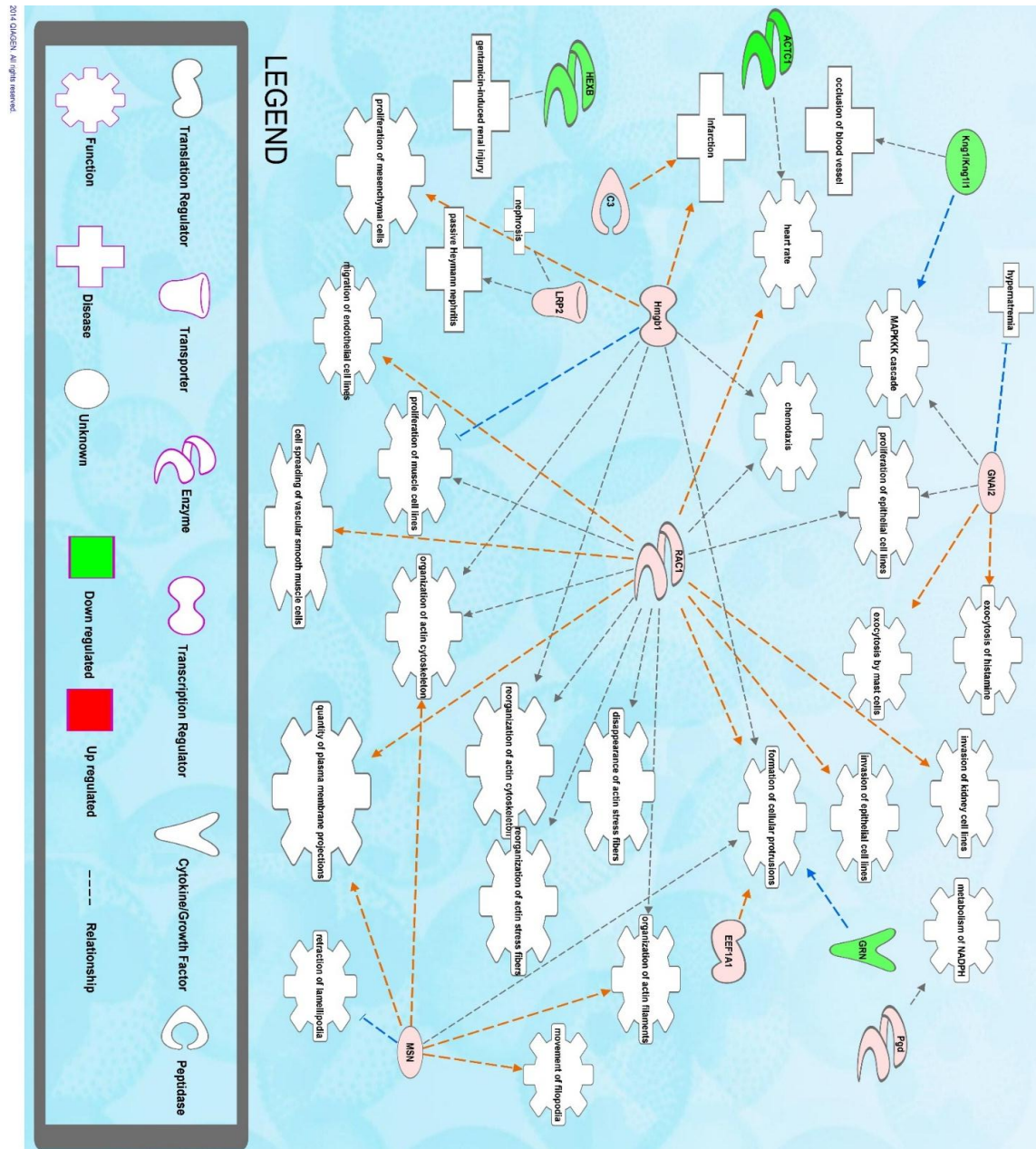


Figure 14: IPA map of insulin-treated rats renal cortex in comparison to diabetic rat renal cortex on cellular processes and diseases that lead to diabetic nephropathy (n=3). **ACTC1**: actin, alpha, cardiac muscle 1; **C3**: complement component 3; **EEF1A1**: ELONGATION FACTOR 1 alpha; **GNAI2**: Guanine nucleotide binding protein (G-protein); **GRN**: Granulin; **HEXB**: HEXOSAMINIDASE beta; **Hmgb1**: high mobility group box 1; **Kng1/Kng11**: kininogen 1; **LRP2**: low density lipoprotein receptor-related protein 2; **MSN**: moesin; **Pgd**: phosphogluconate dehydrogenase; **RAC1**: ras-related C3 botulinum toxin substrate 1

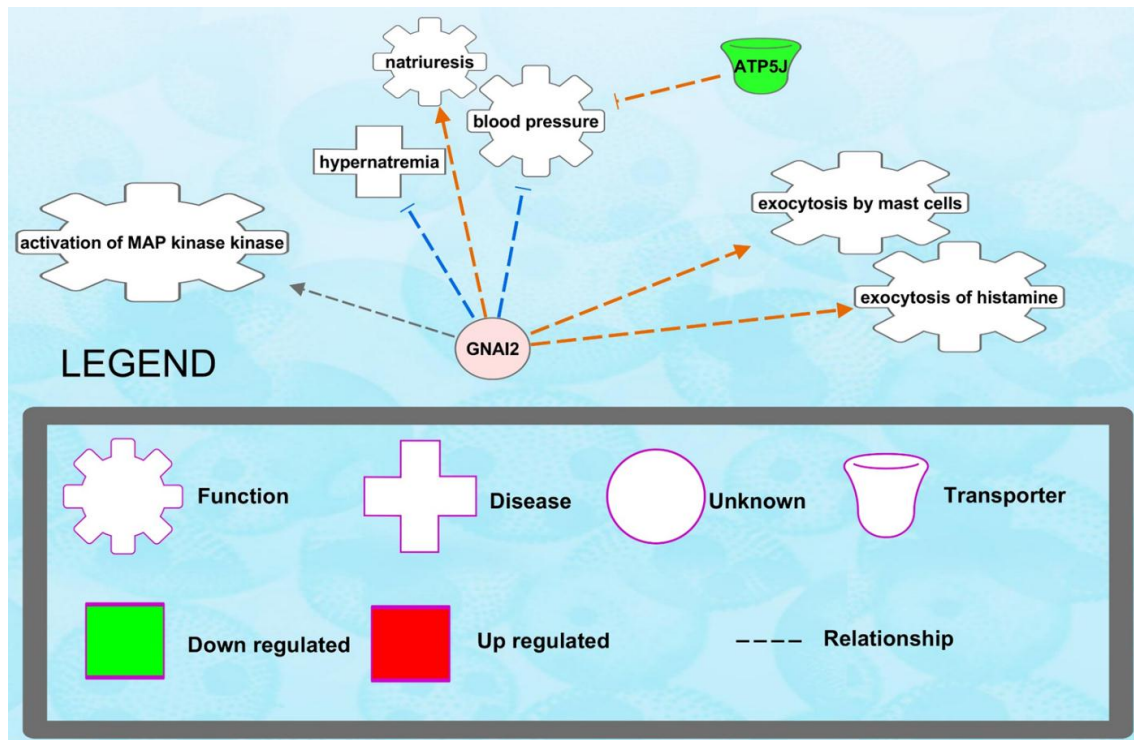


Figure 15: IPA map of insulin-treated rats renal cortex in comparison to control rat renal cortex on cellular processes and diseases that lead to diabetic nephropathy (n=3). **ATP5J**: ATP Synthase; **GNAI2**: Guanine nucleotide binding protein (G-protein)

3. GO analysis

To complement the created pathway maps, it is crucial to know which pathways were up-regulated and which were down-regulated due to the exposure and treatment in the experiment. Results from GO analysis using the KEGG pathway database are illustrated in Figures 16 – 19 for aortic samples and Figures 20 – 23 for renal cortex samples. GO analysis comparing aorta of untreated hyperglycemia to controls (Figures 16-17) showed a dysregulation in ECM homeostasis attributed to lower focal adhesion, ECM-receptor interaction, and regulation of actin cytoskeleton. Metabolic pathways in general were predicted to be both up and down-regulated, suggesting a systemic dysregulation in metabolic processes. Down-regulated metabolic pathways of interest included the insulin signaling pathway, clearly due to lack of insulin, which consequently lowered the starch and sucrose metabolism, despite predicted up

regulation in glycolysis. Glutathione metabolism that maintains NADPH balance in the cell was also lowered, suggesting possible depletion of NADPH as the oxidative phosphorylation pathway was up-regulated. This is also suggestive of increased ROS such as superoxide and hydrogen peroxide following oxidative phosphorylation. Interestingly, cardiovascular pathologies such as Arrhythmogenic right ventricular cardiomyopathy was predicted to be lower. However, cardiac muscle and VSMC contraction were lowered as well, indicating possible cardiovascular ailments. The MAPK, PPAR signaling pathway, and chemokine signaling pathway were predicted to be down-regulated as well. Insulin treatment maintained lowered focal adhesion and regulation of actin cytoskeleton, in addition to lowered metabolic pathways, glutathione metabolism, insulin signaling pathway, starch and sucrose metabolism, and glycolysis. Moreover, the calcium-signaling pathway was reduced as well, possibly leading to the observed lower VSMC and cardiac muscle contraction. Interestingly, oxidative phosphorylation was maintained elevated even after insulin treatment, in addition to activation of the renin-angiotensin system and inositol phosphate metabolism (Figures 18-19). Further analysis comparing renal cortex of untreated hyperglycemia to controls also showed that the metabolic pathways and oxidative phosphorylation were dysregulated and showing paradoxical results, while glutathione metabolism, starch and sucrose metabolism, glycolysis, PPAR, and apoptosis were up-regulated (Figures 20-21). Insulin treatment reversed some of the changes observed in hyperglycemia of the renal cortex by lowering the calcium-signaling pathway, PPAR signaling pathway, oxidative phosphorylation, glutathione metabolism, and glycolysis. Further contrast from the aorta was seen in the up regulation of actin cytoskeleton, glycolysis, and chemokine signaling pathways (Figures 22-23).

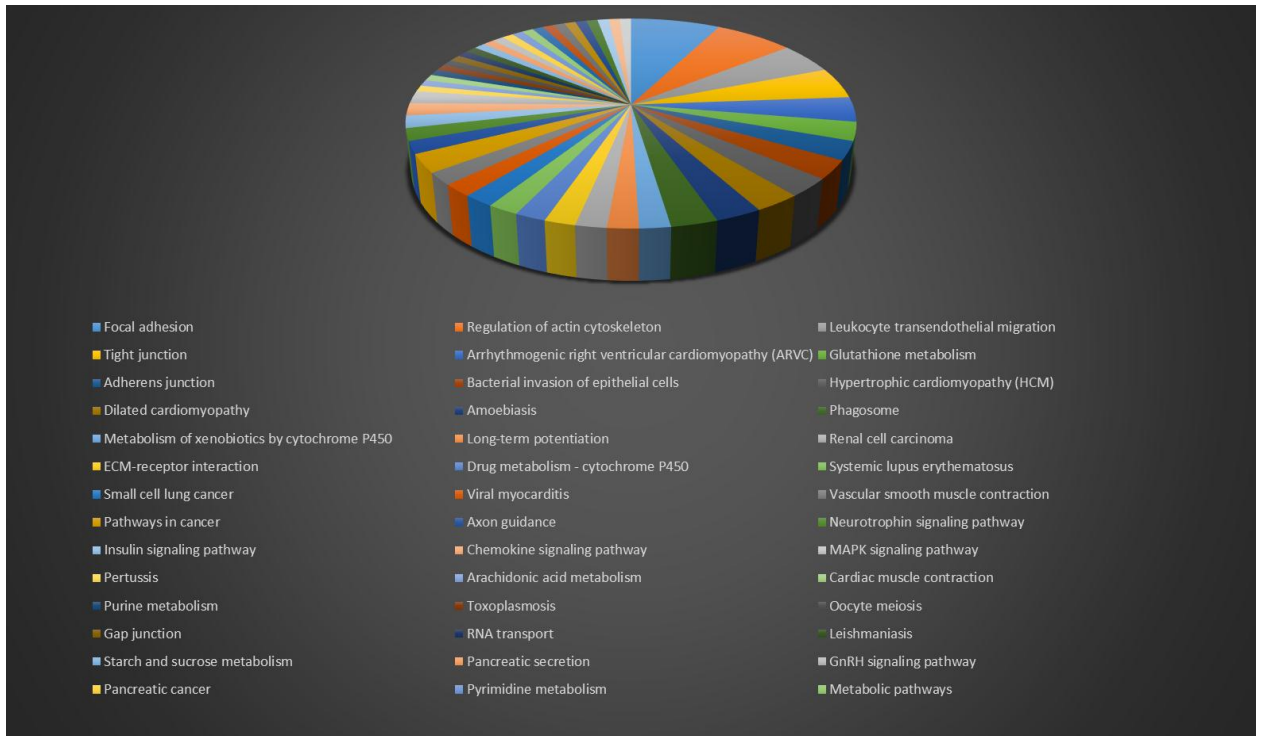


Figure 16: GO analysis illustrating down-regulated pathways and cellular processes in the aorta due to untreated hyperglycemia in comparison to controls

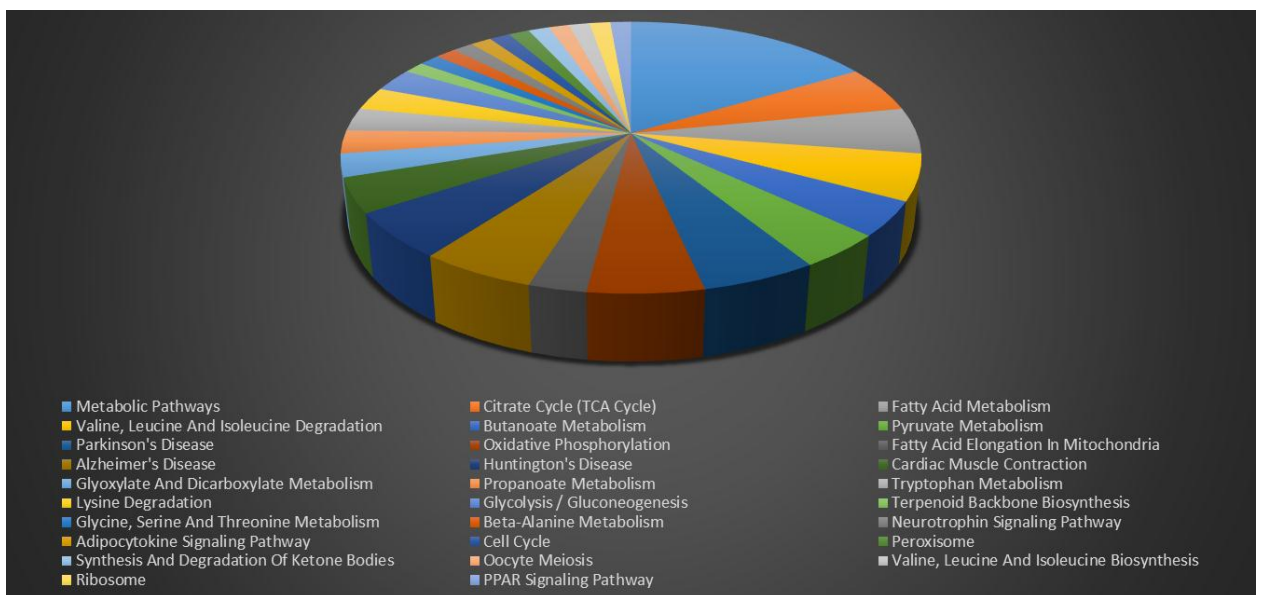


Figure 17: GO analysis illustrating up-regulated pathways and cellular processes in the aorta due to untreated hyperglycemia in comparison to controls

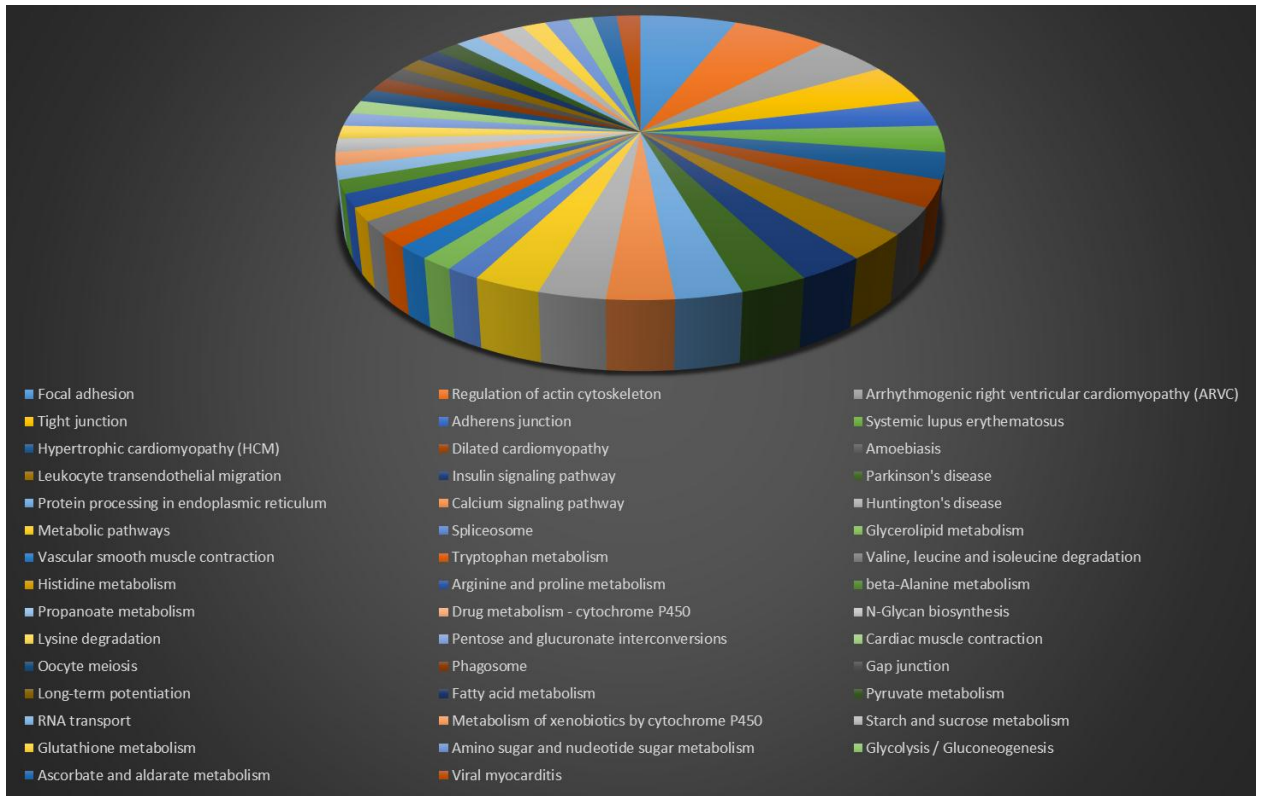


Figure 18: GO analysis illustrating down-regulated pathways and cellular processes in the aorta due to Insulin-treated hyperglycemia in comparison to untreated hyperglycemia

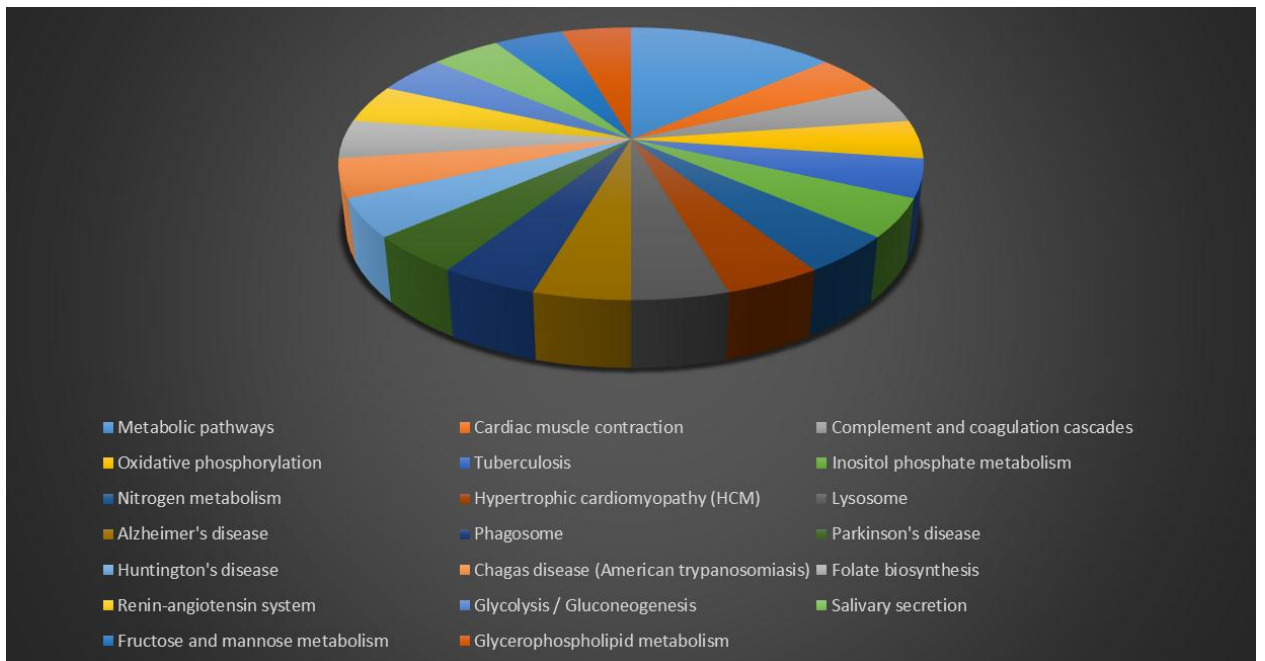


Figure 19: GO analysis illustrating up-regulated pathways and cellular processes in the aorta due to Insulin-treated hyperglycemia in comparison to untreated hyperglycemia

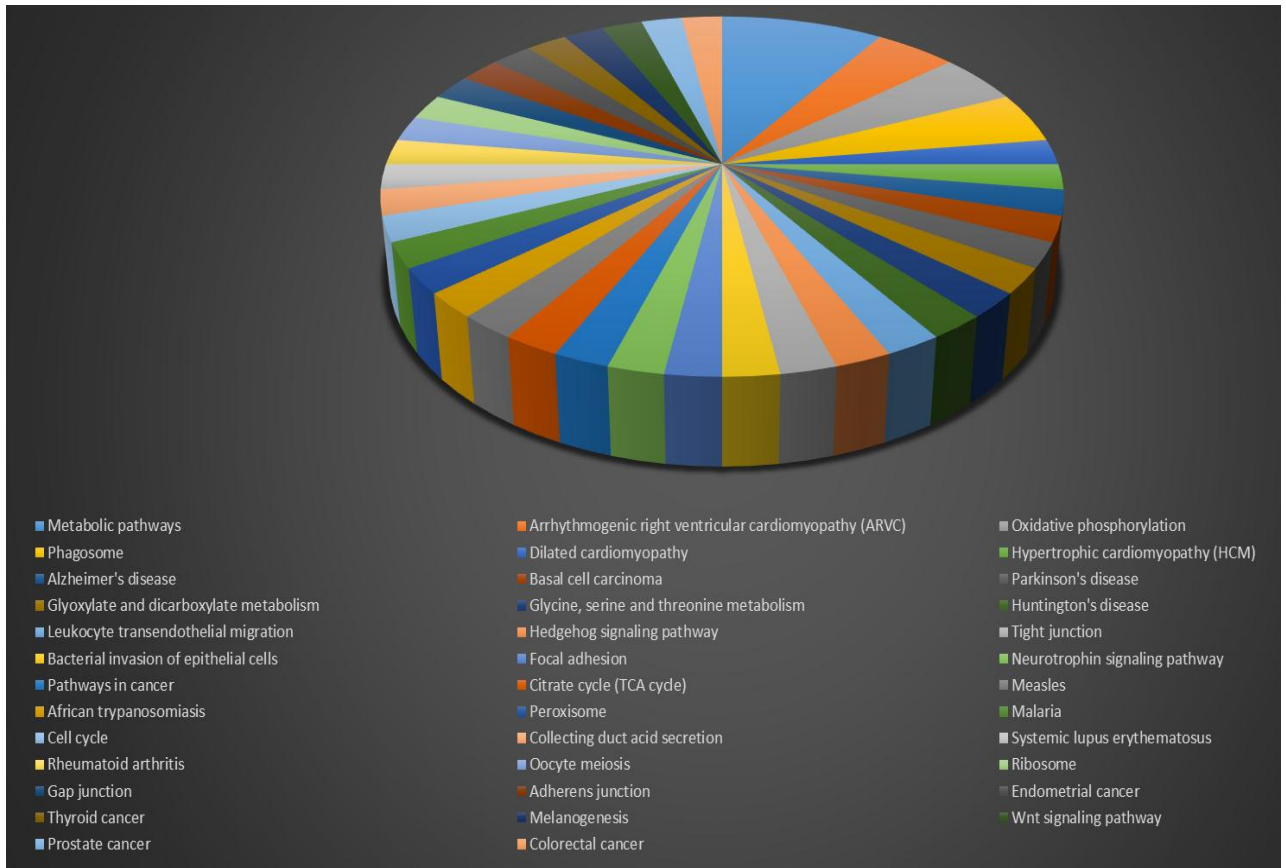


Figure 20: GO analysis illustrating down-regulated pathways and cellular processes in the renal cortex due to untreated hyperglycemia in comparison to controls

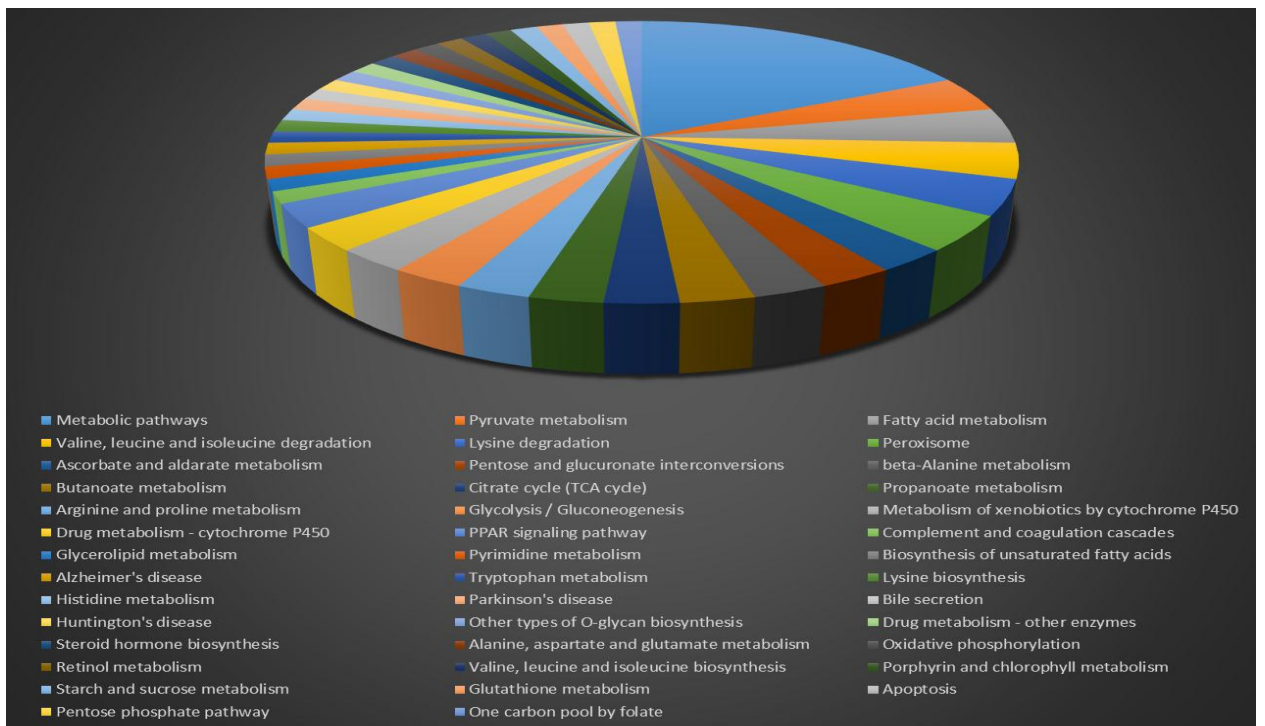


Figure 21: GO analysis illustrating up-regulated pathways and cellular processes in the renal cortex due to untreated hyperglycemia in comparison to controls

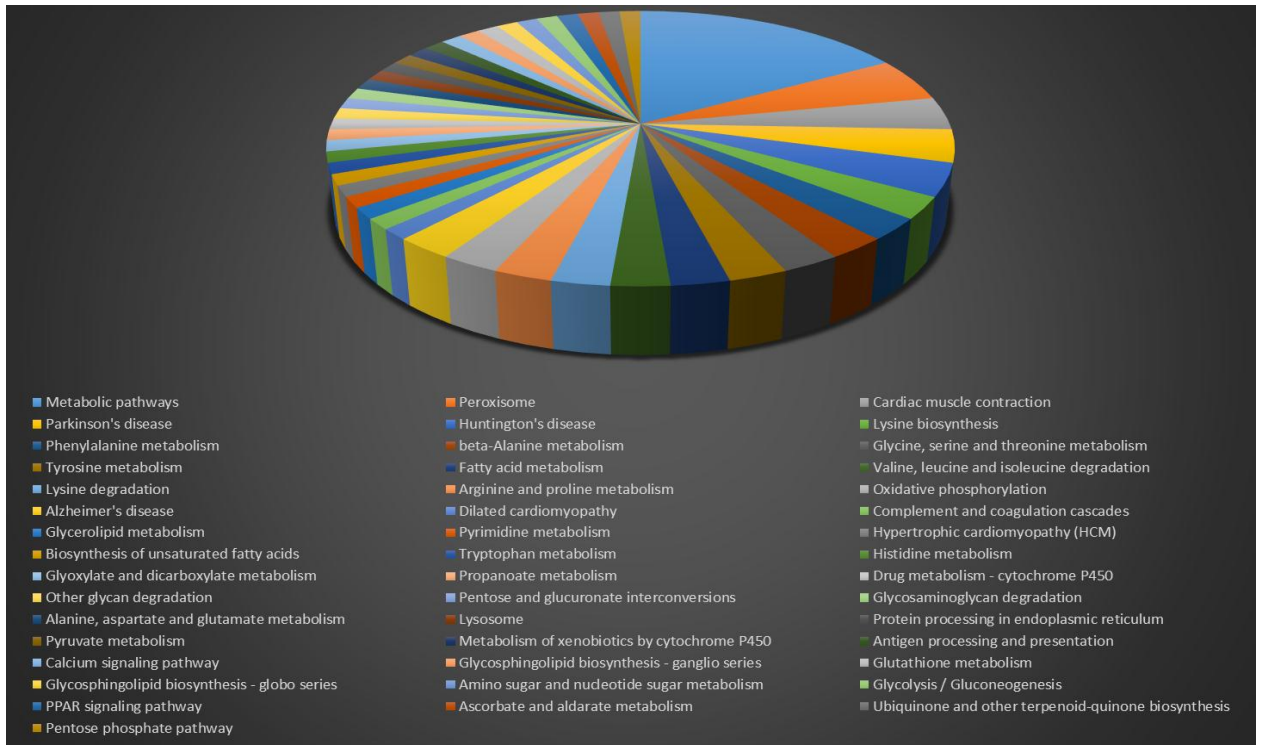


Figure 22: GO analysis illustrating down-regulated pathways and cellular processes in the renal cortex due to Insulin-treated hyperglycemia in comparison to untreated hyperglycemia

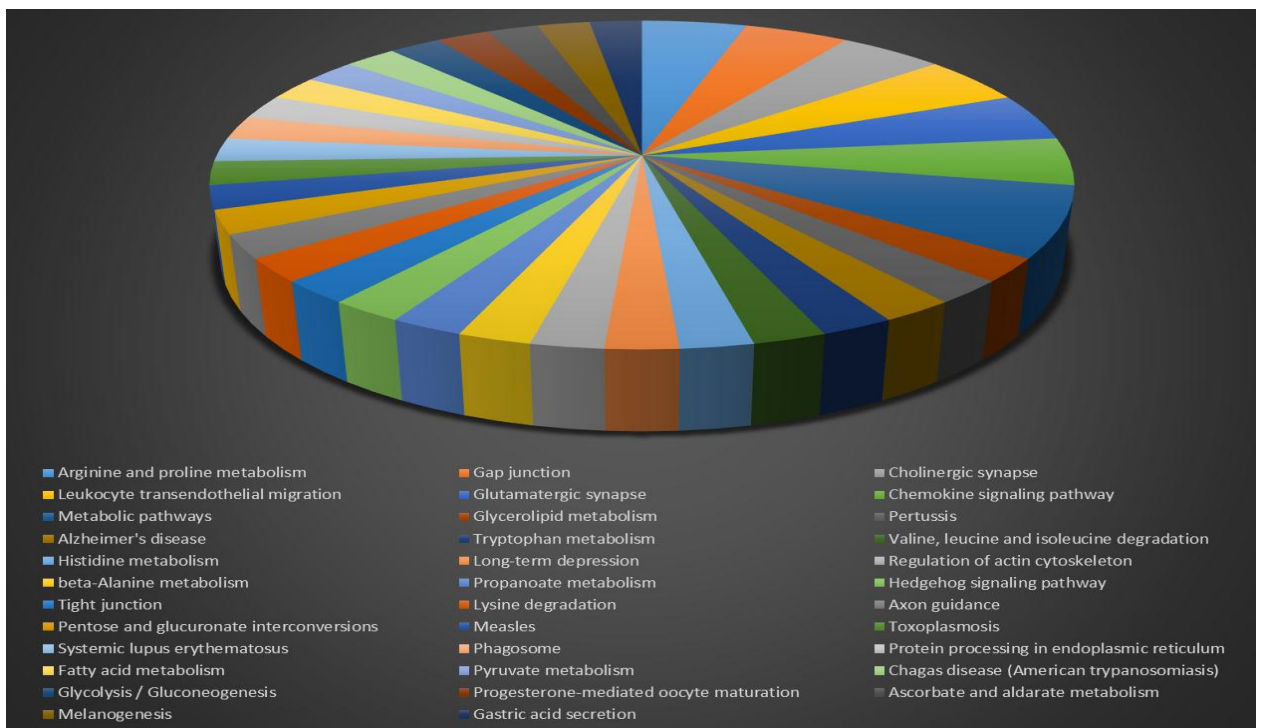


Figure 23: GO analysis illustrating up-regulated pathways and cellular processes in the renal cortex due to Insulin-treated hyperglycemia in comparison to untreated hyperglycemia

CHAPTER VI

DISCUSSION

Hyperglycemia is the one of the primary modifiable mediator of vascular complications in T1DM. The rate of progression and severity of vascular complications such as atherosclerosis, MI, nephropathy, retinopathy, neuropathy, depend on the timeliness and aggressiveness of the treatment. Poor glycemic control and chronic exposure to hyperglycemia result in the phenomenon of metabolic memory. This phenomenon is manifested through several mechanisms, the most notable of which is the mitotically heritable epigenetic modifications that persist despite normalization of blood glucose levels after it is established. The role of the Kinin-Kallikrein system (KKS) in vascular homeostasis and pathology has been extensively studied and correlated with signaling pathways leading to generation of ROS, pro-inflammatory cytokines, and fibrotic proteins that contribute to diabetic vascular complications. However, whether the control of expression of KKS genes in T1DM is a result of epigenetic modifications in the chromatin of vascular smooth muscle cells has not been studied yet. More specifically, no studies have examined the DNA methylation level of *BDKRB1* and *BDKRB2* promoter regions.

Our findings that expression of *BDKRB1* and *BDKRB2* mRNA is increased as a result of hyperglycemia is consistent with earlier studies that also found that B2-kinin receptors are regulated by glucose in vascular smooth muscle cells through the PKC pathway [60] while expression of B1-kinin receptors is increased upon tissue injury, inflammation, and/or diabetes [119]. More importantly, using high resolution melting PCR, we have shown that the promoter regions of *BDKRB1* and *BDKRB2* genes in VSMCs from T1DM rats demonstrated 8.91 and 4.75 fold decrease in DNA methylation level, respectively. These results are in line with the increase of expression

of these genes detected by qPCR. However, *in vitro* studies did not produce the same results as little to no difference in the melting curve was detected between the high glucose treated cells and the control cells. These discrepancies are due to the fact that the microenvironment of VSMCs *in vivo* is quite different than the cell culture environment as it provides signals from other cell types, most notably the endothelium, which is the main regulator of vascular tone and homeostasis [29]. Moreover, endothelium-derived BK may have contributed to the activation of the receptors, a missing element in the *in vitro* studies.

The expression pro-inflammatory cytokines such as TNF α has also been documented to be increased in diabetes [54; 58]. TNF α has been shown to induce ROS production [57] in addition to increasing the expression of other pro-inflammatory agents such as IL-6, IL-1 β , MCSF, and MCP-1 in VSMC from T2DM mice [59]. Our results are in accordance with these studies whereby expression of *TNF α* gene was found to be induced 4.2 ± 0.9 folds by high glucose and 1.3 ± 0.1 folds by hyperglycemia ($p < 0.05$). Moreover, the expression of pro-inflammatory genes downstream of TNF α was higher, especially IL-6 (2.9 ± 1.3) and IL-1 β (2.0 ± 1.0) expression *in vitro*. Next, we explored whether hyperglycemia increases TNF α expression by the DNA methylation level at its promoter methylation levels. Indeed, results revealed that TNF α promoter region had 1.75 lower DNA methylation levels than controls.

Given that CRP acts upstream to TNF α to increase its expression and bioactivity as observed in one study [120], we studied the expression level of CRP and found that it was 5.2 ± 3.2 folds higher *in vitro* and 3.5 ± 0.3 folds higher *in vivo*, in comparison to controls ($p < 0.05$), which suggests that it is also regulating expression of TNF α .

Unexpectedly, one study suggested that hyperglycemia causes both DNA hypomethylation and H3K9/K14 hyperacetylation, a gene-activating epigenetic mark, in HMOX1 promoter, leading to an increase in its expression. HMOX1 is known for activating IL10 and conferring anti-inflammatory activity [96]. These findings are also in line with our results as we demonstrated that IL10 gene expression in VSMCs was increased by 9.7 folds \pm 4.0 due to high glucose in cell culture and by 3.0 folds \pm 0.7 due to hyperglycemia in rats ($p < 0.05$).

The signaling pathway downstream of the kinin receptors leads to increased expression of *Nox1* and *Nox4*, which are the main source of ROS implicated in diabetic vascular complications. Preliminary data from our laboratory have demonstrated that treatment of rat podocytes with BK induced the expression of *Nox1* and *Nox4* (Unpublished data). Since BK and glucose synergise to activate common pathways [76; 121], we tested the effect of hyperglycemia on expression level of *Nox1* and 4 in VSMCs. Results revealed that *Nox1* expression increased 5.0 \pm 3.0 folds *in vitro* and 1.3 \pm 0.1 folds *in vivo* ($p < 0.05$), whereas *Nox4* decreased 0.4 \pm 0.2 folds *in vitro* but increased 1.8 \pm 0.4 folds *in vivo* ($p < 0.05$). More preliminary data from our laboratory have determined a definitive link between B2R activation and *CTGF* gene expression through crosstalk of B2R with S1PR. The enzyme that links the two receptors is SphK1. SphK1 was found to be activated after induction of VSMC with BK through activation of *Nox1* and *Nox4* and ROS production. This was confirmed by using NAC, a scavenger of ROS, that inhibited SphK1 activity. The importance of this pathway is that TGF β and *CTGF* are downstream of S1PR and hence the expression of *Nox1* and *Nox4* lead to expression of *CTGF* and *TGF* leading to increased ECM deposition and fibrosis (Figure 1). In this study we were able to confirm that *CTGF* mRNA levels were up-regulated 2.7 \pm 0.7 folds *in vitro* and 2.3 \pm 1.5 folds *in vivo* ($p < 0.05$).

Cellular fibrosis is a hallmark of diabetic vascular complications due to accumulation of ECM, which plays a pivotal role in progression of atherogenesis [122]. The main ECM component found in atherosclerotic plaques is collagen I, which is synthesized in VSMC in response to stimuli from growth factors. One of the central factors involved in vascular fibrosis is TGF- β as it induces collagen I expression in VSMC, changing them from their contractile state to a synthetic state [78]. Fibrosis in VSMCs has also been attributed to the binding of BK to its receptors, which was observed to lead to autocrine activation of TGF- β 1 [76]. In fact, deletion of DKRB1 was found to ameliorate renal fibrosis, which could mean a role for it in mediating fibrosis [73]. Results from the proteomics studies conducted by our collaborators in Texas Tech University on aorta tissue samples extracted from the same rats that we have extracted DNA and RNA for our experiments demonstrated that several proteins involved in fibrosis were up-regulated. Most notably, TGF- β protein levels were found to be 7.1 folds higher in aorta of diabetic versus control rats ($P < 0.05$). Moreover, its levels did not change upon treatment of T1DM rats with insulin ($P < 0.05$). In our gene expression experiments, levels of *TGF- β 1* expression in T1DM rats and insulin-treated T1DM rats were increased by 1.4 ± 0.1 folds and 1.3 ± 0.3 folds, respectively, compared to control ($p < 0.05$). Moreover, levels of *TGF- β 2* expression showed a 4.0 ± 0.55 fold increase in culture and a 1.3 ± 0.1 fold increase in diabetic rats, compared to controls ($p < 0.05$). High resolution melt analysis also revealed that *TGF- β 2* was hypomethylated at the promoter region by 1.45 fold compared to the control. Taken together, these results show the persistence of expression of fibrosis-mediating proteins despite achieving normal glucose levels with insulin as indicated in Figure 2, hence proving the contribution of metabolic memory, in part through DNA methylation, to cellular fibrosis and ultimately macrovascular complications.

Most *in vitro* results show that mannitol treatment did not cause a fold change as high glucose treatment did, if any. This is direct evidence that the increase in fold change due to high glucose is not due to osmotic pressure, but due to intracellular signaling pathways and epigenetic modifications as demonstrated in the melt curve analysis.

Another component of ECM, FN1, is also known to increase due to hyperglycemia and contributes to fibrosis. Several studies also found that BK stimulates FN1 production. In fact, studies confirm that hyperglycemia and BK signaling synergize to induce expression of FN1, in addition to collagen I subunits and TGF- β [76; 121]. In our study, consistent results were obtained for FN1 gene expression which increased by 1.3 ± 0.3 and 3.2 ± 0.7 folds *in vitro* and *in vivo*, respectively, compared to the controls ($p < 0.05$). Similarly, FN1 protein quantification was up-regulated by 2.78 folds in T1DM rats versus controls. Systems Biology Assessment of FN1 role in diabetic complications have shown that it was predicted to contribute to several atherosclerosis-promoting pathologies including infarction of blood vessels, diabetes, accumulation of ECM and fibrosis. It also activated cell movement directly and through formation of cellular protrusions, focal adhesions, actin stress fibers, and filopodia, in addition to promotion of cell spreading, attachment, and adhesion.

Proteomics data on our samples have also indicated that ACE (or kininase II) was elevated in the insulin-treated T1DM rats *versus* the control and T1DM rats in which it was not detected. ACE is an endogenous metalloproteases that quickly metabolizes BK and attenuates its activity. Given the protective role BK plays in stimulating the production of eNOS, the upregulation of ACE could be contributing to the persistence of the aberrant gene expression in the insulin-treated rats [123].

In the aorta, GO analysis revealed that hyperglycemia induced oxidative phosphorylation pathway which is a significant source of ROS. The interesting finding, is that even after treatment with insulin, the oxidative phosphorylation pathway remained up-regulated . The persisting dysregulations of some of these pathways and processes even upon treatment of hyperglycemia are suggestive of a metabolic memory maintained by epigenetic modifications due to changes in the microenvironment of the cell. Moreover, an interesting link between diabetic kidney disease and CVD emerged as the levels of Rac1 and Hmgb1 proteins in the renal cortex increased upon insulin treatment in comparison to the untreated T1DM rats. IPA analysis revealed that Rac1 was predicted to cause heart rate disturbances and promote migration and proliferation of VSMC. While elevated Hmgb1 and C3 were predicted to cause vascular infarction.

CHAPTER VII

CONCLUSIONS

A. Main findings of the study

Our results revealed that hyperglycemia induced the overexpression of *BDKRB1*, *BDKRB2*, and the pathways downstream of these receptors in VSMCs, known to cause oxidative stress, cellular fibrosis, and inflammation; hallmarks of atherosclerosis. DNA hypomethylation at the promoter region of *BDKRB1* and *BDKRB2* was recorded and might contribute to the overexpression observed. Moreover, DNA of pro-inflammatory gene *TNF α* and fibrosis-inducing gene *TGF- β* were also hypomethylated at the promoter region, possibly contributing to their overexpression. Pathways downstream of the kinin receptors have also been found to be up-regulated in the aorta and persist as such even after lowering blood glucose with intensive insulin treatment. In fact, the expression of many genes was higher after insulin treatment in comparison to T1DM rats. This correlation is in line with studies which have demonstrated that insulin acts as a pro-atherogenic growth factor [124]. Moreover, clinical studies have shown that intensive insulin treatment of patients with established vascular complications is counterproductive and leads to worsening of cardiovascular outcomes [16]. Hence, the question of whether these observations are due to hyperglycemic metabolic memory or insulin treatment must be addressed.

B. Limitations of the study

Our melt curve analysis results need to be verified against a standard method for assessing DNA methylation level such as DNA sequencing. In addition, low sample size, in addition to the method complexity, might have caused sample-to-sample

variability and hence lowered the statistical significance. Moreover, while MS-HRM uses primers to amplify and melt only specific regions expected to show aberrant DNA methylation, global DNA methylation studies would detect any change in methylation across the entire promoter and gene sequence.

C. Future prospects

Sequencing of target genes for detection of alterations in DNA methylation at CpG sites as an alternative to MS-HRM would verify the obtained results and determine which sites are specifically methylated and whether any known binding sites for transcription factors are affected, thus affecting transcription. Moreover, further analysis of the proteomics data with IPA will help explore common pathways between diabetic nephropathy in the kidney cortex and atherosclerosis in the aorta. The proteomics data can also be analyzed to look at post translational modifications of proteins such as phosphorylation, glycosylation and oxidation and their effect on protein activity. Validation of the proteomics data can be done via MRM experiments.

Ideally, it would be crucial to repeat these experiments in ApoE knockout mice as a model of atherosclerosis to link the effect of methylation to vascular complications. Given that BK and glucose synergize to activate pro-inflammatory and fibrosis inducing pathways that lead to vascular complications, it would be interesting to see if BK treatment of VSMCs adds another layer of alterations in DNA methylation. Hence, co treatment of VSMC with glucose and BK in culture could help assimilate the *in vitro* observations to those seen *in vivo*. Finally, an assessment of ROS generation using DHE staining would help confirm the predicted outcomes by systems biology and GO studies.

BIBLIOGRAPHY

1. "International Diabetes Federation. *Idf Diabetes Atlas*, 6th Edn. Brussels, Belgium: International Diabetes Federation, 2013."
2. Onkamo, P., S. Vaananen, M. Karvonen, and J. Tuomilehto. "Worldwide Increase in Incidence of Type I Diabetes--the Analysis of the Data on Published Incidence Trends." *Diabetologia* 42, no. 12 (1999): 1395-403.
3. Pundziute-Lycka, A., G. Dahlquist, L. Nystrom, H. Arnqvist, E. Bjork, G. Blohme, J. Bolinder, J. W. Eriksson, G. Sundkvist, and J. Ostman. "The Incidence of Type I Diabetes Has Not Increased but Shifted to a Younger Age at Diagnosis in the 0-34 Years Group in Sweden 1983-1998." *Diabetologia* 45, no. 6 (2002): 783-91.
4. Narayan, K. M., J. P. Boyle, T. J. Thompson, S. W. Sorensen, and D. F. Williamson. "Lifetime Risk for Diabetes Mellitus in the United States." *JAMA* 290, no. 14 (2003): 1884-90.
5. "The Effect of Intensive Treatment of Diabetes on the Development and Progression of Long-Term Complications in Insulin-Dependent Diabetes Mellitus. The Diabetes Control and Complications Trial Research Group." *N Engl J Med* 329, no. 14 (1993): 977-86.
6. Holman, R. R., S. K. Paul, M. A. Bethel, D. R. Matthews, and H. A. Neil. "10-Year Follow-up of Intensive Glucose Control in Type 2 Diabetes." *N Engl J Med* 359, no. 15 (2008): 1577-89.
7. Zinman, B., S. Genuth, and D. M. Nathan. "The Diabetes Control and Complications Trial/Epidemiology of Diabetes Interventions and Complications Study: 30th Anniversary Presentations." *Diabetes Care* 37, no. 1 (2014): 8.
8. Turner, R. C., C. A. Cull, V. Frighi, and R. R. Holman. "Glycemic Control with Diet, Sulfonylurea, Metformin, or Insulin in Patients with Type 2 Diabetes Mellitus: Progressive Requirement for Multiple Therapies (Ukpds 49). Uk Prospective Diabetes Study (Ukpds) Group." *JAMA* 281, no. 21 (1999): 2005-12.
9. "Uk Prospective Diabetes Study (Ukpds). Viii. Study Design, Progress and Performance." *Diabetologia* 34, no. 12 (1991): 877-90.
10. "Intensive Blood-Glucose Control with Sulphonylureas or Insulin Compared with Conventional Treatment and Risk of Complications in Patients with Type 2 Diabetes (Ukpds 33). Uk Prospective Diabetes Study (Ukpds) Group." *Lancet* 352, no. 9131 (1998): 837-53.
11. Gaede, P. H., P. V. Jepsen, J. N. Larsen, G. V. Jensen, H. H. Parving, and O. B. Pedersen. "[the Steno-2 Study. Intensive Multifactorial Intervention Reduces the Occurrence of Cardiovascular Disease in Patients with Type 2 Diabetes]." *Ugeskr Laeger* 165, no. 26 (2003): 2658-61.

12. Gaede, P., P. Vedel, N. Larsen, G. V. Jensen, H. H. Parving, and O. Pedersen. "Multifactorial Intervention and Cardiovascular Disease in Patients with Type 2 Diabetes." *N Engl J Med* 348, no. 5 (2003): 383-93.
13. Gaede, P., H. Lund-Andersen, H. H. Parving, and O. Pedersen. "Effect of a Multifactorial Intervention on Mortality in Type 2 Diabetes." *N Engl J Med* 358, no. 6 (2008): 580-91.
14. Dormandy, J. A., B. Charbonnel, D. J. Eckland, E. Erdmann, M. Massi-Benedetti, I. K. Moules, A. M. Skene, M. H. Tan, P. J. Lefebvre, G. D. Murray, E. Standl, R. G. Wilcox, L. Wilhelmsen, J. Betteridge, K. Birkeland, A. Golay, R. J. Heine, L. Koranyi, M. Laakso, M. Mokan, A. Norkus, V. Pirags, T. Podar, A. Scheen, W. Scherbaum, G. Schernthaner, O. Schmitz, J. Skrha, U. Smith, and J. Taton. "Secondary Prevention of Macrovascular Events in Patients with Type 2 Diabetes in the Proactive Study (Prospective Pioglitazone Clinical Trial in Macrovascular Events): A Randomised Controlled Trial." *Lancet* 366, no. 9493 (2005): 1279-89.
15. Patel, A., S. MacMahon, J. Chalmers, B. Neal, M. Woodward, L. Billot, S. Harrap, N. Poulter, M. Marre, M. Cooper, P. Glasziou, D. E. Grobbee, P. Hamet, S. Heller, L. S. Liu, G. Mancia, C. E. Mogensen, C. Y. Pan, A. Rodgers, and B. Williams. "Effects of a Fixed Combination of Perindopril and Indapamide on Macrovascular and Microvascular Outcomes in Patients with Type 2 Diabetes Mellitus (the Advance Trial): A Randomised Controlled Trial." *Lancet* 370, no. 9590 (2007): 829-40.
16. Gerstein, H. C., M. E. Miller, R. P. Byington, D. C. Goff, Jr., J. T. Bigger, J. B. Buse, W. C.ushman, S. Genuth, F. Ismail-Beigi, R. H. Grimm, Jr., J. L. Probstfield, D. G. Simons-Morton, and W. T. Friedewald. "Effects of Intensive Glucose Lowering in Type 2 Diabetes." *N Engl J Med* 358, no. 24 (2008): 2545-59.
17. Duckworth, W., C. Abraira, T. Moritz, D. Reda, N. Emanuele, P. D. Reaven, F. J. Zieve, J. Marks, S. N. Davis, R. Hayward, S. R. Warren, S. Goldman, M. McCarren, M. E. Vitek, W. G. Henderson, and G. D. Huang. "Glucose Control and Vascular Complications in Veterans with Type 2 Diabetes." *N Engl J Med* 360, no. 2 (2009): 129-39.
18. Home, P. D., S. J. Pocock, H. Beck-Nielsen, P. S. Curtis, R. Gomis, M. Hanefeld, N. P. Jones, M. Komajda, and J. J. McMurray. "Rosiglitazone Evaluated for Cardiovascular Outcomes in Oral Agent Combination Therapy for Type 2 Diabetes (Record): A Multicentre, Randomised, Open-Label Trial." *Lancet* 373, no. 9681 (2009): 2125-35.
19. Levin, B. E. "Metabolic Imprinting: Critical Impact of the Perinatal Environment on the Regulation of Energy Homeostasis." *Philos Trans R Soc Lond B Biol Sci* 361, no. 1471 (2006): 1107-21.

20. El-Osta, A., D. Brasacchio, D. Yao, A. Pocai, P. L. Jones, R. G. Roeder, M. E. Cooper, and M. Brownlee. "Transient High Glucose Causes Persistent Epigenetic Changes and Altered Gene Expression During Subsequent Normoglycemia." *J Exp Med* 205, no. 10 (2008): 2409-17.
21. Nathan, D. M., P. A. Cleary, J. Y. Backlund, S. M. Genuth, J. M. Lachin, T. J. Orchard, P. Raskin, and B. Zinman. "Intensive Diabetes Treatment and Cardiovascular Disease in Patients with Type 1 Diabetes." *N Engl J Med* 353, no. 25 (2005): 2643-53.
22. Ihnat, M. A., J. E. Thorpe, and A. Ceriello. "Hypothesis: The 'Metabolic Memory', the New Challenge of Diabetes." *Diabet Med* 24, no. 6 (2007): 582-6.
23. Blomen, V. A., and J. Boonstra. "Stable Transmission of Reversible Modifications: Maintenance of Epigenetic Information through the Cell Cycle." *Cell Mol Life Sci* 68, no. 1 (2011): 27-44.
24. Riggs, A.D., and T.N. Porter. *Epigenetic Mechanisms of Gene Regulation*. Vol. 32 Mechanisms of Gene Regulation, Edited by V.E.A Russo, R.A. Martienssen and A.D. Riggs. Cold Spring Harbor, NY: Cold Spring Harbor Laboratory Press, 1996.
25. Suganuma, T., and J. L. Workman. "Signals and Combinatorial Functions of Histone Modifications." *Annu Rev Biochem* 80, (2011): 473-99.
26. Yoder, J. A., N. S. Soman, G. L. Verdine, and T. H. Bestor. "DNA (Cytosine-5)-Methyltransferases in Mouse Cells and Tissues. Studies with a Mechanism-Based Probe." *Journal of Molecular Biology* 270, no. 3 (1997): 385-395.
27. Kannel, W. B., and D. L. McGee. "Diabetes and Cardiovascular Disease. The Framingham Study." *JAMA* 241, no. 19 (1979): 2035-8.
28. Ross, R. "Atherosclerosis--an Inflammatory Disease." *N Engl J Med* 340, no. 2 (1999): 115-26.
29. Davignon, J., and P. Ganz. "Role of Endothelial Dysfunction in Atherosclerosis." *Circulation* 109, no. 23 Suppl 1 (2004): III27-32.
30. Luscher, T. F., and M. Barton. "Biology of the Endothelium." *Clin Cardiol* 20, no. 11 Suppl 2 (1997): II-3-10.
31. Luscher, T. F., F. C. Tanner, M. R. Tschudi, and G. Noll. "Endothelial Dysfunction in Coronary Artery Disease." *Annu Rev Med* 44, (1993): 395-418.
32. Gordon, J. L., and W. Martin. "Endothelium-Dependent Relaxation of the Pig Aorta: Relationship to Stimulation of 86rb Efflux from Isolated Endothelial Cells." *Br J Pharmacol* 79, no. 2 (1983): 531-41.

33. Siragy, H. M., A. A. Jaffa, and H. S. Margolius. "Bradykinin B2 Receptor Modulates Renal Prostaglandin E2 and Nitric Oxide." *Hypertension* 29, no. 3 (1997): 757-62.
34. Toda, N., K. Bian, T. Akiba, and T. Okamura. "Heterogeneity in Mechanisms of Bradykinin Action in Canine Isolated Blood Vessels." *Eur J Pharmacol* 135, no. 3 (1987): 321-9.
35. Briner, V. A., P. Tsai, and R. W. Schrier. "Bradykinin: Potential for Vascular Constriction in the Presence of Endothelial Injury." *Am J Physiol* 264, no. 2 Pt 2 (1993): F322-7.
36. Velarde, V., P. M. de la Cerda, C. Duarte, F. Arancibia, E. Abbott, A. Gonzalez, F. Moreno, and A. A. Jaffa. "Role of Reactive Oxygen Species in Bradykinin-Induced Proliferation of Vascular Smooth Muscle Cells." *Biol Res* 37, no. 3 (2004): 419-30.
37. Bhoola, K. D., C. D. Figueroa, and K. Worthy. "Bioregulation of Kinins: Kallikreins, Kininogens, and Kininases." *Pharmacol Rev* 44, no. 1 (1992): 1-80.
38. Marceau, F., J. Barabe, S. St-Pierre, and D. Regoli. "Kinin Receptors in Experimental Inflammation." *Can J Physiol Pharmacol* 58, no. 5 (1980): 536-42.
39. Kaiser, N., S. Sasson, E. P. Feener, N. Boukobza-Vardi, S. Higashi, D. E. Moller, S. Davidheiser, R. J. Przybylski, and G. L. King. "Differential Regulation of Glucose Transport and Transporters by Glucose in Vascular Endothelial and Smooth Muscle Cells." *Diabetes* 42, no. 1 (1993): 80-9.
40. Heilig, C. W., L. A. Concepcion, B. L. Riser, S. O. Freytag, M. Zhu, and P. Cortes. "Overexpression of Glucose Transporters in Rat Mesangial Cells Cultured in a Normal Glucose Milieu Mimics the Diabetic Phenotype." *J Clin Invest* 96, no. 4 (1995): 1802-14.
41. Lee, A. Y., and S. S. Chung. "Contributions of Polyol Pathway to Oxidative Stress in Diabetic Cataract." *FASEB J* 13, no. 1 (1999): 23-30.
42. Giardino, I., D. Edelstein, and M. Brownlee. "Nonenzymatic Glycosylation in Vitro and in Bovine Endothelial Cells Alters Basic Fibroblast Growth Factor Activity. A Model for Intracellular Glycosylation in Diabetes." *J Clin Invest* 94, no. 1 (1994): 110-7.
43. Shinohara, M., P. J. Thornalley, I. Giardino, P. Beisswenger, S. R. Thorpe, J. Onorato, and M. Brownlee. "Overexpression of Glyoxalase-I in Bovine Endothelial Cells Inhibits Intracellular Advanced Glycation Endproduct Formation and Prevents Hyperglycemia-Induced Increases in Macromolecular Endocytosis." *J Clin Invest* 101, no. 5 (1998): 1142-7.
44. Abordo, E. A., and P. J. Thornalley. "Synthesis and Secretion of Tumour Necrosis Factor-Alpha by Human Monocytic Thp-1 Cells and Chemotaxis

- Induced by Human Serum Albumin Derivatives Modified with Methylglyoxal and Glucose-Derived Advanced Glycation Endproducts." *Immunol Lett* 58, no. 3 (1997): 139-47.
45. McLellan, A. C., P. J. Thornalley, J. Benn, and P. H. Sonksen. "Glyoxalase System in Clinical Diabetes Mellitus and Correlation with Diabetic Complications." *Clin Sci (Lond)* 87, no. 1 (1994): 21-9.
 46. Charonis, A. S., L. A. Reger, J. E. Dege, K. Kouzi-Koliakos, L. T. Furcht, R. M. Wohlhueter, and E. C. Tsilibary. "Laminin Alterations after in Vitro Nonenzymatic Glycosylation." *Diabetes* 39, no. 7 (1990): 807-14.
 47. Kolm-Litty, V., U. Sauer, A. Nerlich, R. Lehmann, and E. D. Schleicher. "High Glucose-Induced Transforming Growth Factor Beta 1 Production Is Mediated by the Hexosamine Pathway in Porcine Glomerular Mesangial Cells." *Journal of Clinical Investigation* 101, no. 1 (1998): 160-169.
 48. Koya, D., and G. L. King. "Protein Kinase C Activation and the Development of Diabetic Complications." *Diabetes* 47, no. 6 (1998): 859-866.
 49. Koya, D., M. R. Jirousek, Y. W. Lin, H. Ishii, K. Kuboki, and G. L. King. "Characterization of Protein Kinase C Beta Isoform Activation on the Gene Expression of Transforming Growth Factor-Beta, Extracellular Matrix Components, and Prostanoids in the Glomeruli of Diabetic Rats." *Journal of Clinical Investigation* 100, no. 1 (1997): 115-126.
 50. Mueller, C. F., K. Laude, J. S. McNally, and D. G. Harrison. "Atvb in Focus: Redox Mechanisms in Blood Vessels." *Arterioscler Thromb Vasc Biol* 25, no. 2 (2005): 274-8.
 51. Du, X. L., D. Edelstein, L. Rossetti, I. G. Fantus, H. Goldberg, F. Ziyadeh, J. Wu, and M. Brownlee. "Hyperglycemia-Induced Mitochondrial Superoxide Overproduction Activates the Hexosamine Pathway and Induces Plasminogen Activator Inhibitor-1 Expression by Increasing Sp1 Glycosylation." *Proc Natl Acad Sci U S A* 97, no. 22 (2000): 12222-6.
 52. Fatehi-Hassanabad, Z., C. B. Chan, and B. L. Furman. "Reactive Oxygen Species and Endothelial Function in Diabetes." *Eur J Pharmacol* 636, no. 1-3 (2010): 8-17.
 53. Pieper, G. M., and Haq Riaz ul. "Activation of Nuclear Factor-Kappab in Cultured Endothelial Cells by Increased Glucose Concentration: Prevention by Calphostin C." *J Cardiovasc Pharmacol* 30, no. 4 (1997): 528-32.
 54. Yerneni, K. K., W. Bai, B. V. Khan, R. M. Medford, and R. Natarajan. "Hyperglycemia-Induced Activation of Nuclear Transcription Factor Kappab in Vascular Smooth Muscle Cells." *Diabetes* 48, no. 4 (1999): 855-64.
 55. Hofmann, M. A., S. Schiekofer, M. Kanitz, M. S. Klevesath, M. Joswig, V. Lee, M. Morcos, H. Tritschler, R. Ziegler, P. Wahl, A. Bierhaus, and P. P. Nawroth.

- "Insufficient Glycemic Control Increases Nuclear Factor-Kappa B Binding Activity in Peripheral Blood Mononuclear Cells Isolated from Patients with Type 1 Diabetes." *Diabetes Care* 21, no. 8 (1998): 1310-6.
56. Zhang, M., P. Song, J. Xu, and M. H. Zou. "Activation of Nad(P)H Oxidases by Thromboxane A2 Receptor Uncouples Endothelial Nitric Oxide Synthase." *Arterioscler Thromb Vasc Biol* 31, no. 1 (2011): 125-32.
 57. Hsieh, H. L., H. H. Wang, W. B. Wu, P. J. Chu, and C. M. Yang. "Transforming Growth Factor-Beta1 Induces Matrix Metalloproteinase-9 and Cell Migration in Astrocytes: Roles of Ros-Dependent Erk- and Jnk-Nf-Kappab Pathways." *J Neuroinflammation* 7, (2010): 88.
 58. Bierhaus, A., S. Schiekofler, M. Schwaninger, M. Andrassy, P. M. Humpert, J. Chen, M. Hong, T. Luther, T. Henle, I. Kloting, M. Morcos, M. Hofmann, H. Tritschler, B. Weigle, M. Kasper, M. Smith, G. Perry, A. M. Schmidt, D. M. Stern, H. U. Haring, E. Schleicher, and P. P. Nawroth. "Diabetes-Associated Sustained Activation of the Transcription Factor Nuclear Factor-Kappab." *Diabetes* 50, no. 12 (2001): 2792-808.
 59. Villeneuve, L. M., M. A. Reddy, L. L. Lanting, M. Wang, L. Meng, and R. Natarajan. "Epigenetic Histone H3 Lysine 9 Methylation in Metabolic Memory and Inflammatory Phenotype of Vascular Smooth Muscle Cells in Diabetes." *Proc Natl Acad Sci U S A* 105, no. 26 (2008): 9047-9052.
 60. Christopher, J., V. Velarde, D. Zhang, D. Mayfield, R. K. Mayfield, and A. A. Jaffa. "Regulation of B(2)-Kinin Receptors by Glucose in Vascular Smooth Muscle Cells." *Am J Physiol Heart Circ Physiol* 280, no. 4 (2001): H1537-46.
 61. Higashida, H., R. A. Streaty, W. Klee, and M. Nirenberg. "Bradykinin-Activated Transmembrane Signals Are Coupled Via No or Ni to Production of Inositol 1,4,5-Trisphosphate, a Second Messenger in Ng108-15 Neuroblastoma-Glioma Hybrid Cells." *Proc Natl Acad Sci U S A* 83, no. 4 (1986): 942-6.
 62. Menke, J. G., J. A. Borkowski, K. K. Bierilo, T. MacNeil, A. W. Derrick, K. A. Schneck, R. W. Ransom, C. D. Strader, D. L. Linemeyer, and J. F. Hess. "Expression Cloning of a Human B1 Bradykinin Receptor." *J Biol Chem* 269, no. 34 (1994): 21583-6.
 63. Eggerickx, D., E. Raspe, D. Bertrand, G. Vassart, and M. Parmentier. "Molecular Cloning, Functional Expression and Pharmacological Characterization of a Human Bradykinin B2 Receptor Gene." *Biochem Biophys Res Commun* 187, no. 3 (1992): 1306-13.
 64. Figueroa, C. D., A. Marchant, U. Novoa, U. Forsternann, K. Jarnagin, B. Scholkens, and W. Muller-Esterl. "Differential Distribution of Bradykinin B(2) Receptors in the Rat and Human Cardiovascular System." *Hypertension* 37, no. 1 (2001): 110-120.

65. Oza, N. B., J. H. Schwartz, H. D. Goud, and N. G. Levinsky. "Rat Aortic Smooth Muscle Cells in Culture Express Kallikrein, Kininogen, and Bradykininase Activity." *J Clin Invest* 85, no. 2 (1990): 597-600.
66. Margolius, HS. "Kallikrein and Kinins. Some Unanswered Questions About System Characteristics and Roles in Human Disease." *Hypertension* 26, (1995): 221-229.
67. Mombouli, J. V., and P. M. Vanhoutte. "Kinins and Endothelial Control of Vascular Smooth Muscle." *Annu Rev Pharmacol Toxicol* 35, (1995): 679-705.
68. Ahluwalia, A., and M. Perretti. "B1 Receptors as a New Inflammatory Target. Could This Be the 1?" *Trends Pharmacol Sci* 20, no. 3 (1999): 100-4.
69. McLean, P. G., M. Perretti, and A. Ahluwalia. "Kinin B(1) Receptors and the Cardiovascular System: Regulation of Expression and Function." *Cardiovasc Res* 48, no. 2 (2000): 194-210.
70. Madeddu, P., A. F. Milia, M. B. Salis, L. Gaspa, W. Gross, A. Lippoldt, and C. Emanuelli. "Renovascular Hypertension in Bradykinin B2-Receptor Knockout Mice." *Hypertension* 32, no. 3 (1998): 503-9.
71. Schanstra, J. P., M. Bachvarova, E. Neau, J. L. Bascands, and D. Bachvarov. "Gene Expression Profiling in the Remnant Kidney Model of Wild Type and Kinin B1 and B2 Receptor Knockout Mice." *Kidney Int* 72, no. 4 (2007): 442-54.
72. Jaffa, M. A., F. Kobeissy, M. Al Hariri, H. Chalhoub, A. Eid, F. N. Ziyadeh, and A. A. Jaffa. "Global Renal Gene Expression Profiling Analysis in B2-Kinin Receptor Null Mice: Impact of Diabetes." *PLoS One* 7, no. 9 (2012): e44714.
73. Wang, P. H., M. A. Cenedeze, G. Campanholle, D. M. Malheiros, H. A. Torres, J. B. Pesquero, A. Pacheco-Silva, and N. O. Camara. "Deletion of Bradykinin B1 Receptor Reduces Renal Fibrosis." *Int Immunopharmacol* 9, no. 6 (2009): 653-7.
74. Abdouh, M., A. Khanjari, N. Abdelazziz, B. Ongali, R. Couture, and H. M. Hassessian. "Early Upregulation of Kinin B1 Receptors in Retinal Microvessels of the Streptozotocin-Diabetic Rat." *Br J Pharmacol* 140, no. 1 (2003): 33-40.
75. Rodriguez, A. I., K. Pereira-Flores, R. Hernandez-Salinas, M. P. Boric, and V. Velarde. "High Glucose Increases B1-Kinin Receptor Expression and Signaling in Endothelial Cells." *Biochem Biophys Res Commun* 345, no. 2 (2006): 652-9.
76. Douillet, C. D., V. Velarde, J. T. Christopher, R. K. Mayfield, M. E. Trojanowska, and A. A. Jaffa. "Mechanisms by Which Bradykinin Promotes Fibrosis in Vascular Smooth Muscle Cells: Role of Tgf-Beta and Mapk." *Am J Physiol Heart Circ Physiol* 279, no. 6 (2000): H2829-37.

77. Pugliese, G., F. Pricci, F. Pugliese, P. Mene, L. Lenti, D. Andreani, G. Galli, A. Casini, S. Bianchi, C. M. Rotella, and et al. "Mechanisms of Glucose-Enhanced Extracellular Matrix Accumulation in Rat Glomerular Mesangial Cells." *Diabetes* 43, no. 3 (1994): 478-90.
78. Campbell, GR, JH Campbell, AH Ang, IL Campbell, S Horrigan, JA Manderson, PRL Mosse, and RA Rennick. *Phenotypic Changes in Smooth Muscle Cells of Human Atherosclerotic Plaques* Pathophysiology of the Atherosclerotic Plaque, edited by S Glagove, WP Newman and and SA Schaffer. New York: Springer-Verlag, 1990.
79. Ross, R. "Cell Biology of Atherosclerosis." *Annu Rev Physiol* 57, (1995): 791-804.
80. Zhang, H., X. Cai, B. Yi, J. Huang, J. W. Wang, and J. Sun. "Correlation of Ctgf Gene Promoter Methylation with Ctgf Expression in Type 2 Diabetes Mellitus with or without Nephropathy." *Molecular Medicine Reports* 9, no. 6 (2014): 2138-2144.
81. Oemar, B. S., A. Werner, J. M. Garnier, D. D. Do, N. Godoy, M. Nauck, W. Marz, J. Rupp, M. Pech, and T. F. Luscher. "Human Connective Tissue Growth Factor Is Expressed in Advanced Atherosclerotic Lesions." *Circulation* 95, no. 4 (1997): 831-9.
82. Sohn, M., Y. Tan, R. L. Klein, and A. A. Jaffa. "Evidence for Low-Density Lipoprotein-Induced Expression of Connective Tissue Growth Factor in Mesangial Cells." *Kidney Int* 67, no. 4 (2005): 1286-96.
83. Ling, C., and L. Groop. "Epigenetics: A Molecular Link between Environmental Factors and Type 2 Diabetes." *Diabetes* 58, no. 12 (2009): 2718-2725.
84. Litherland, S. A. "Immunopathogenic Interaction of Environmental Triggers and Genetic Susceptibility in Diabetes Is Epigenetics the Missing Link?" *Diabetes* 57, no. 12 (2008): 3184-3186.
85. Villeneuve, L. M., and R. Natarajan. "The Role of Epigenetics in the Pathology of Diabetic Complications." *Am J Physiol Renal Physiol* 299, no. 1 (2010): F14-25.
86. Reddy, M. A., L. M. Villeneuve, M. Wang, L. Lanting, and R. Natarajan. "Role of the Lysine-Specific Demethylase 1 in the Proinflammatory Phenotype of Vascular Smooth Muscle Cells of Diabetic Mice." *Circ Res* 103, no. 6 (2008): 615-23.
87. Fuks, F., P. J. Hurd, R. Deplus, and T. Kouzarides. "The DNA Methyltransferases Associate with Hp1 and the Suv39h1 Histone Methyltransferase." *Nucleic Acids Res* 31, no. 9 (2003): 2305-12.
88. Brasacchio, D., J. Okabe, C. Tikellis, A. Balcerzyk, P. George, E. K. Baker, A. C. Calkin, M. Brownlee, M. E. Cooper, and A. El-Osta. "Hyperglycemia

Induces a Dynamic Cooperativity of Histone Methylase and Demethylase Enzymes Associated with Gene-Activating Epigenetic Marks That Coexist on the Lysine Tail." *Diabetes* 58, no. 5 (2009): 1229-1236.

89. Villeneuve, L. M., M. Kato, M. A. Reddy, M. Wang, L. Lanting, and R. Natarajan. "Enhanced Levels of MicroRNA-125b in Vascular Smooth Muscle Cells of Diabetic Db/Db Mice Lead to Increased Inflammatory Gene Expression by Targeting the Histone Methyltransferase Suv39h1." *Diabetes* 59, no. 11 (2010): 2904-15.
90. Wang, Q., Y. Wang, A. W. Minto, J. Wang, Q. Shi, X. Li, and R. J. Quigg. "MicroRNA-377 Is up-Regulated and Can Lead to Increased Fibronectin Production in Diabetic Nephropathy." *FASEB J* 22, no. 12 (2008): 4126-35.
91. Du, B., L. M. Ma, M. B. Huang, H. Zhou, H. L. Huang, P. Shao, Y. Q. Chen, and L. H. Qu. "High Glucose Down-Regulates Mir-29a to Increase Collagen Iv Production in Hk-2 Cells." *FEBS Lett* 584, no. 4 (2010): 811-6.
92. Reddy, M. A., W. Jin, L. Villeneuve, M. Wang, L. Lanting, I. Todorov, M. Kato, and R. Natarajan. "Pro-Inflammatory Role of MicroRNA-200 in Vascular Smooth Muscle Cells from Diabetic Mice." *Arterioscler Thromb Vasc Biol* 32, no. 3 (2012): 721-9.
93. Sharma, S., T. K. Kelly, and P. A. Jones. "Epigenetics in Cancer." *Carcinogenesis* 31, no. 1 (2010): 27-36.
94. Kuroda, A., T. A. Rauch, I. Todorov, H. T. Ku, I. H. Al-Abdullah, F. Kandeel, Y. Mullen, G. P. Pfeifer, and K. Ferreri. "Insulin Gene Expression Is Regulated by DNA Methylation." *PLoS One* 4, no. 9 (2009): e6953.
95. Park, J. H., D. A. Stoffers, R. D. Nicholls, and R. A. Simmons. "Development of Type 2 Diabetes Following Intrauterine Growth Retardation in Rats Is Associated with Progressive Epigenetic Silencing of Pdx1." *J Clin Invest* 118, no. 6 (2008): 2316-24.
96. Pirola, L., A. Balcerczyk, R. W. Tothill, I. Haviv, A. Kaspi, S. Lunke, M. Ziemann, T. Karagiannis, S. Tonna, A. Kowalczyk, B. Beresford-Smith, G. Macintyre, K. L. Ma, H. Y. Zhang, J. Zhu, and A. El-Osta. "Genome-Wide Analysis Distinguishes Hyperglycemia Regulated Epigenetic Signatures of Primary Vascular Cells." *Genome Research* 21, no. 10 (2011): 1601-1615.
97. Kim, M., T. I. Long, K. Arakawa, R. W. Wang, M. C. Yu, and P. W. Laird. "DNA Methylation as a Biomarker for Cardiovascular Disease Risk." *PLoS One* 5, no. 3 (2010).
98. Ingrosso, D., and A. F. Perna. "Epigenetics in Hyperhomocysteinemic States. A Special Focus on Uremia." *Biochimica Et Biophysica Acta-General Subjects* 1790, no. 9 (2009): 892-899.

99. Ekstrom, T. J., and P. Stenvinkel. "The Epigenetic Conductor: A Genomic Orchestrator in Chronic Kidney Disease Complications?" *Journal of Nephrology* 22, no. 4 (2009): 442-449.
100. Stenvinkel, P., M. Karimi, S. Johansson, J. Axelsson, M. Suliman, B. Lindholm, O. Heimbürger, P. Barany, A. Alvestrand, L. Nordfors, A. R. Qureshi, T. J. Ekstrom, and M. Schalling. "Impact of Inflammation on Epigenetic DNA Methylation - a Novel Risk Factor for Cardiovascular Disease?" *Journal of Internal Medicine* 261, no. 5 (2007): 488-499.
101. Jamaluddin, M. S., X. F. Yang, and H. Wang. "Hyperhomocysteinemia, DNA Methylation and Vascular Disease." *Clinical Chemistry and Laboratory Medicine* 45, no. 12 (2007): 1660-1666.
102. Zhang, D. Q., X. H. Jiang, P. Fang, Y. Yan, J. Song, S. Gupta, A. I. Schafer, W. Durante, W. D. Kruger, X. F. Yang, and H. Wang. "Hyperhomocysteinemia Promotes Inflammatory Monocyte Generation and Accelerates Atherosclerosis in Transgenic Cystathionine Beta-Synthase-Deficient Mice." *Circulation* 120, no. 19 (2009): 1893-U138.
103. Zhang, Y., N. Fatima, and M. L. Dufau. "Coordinated Changes in DNA Methylation and Histone Modifications Regulate Silencing/Derepression of Luteinizing Hormone Receptor Gene Transcription." *Mol Cell Biol* 25, no. 18 (2005): 7929-39.
104. Kondo, Y., L. Shen, and J. P. Issa. "Critical Role of Histone Methylation in Tumor Suppressor Gene Silencing in Colorectal Cancer." *Mol Cell Biol* 23, no. 1 (2003): 206-15.
105. Barzily-Rokni, M., N. Friedman, S. Ron-Bigger, S. Isaac, D. Michlin, and A. Eden. "Synergism between DNA Methylation and Macroh2a1 Occupancy in Epigenetic Silencing of the Tumor Suppressor Gene P16(Cdkn2a)." *Nucleic Acids Research* 39, no. 4 (2011): 1326-1335.
106. Lister, R., M. Pelizzola, R. H. Dowen, R. D. Hawkins, G. Hon, J. Tonti-Filippini, J. R. Nery, L. Lee, Z. Ye, Q. M. Ngo, L. Edsall, J. Antosiewicz-Bourget, R. Stewart, V. Ruotti, A. H. Millar, J. A. Thomson, B. Ren, and J. R. Ecker. "Human DNA Methylomes at Base Resolution Show Widespread Epigenomic Differences." *Nature* 462, no. 7271 (2009): 315-322.
107. Rossini, A.A., A.A. Like, W.L. Chick, M.C. Appel, and G.F. Cahill Jr. "Studies of Streptozotocin-Induced Insulinitis and Diabetes." *Proceedings of the National Academy of Sciences of the United States of America* 6, no. 74 (1977): 2485–2489.
108. Luo, M., F. Qiu, J. Qiu, Y. Liu, Y. Fan, and Y. Guo. "An Optimized Method of Vessel Dissection in Establishment of the Rat Aortic Transplantation Model." *J Reconstr Microsurg* 27, no. 6 (2011): 331-6.

109. Li, L. C., and R. Dahiya. "Methprimer: Designing Primers for Methylation Pers." *Bioinformatics* 18, no. 11 (2002): 1427-31.
110. Gardiner-Garden, M., and M. Frommer. "Cpg Islands in Vertebrate Genomes." *J Mol Biol* 196, no. 2 (1987): 261-82.
111. Hulsege, I, A Kommadath, and MA Smits MA. "Globaltest and Goeast: Two Different Approaches for Gene Ontology Analysis." *BMC Proc 3 (Suppl 4), S10, BioMed Central Ltd. , (2009).*
112. Kanehisa, M., and S. Goto. "Kegg: Kyoto Encyclopedia of Genes and Genomes." *Nucleic Acids Research* 28, no. 1 (2000): 27-30.
113. Franceschini, A., D. Szklarczyk, S. Frankild, M. Kuhn, M. Simonovic, A. Roth, J. Y. Lin, P. Minguez, P. Bork, C. von Mering, and L. J. Jensen. "String V9.1: Protein-Protein Interaction Networks, with Increased Coverage and Integration." *Nucleic Acids Research* 41, no. D1 (2013): D808-D815.
114. Stark, C., B. J. Breitkreutz, T. Reguly, L. Boucher, A. Breitkreutz, and M. Tyers. "Biogrid: A General Repository for Interaction Datasets." *Nucleic Acids Research* 34, (2006): D535-D539.
115. Bader, G. D., D. Betel, and C. W. V. Hogue. "Bind: The Biomolecular Interaction Network Database." *Nucleic Acids Research* 31, no. 1 (2003): 248-250.
116. Xenarios, I., L. Salwinski, X. Q. J. Duan, P. Higney, S. M. Kim, and D. Eisenberg. "Dip, the Database of Interacting Proteins: A Research Tool for Studying Cellular Networks of Protein Interactions." *Nucleic Acids Research* 30, no. 1 (2002): 303-305.
117. Licata, L., L. Briganti, D. Peluso, L. Perfetto, M. Iannuccelli, E. Galeota, F. Sacco, A. Palma, A. P. Nardoza, E. Santonico, L. Castagnoli, and G. Cesareni. "Mint, the Molecular Interaction Database: 2012 Update." *Nucleic Acids Research* 40, no. D1 (2012): D857-D861.
118. Jolliffe, I.T. *Principal Component Analysis*. Vol. XXX. 2nd ed ed. NY: Springer, 2002.
119. Marceau, F., J. F. Hess, and D. R. Bachvarov. "The B-1 Receptors for Kinins." *Pharmacological Reviews* 50, no. 3 (1998): 357-386.
120. Galve-de Rochemonteix, B., K. Wiktorowicz, I. Kushner, and J. M. Dayer. "C-Reactive Protein Increases Production of Il-1 Alpha, Il-1 Beta, and Tnf-Alpha, and Expression of Mrna by Human Alveolar Macrophages." *J Leukoc Biol* 53, no. 4 (1993): 439-45.
121. Greene, E. L., V. Velarde, and A. A. Jaffa. "Role of Reactive Oxygen Species in Bradykinin-Induced Mitogen-Activated Protein Kinase and C-Fos Induction in Vascular Cells." *Hypertension* 35, no. 4 (2000): 942-7.

122. Barnes, M. J. "Collagens in Atherosclerosis." *Coll Relat Res* 5, no. 1 (1985): 65-97.
123. Kaplan, A. P., K. Joseph, and M. Silverberg. "Pathways for Bradykinin Formation and Inflammatory Disease." *J Allergy Clin Immunol* 109, no. 2 (2002): 195-209.
124. Breen, D. M., and A. Giacca. "Effects of Insulin on the Vasculature." *Curr Vasc Pharmacol* 9, no. 3 (2011): 321-32.